Small scale investigation and statistical modelling of mountain snow depth

PAR

Thomas GRÜNEWALD

EPFL

ÉCOLE POLYTECHNIQUE
FÉDÉRALE DE LAUSANNE

Suisse
2014

Abstract

The spatial distribution of the mountain snow cover is of high importance for many issues in hydrology (e.g. water supply, flooding), natural hazards (e.g. snow avalanches) or mountain ecology. The snow distribution is typically characterised by a strong spatial heterogeneity, that is the result of different processes interacting with the local topography. Characterising this spatial heterogeneity is a challenging task. Nevertheless, many hydrological applications do not consider the spatial characteristics of the mountain snow cover on the local to regional scale.

This thesis addresses several currently unanswered questions that are of critical importance when describing or modelling the mountain snow cover based on simple, statistical relationships. For the purpose of this thesis we collected a large data set of high resolution snow-depth measurements from different mountain regions obtained by airborne laser scanning and airborne digital photogrammetry. The combination of spatially continuous data in high spatial resolution (metres) with the high accuracy of few decimetres allowed to systematically address questions related to the spatial variability of snow, particularly in relationship with terrain parameters.

In the first study the representativeness of typical index sites for snow-depth measurements was analysed. Based on their topographic characteristics, potential index stations were defined for each of the data sets. The snow cover at these points was then related to the mean snow depth in its vicinity (ranging from metres to hundreds of metres) and to the mean snow depth of the entire investigation area. The analysis showed that the vast majority of these index stations strongly overestimate snow depth of its surrounding and of the complete catchments. Secondly, the topographic characteristics of cells with snow depths that deviate less than 10 % from the catchment mean were analysed. It appears that these "representative" cells are rather randomly distributed and cannot be identified a priori. In summary, our results show large potential biases of index stations with respect to snow distribution.

In the second study we aimed to develop statistical models to explain the spatial variability of the snow depth on the scale of small catchments. Multiple linear regression was applied to model snow depth solely based on topographical parameters. We show that substantial portions of the snow-depth variability (30 to 91 %) could be explained when aggregating the data to a cell-size of 400 m. Such aggregation is required to smooth the effect of small scale accumulation features such as drifts. Similar parameters such as elevation, slope and northing appeared as the best predictors of snow distribution. However, the models deviate between the sites and a "global" model could only explain 23 % of the overall variability.

Due to the dominant impact of elevation on the mountain snow cover and its large importance for hydrological models, a strong focus of the thesis was the altitudinal dependency of precipitation and snow depth. The third and fourth study of the thesis systematically assessed the relationship between snow depth and elevation as reflected in the data sets. The former focuses on the capability of climatological gradients and gradients obtained from meteorological stations to represent the elevation – snow-depth relationship found in reality. It demonstrates that neither climatological nor station-based gradients reflect catchment-wide snow amounts accurately. While the climatological gradient showed different trends, the snow stations tended to overestimate mean snow amounts which is in agreement with the first study. The latter study on elevation gradients presents a detailed analysis of typical shapes of the elevation – snow-depth relationship. The assessment was performed at three scales ranging from the complete data sets of each site to km-scale sub-catchments and finally to 100 m wide slope transects. Results indicate that the elevation – snow-depth curves of most subareas at all scales were characterised by a typical shape. Mean snow depths increase with elevation up to a certain level where they have a distinct peak followed by a decrease at the highest elevations. Rescaling of the data results in a fairly nice collapse of the curves. This shape can be explained with a generally positive elevation gradient of snow fall that is modified by the interrelation of snow cover and topography. These processes are the interaction of snow with the wind that is amplified in rather exposed higher elevations and the relocation of snow from steep to flatter slopes due to gravitational forces. The finding that the elevation level of the maximum of mean snow depth correlates with the dominant elevation level of rocks in the respective subarea seems to confirm this hypothesis. However, more detailed investigation will be required to consolidate that interpretation.

In summary the thesis confirmed the large potential of simple statistical and descriptive approaches

for the assessment of the snow-cover variability on larger scales. While the work was able to characterise general patterns of snow distribution in complex Alpine terrain and to develope statistical descriptions of these patterns, it also demonstrated the limited quantitative generality of these patterns. Therefore, future progress in assessment and prediction will depend on improved physical process representation possibly in combination with statistical approaches.

Zusammenfassung

Der räumlichen Verteilung der Schneedecke im Gebirge kommt in vielen Themengebieten der Hydrologie (z.B. Wasserversorgung und Hochwasser), Naturgefahren (z.B. Lawinen) oder Gebirgsökologie eine entscheidende Bedeutung zu. Grundsätzlich ist die Schneeverteilung durch eine grosse Variabilität gekennzeichnet, die durch das Zusammenspiel verschiedener Prozesse mit der Topographie bedingt ist. Der Umgang mit dieser Variabilität stellt eine grosse Herausforderung dar. Nichts desto trotz werden die räumlich Unterschiede der Schneedecken bei vielen hydrologischen Fragestellungen nicht oder nur unzureichend berücksichtigt. Vor diesem Hintergrund beschäftigt sich die vorliegende Arbeit mit offenen Fragen, die für die statistische Beschreibung und Modellierung der Schneedecke eine wichtige Rolle spielen. Zu diesem Zweck wurde ein umfangreicher Datensatz, bestehend aus grossflächigen Schneehöhenmessungen in hoher räumlicher Auflösung zusammengestellt. Die Daten wurden in verschiedenen Gebirgsregionen mit luftgestützten Laseraufnahmen oder Photogrammmetrie erhoben. Die räumliche Kontinuität in einer Auflösung von wenigen Metern und die Genauigkeit der Schneehöhenmessungen im Dezimeterbereich, ermöglichen eine systematische Herangehensweise an Fragen der räumlichen Variabilität der Schneedecke, insbesondere unter Berücksichtigung des Zusammenhangs mit der Topographie.

Die erste Veröffentlichung dieser Doktorarbeit beschäftigt sich mit der Repräsentativität von typischen Standorten zur Schneehöhenmessung in Flachfeldern. Für die vorhandenen Datensätze wurden solche möglichen Standorte auf Grundlage üblicher Geländeeigenschaften ausgewählt. Die Schneehöhen an diesen Standorten wurden in der Folge mit den mittleren Schneehöhen der umliegenden Referenzgebiete verglichen. Als Referenzgebiet wurden Kreise mit zunehmendem Radius (20 bis 400 m) und letztendlich die gesamte Fläche der Untersuchungsgebiete verwendet. Es zeigte sich, dass die überwältigende Mehrheit der Messstandorte die mittleren Schneehöhen der Referenzgebiete deutlich überschätzt. Zusätzlich wurden die topographischen Charakteristika von Gitterzellen, deren Schneehöhe nur wenig (10 %) vom Flächenmittel abweichen untersucht. Solche "repräsentative" Zellen scheinen relativ zufällig über die Untersuchungsgebiete verteilt, so dass eine Festlegung repräsentativer Standorte auf Grundlage der Topographie nicht möglich erscheint. Zusammenfassend muss festgestellt werden, dass typische Standorte für Schneehöhenmessungen im Bezug auf die grossflächigere Schneeverteilung mit einem grossen potentiellen Fehler behaftet sind.

Die zweite Studie zielt darauf statistische Modelle (multiple lineare Regression) zu entwickeln die die räumliche Variabilität der Schneedecke auf der Skala kleiner Einzugsgebiete mit Hilfe von Geländeeigenschaften erklären. Wir konnten zeigen, dass solche Modelle einen wesentlichen Anteil (30 – 91 %) der Variabilität erklären können. Die Daten müssen jedoch zu Clustern mit einigen hundert Metern Kantenlänge (hier 400 m) aggregiert werden, um die Einflüsse kleinskaliger Akkumulationsformen, wie z.B. Wächten abzuschwächen. In den verschiedenen Untersuchungsgebieten wurden meist ähnliche Geländeparameter, vor allem Seehöhe, Hangneigung und Exposition in die Modelle eingebaut. Ausgewählt wurden die Parameter, die den grössten Teil der Variabilität erklären. Dennoch gibt es deutliche Unterschiede zwischen den Modellen und eine Übertragbarkeit eines Modells auf ein anderes Gebiet scheint nur sehr eingeschränkt möglich. So konnte ein "globales Modell" nur 23 % der Schneehöhenvariabilität erklären.

Die Höhenlage hat einen prägenden Einfluss auf die Schneeverteilung im Gebirge und wird häufig als Variable in hydrologischen Modellen eingesetzt. Deshalb wurde ein Hauptaugenmerk dieser Arbeit auf Höhengradienten von Niederschlag und Schnee gesetzt. Die letzten beiden Studien dieser Arbeit befassen sich systematisch mit dem Zusammenhang zwischen Höhenlage und Schneehöhensignal in den vorhandenen Datensätzen. In der ersten der beiden Studien wurde untersucht ob klimatologische Niederschlagsgradienten und Gradienten die von einzelnen Messstationen abgeleitet wurden, in der Lage sind, die beobachtete Schneeverteilung wiederzugeben. Während die klimatologischen Gradienten unterschiedliche Muster aufwiesen, tendierten die Gradienten auf Grundlage der Messstationen zu einer deutlichen Überschätzung der realen Schneeverteilung. In einer zweiten Studie wurden typische Formen von Höhengradienten der Schneedecke untersucht. Die Analysen wurden auf drei Skalen durchgeführt: Auf der Skala der gesamten Untersuchungsgebiete, auf der Skala hydrologischer Untergebiete und für kleinräumige Hangtransekte. Die Ergebnisse deuten darauf hin, dass auf allen Skalen eine typische Form der Höhengradienten vorherrscht: Die Schneehöhe steigt zunächst mit der Höhe an und erreicht schliesslich ein ausgeprägtes Maximum. Danach fallen die Kurven wieder deutlich ab. Wenn die Kurven skaliert werden, stimmen sie in ihrer Form relative gut überein. Die Form der Kurven kann durch eine

Zunahme der Niederschlags mit der Höhe erklärt werden. Im Zusammenspiel mit der Topographie wird die Schneedecke auf der Oberfläche modifiziert. Vor allem in den exponierten Hochlagen hat der Wind grossen Einfluss auf den Schnee. Ausserdem wird durch die Gravitation Schnee von steilen in flachere Hangbereiche umgelagert. Eine hohe Korrelation zwischen der Höhenlage der maximalen Schneehöhe und der Höhenlage ausgeprägter Felspartien scheint diese Interpretation zu bestätigen. Dennoch sind weitere Analysen notwendig um das Wirken der vorherrschenden Prozesse genauer zu verstehen.

Insgesamt bestätigt die vorliegende Arbeit das grosse Potential relativ einfacher, statistischer Ansätze zur Charakterisierung der Schneehöhenverteilung. Zum einen wurde gezeigt, dass die grobskaligen Muster der Schneeverteilung im Gebirge gut mit statistischen Modellen abgebildet werden können. Zum anderen wurde jedoch die beschränkte qualitative Übertragbarkeit dieser Ansätze klar herausgestellt. Zukünftige Fortschritte in Modellierung und Vorhersage werden deshalb von Verbesserungen der Beschreibung relevanten physikalischen Prozesse abhängen, möglicherweise ergänzt durch statistische Ansätze.

Schlüsselwörter: Alpine Schneedecke, Schneehöhenvariabilität, Schneehöhen, räumliche Variabilität, Representativiät, Index Station, Einzugsgebiet Skala, statistische Modellierung, Höhengradient, LiDAR, Laserscanning

Contents

1.1 Motivation

One of the most apparent characteristics of the snow cover in mountain regions is its spatial heterogeneity (Blöschl, 1999; McKay and Gray, 1981; Seligman, 1936; Sturm and Benson, 2004; Zingg, 1963). This spatial variability is present at a large range of scales, ranging from the sub-metre scale to hundreds of kilometres.

The spatial and temporal heterogeneity of the mountain snow cover has a significant influence on avalanche formation (Schweizer et al., 2003; Birkeland et al., 1995), local ecology (Litaor et al., 2008; Wipf et al., 2009) and hydrology (Balk and Elder, 2000; Barnett et al., 2005; Lundquist and Dettinger, 2005). Information on the amount of water stored in the snow cover and how it is spatially distributed is important for predicting the timing, magnitude and duration of snowmelt and run-off (Lundquist and Dettinger, 2005) and for managing discharge and water supply e.g. for hydropower and irrigation.

Recent years have seen advance in modelling snow distributions by applying sophisticated physical based models such as Alpine3D (Lehning et al., 2006). To capture the small scale variability of the snow, such models have to be operated at grid resolutions of a few metres (Mott and Lehning, 2010; Mott et al., 2010). Nevertheless such sophisticated models require high level input, including high resolution meteorological data (Magnusson et al., 2010), detailed flow fields (Raderschall et al., 2008) and high resolution digital elevation models. They are therefore very expensive in terms of required computational resources and not capable for larger areas or longer time series.

When considering hydrological questions on water resources or climate change, such high resolutions are not necessarily required. It has therefore been attempted to describe the snow-depth distribution with simple models (Winstral and Marks, 2002). For highly complex and steep terrain, however, these simpler models necessitate a similar accuracy of wind field estimates as the more complex models, which can only be obtained by applying the demanding task of running a full 3D atmospheric flow model as for the detailed model.

It is a well-known fact that topography strongly influences the snow distribution (Gerrard, 1990; McKay and Gray, 1981). The spatial heterogeneity of the snow cover is attributed to a number of different processes which act on different scales: Local precipitation amounts are strongly affected by the interaction of the terrain with the local weather and climate (Beniston, 1997; Daly et al., 1994; Mott et al., 2014). Wind plays a major role for the deposition and redistribution of snow (Lehning et al., 2008; McKay and Gray, 1981; Trujillo et al., 2007). Moreover snow can be relocated by avalanches and sloughing (Bernhardt and Schulz, 2010; Blöschl and Kirnbauer, 1992; Elder et al., 1991) and the local radiation and energy balance influence the spatially varying ablation processes (Cline et al., 1998; Mott et al., 2011a; Pohl et al., 2006; Pomeroy et al., 1998).

Due to this obvious relation between snow cover and terrain, statistical approaches seem promising to model snow characteristics such as snow depth or snow water equivalent (SWE) based on their topographic settings. A large number of studies have therefore aimed to analyse these statistical relationships for different landscapes worldwide and at different spatial scales. Many of these approaches are described in the following sections. However, a comprehensive review shows that the findings are contradictory: Dependent on the site and the spatial scale, different parameters appear to affect the snow distribution, and the amount of variability that could be explained by the models varied considerably. Most of the studies were limited by the data available for the analysis. A lack of spatial continuous snow depth observations in appropriate accuracy and spatial resolution is the reason that most of these studies are limited to relatively small study areas or a spatially sparse number of point observations. Such point observations

are not necessarily representing the snow cover in their surrounding and impose large potential biases. Furthermore, comprehensive studies, merging data sets from diverse climatic and morphologic regions are currently missing.

The availability of a large data set consisting of spatial continuous snow-depth data from several large study domains of different mountain regions now allows to address some of these shortcomings.

1.2 Research questions

Specifically this thesis aims to address the following research questions:

1. **Representativeness of flat-field measurements:**
   How representative are snow-depth measurements at typical flat-field sites in comparison to slopes in the surrounding and to entire catchments or mountain sites?

2. **Statistical modelling:**

   (a) Can we explain the small-scale snow-depth variability with simple statistical models? Which parameters are important? How universal are such relationships and how do they vary between different regions?

   (b) To what degree must the data be spatially aggregated to produce meaningful statistical models and how can such an aggregation be performed?

3. **Altitudinal gradients:**

   (a) How are altitudinal gradients reflected in snow-depth measurements? How universal are they and how do they compare to published results?

   (b) Where is the maximum of the precipitation-elevation relationship and how is the flattening of the gradients reflected in the snow distribution on the ground? Which variables have a significant impact on the characteristics of these gradients?

1.3 Background

1.3.1 Spatial variability of snow depth

It has been shown that different processes are controlling the snow distribution at different scales (Blöschl, 1999). At the point scale ($< 5\,\mathrm{m}$) small scale surface roughness is dominating the snow distribution. Small obstacles like shallow vegetation or rock boulders have a sheltering effect and snow can be accumulated on their leeward sides or in small depressions (Clark et al., 2011). At the hillslope scale (metres to hundreds of metres) the local wind field is the driving factor for the processes of preferential deposition of precipitation (Lehning et al., 2008; Mott and Lehning, 2010; Mott et al., 2011b) and drifting of snow (Gauer, 2001; Mott et al., 2010; Trujillo et al., 2007). Avalanching and sloughing also affect the snow distribution at that scale (Bernhardt and Schulz, 2010; Blöschl and Kirnbauer, 1992; Gruber, 2007; Sovilla et al., 2010). At the watershed scale (hundreds of metres to kilometres), the most important factors are variations in melt energy and freezing levels (Clark et al., 2011) and orographic precipitation gradients (Frei and Schär, 1998; Grünewald and Lehning, 2011).

Vertical elevation gradients of precipitation are caused by orographic lifting of the air and are common for mountainous areas. This effect usually accounts for an increase in precipitation with altitude (Daly et al., 1994; Frei and Schär, 1998; Kirchhofer and Sveruk, 1992; Lang, 1985; Zängl, 2008). Nevertheless, due to the large effect of topography and climatology, precipitation gradients are known to vary on a regional scale (Mott et al., 2014; Schwarb et al., 2001; Sevruk, 1997; Wastl and Zängl, 2008). As snow distribution is strongly affected by precipitation, the increase in precipitation is reflected in an increase in snow amounts with elevation as confirmed by several studies (Bavay et al., 2009; Bavera and De Michele, 2009; Foppa et al., 2005; Jonas et al., 2009; Lopez-Moreno and Stähli, 2008; Pipp, 1998; Rohrer et al., 1994). However, such gradients can significantly differ over a specific elevation range. Especially at high altitudes a flattening or even a decrease in the gradient is present (Grünewald and Lehning, 2011). This

flattening might on the one hand be attributed to the fact that a precipitation maximum is reached at a certain elevation (Blanchet et al., 2009). The reason for such a limit is that the decreasing air density in higher elevations reduces the amount of moisture available for condensation and therefore counteracts further precipitation increase. Following theoretical considerations, Havlik (1969) expected such a precipitation maximum above 3500 m for the Alps. However, we are not aware of any study which could provide evidence for such a maximum, probably due to a general lack of observational data from such high elevations. On the other hand, high elevations are usually steeper and more exposed which results in an redistribution of snow by avalanches (Bernhardt and Schulz, 2010) and by wind (Winstral et al., 2002) from the summit regions to lower elevations. Nevertheless the information on precipitation amounts and gradients in high elevations is very limited. This is due to measurement difficulties of snowfall and rain in exposed areas (Rasmussen et al., 2001, 2011; Sevruk, 1997; Yang et al., 1998) and to an insufficient coverage of these regions by measurement stations (Blanchet et al., 2009; Daly et al., 2008).

1.3.2 Statistical modelling of the spatial variability

Statistics provide a simple and straightforward approach for modelling snow-cover variables such as snow depth, SWE or snow-cover duration. Many statistical models aim to explain the variability of the snow-cover as a function of topographic indices.

1.3.2.1 Terrain parameters

Elevation is probably the most common variable applied in such models. On the one hand, elevation reflects the effect of decreasing air temperatures with altitude and can therefore be used as a proxy for parameters like freezing level and therefore snow – rain transition, or the amount of energy available for melting (Clark et al., 2011). On the other hand, as discussed above, elevation has an important effect on the distribution of precipitation, especially at larger scales. Obviously these altitudinal effects are reflected in the snow-depth distribution.

A second variable which is commonly used as explanatory parameter is the slope. The slope is the first derivative of the elevation and is important for gravitative processes like sloughing and avalanching which have a significant effect on the snow distribution (Bernhardt and Schulz, 2010; Blöschl and Kirnbauer, 1992; Elder et al., 1991; Sovilla et al., 2010). Snow is removed from steep areas and relocated towards flat slopes and terrain depressions. Moreover the slope also strongly affects the local energy balance. The slope angle is related to the albedo and therefore to the amount of solar radiation which arrives at the snow cover (Helbig et al., 2009) and is available as a source for melt. The albedo of the surface is directly related to the impact angle of the radiation. The higher the impact angle, the lower the albedo which is the portion of energy that is scattered back to the atmosphere. The impact angle is affected by the combination of the elevation of the sun, the slope and aspect of the terrain (Odermatt et al., 2005; Warren, 1982).

A further variable which has an effect on the snow cover is the aspect. Similar to the slope, the aspect is directly related to the radiation input. On the Northern hemisphere, east- and south-facing slopes are getting much larger portions of solar radiation, especially during the winter, when the elevation of the sun is low. Aspect is usually given in degrees. For physical reasons the definition of North as being 0 and 360 degrees is not very meaningful, aspect is therefore often divided into sectors (e.g. NW to NE, NE to SE...) or transformed to a continuous variable like Northing (deviation from North) (Grünewald et al., 2010). Furthermore the aspect is also important for the deposition and redistribution of snow by wind (Lehning et al., 2008; Seyfried and Wilcox, 1995). More snow is usually accumulated on the leeward sides of slopes and mountains.

Nevertheless, more sophisticated parameters have been developed to account for the effect of shelter and exposure (Anderton et al., 2004; Purves et al., 1998; Winstral et al., 2002). The sheltering index Sx introduced by Winstral et al. (2002) calculates the upslope angle of the terrain in the direction of the dominating wind for each cell of a digital elevation model. Several studies showed that Sx is a good measure for sheltering and exposure of the local terrain which gives a simple but reasonable representation of the local flow field and therefore of the redistribution of snow by wind (Anderton et al., 2004; Erickson

et al., 2005; Litaor et al., 2008; Molotch et al., 2005; Schirmer et al., 2011; Winstral et al., 2002; Winstral and Marks, 2002).

Solar radiation has a direct effect on snow density and snow depth resulting from a combination of sublimation and melt (Elder et al., 1991). Many studies have used potential solar radiation as an explanatory variable (Elder et al., 1991, 1998; Erickson et al., 2005; Erxleben et al., 2002; Hosang and Dettwiler, 1991; Litaor et al., 2008; Lopez-Moreno and Nogues-Bravo, 2006; Schmidt et al., 2009). In almost all of these studies the potential radiation for the specific spot is calculated assuming clear sky conditions. This means that in such models radiation is simply a function of the solar angle and the terrain.

If present, vegetation can have a remarkable impact on the snow distribution (Clark et al., 2011; Deems et al., 2006; Trujillo et al., 2007; Varhola et al., 2010). Trees and shrubs have – as long as not completely covered by snow – an effect on the local wind field and therefore on the deposition and redistribution of snow. Moreover interception and sublimation of snow in the canopy and the effect of vegetation on the local energy balance are influencing the snow distribution in forests (Varhola et al., 2010). The presence or absence of vegetation as well as the size and spacing of trees is therefore an important factor for the spatial distribution of snow.

A measure that reflects the local exposure of the relief is the surface roughness which is an expression of the irregularity of the terrain (Mark, 1975) and is a very important measure to characterise the topography of the earth on different scales. The surface roughness strongly affects the redistribution of snow via wind and gravitative processes (Jost et al., 2007) and can be seen as the capability of the surface to trap snow. Many different morphometric parameters, including deviation of elevation, slope, aspect and curvature (Evans, 1972; Shepard et al., 2001; Speight, 1974; Wood, 1996) have been applied in order to characterise the roughness of the terrain, whereas the local deviation of elevation is the most common roughness index (Alvarez-Mozos et al., 2011). Nevertheless Mark (1975) and Evans (1972) already noted that a single measure is usually not capable to adequately capture surface roughness and that combinations of different parameters are required.

Since Mandelbrot (1977, 1982) introduced his concept of fractals, this approach was widely applied in order to characterise surface roughness. A large variety of natural phenomena, including topography, show fractal behaviour and spatial self-similarity over a distinct range of scales (Goodchild and Mark, 1987). The most important fractal parameters are the fractal dimension D, which is a measure of the irregularity of the object in consideration (Sun et al., 2006) and the ordinal intercept γ, which is the "expected squared difference an unit distance apart" (Xu et al., 1993) and therefore reflects the roughness of the object on the scale of the measurement resolution. Fractal parameters, especially D and γ have been identified to be good measures to characterise surface roughness (Goodchild and Mark, 1987; Klinkenberg, 1992; Klinkenberg and Goodchild, 1992; Power and Tullis, 1991; Sun et al., 2006; Taud and Parrot, 2006; Xu et al., 1993). In this context large D indicate very rough surfaces and small fractal dimensions are linked to smooth surfaces (Burrough, 1981, 1993; Klinkenberg, 1992; Pentland, 1984; Sun et al., 2006). D can also be applied to identify the scale at which different processes dominate (Emerson et al., 1999; Shepard et al., 2001; Sun et al., 2006) and also to distinguish between such processes (Goodchild and Mark, 1987; Klinkenberg, 1992; Klinkenberg and Goodchild, 1992). Klinkenberg (1992) and Klinkenberg and Goodchild (1992) noticed that D only shows weak correlations with traditional roughness measures and reasoned that D reflects a different aspect of surface roughness (Xu et al., 1993). On the contrary, γ appears to very well correlate with such morphometric parameters, especially with those related to gradients: Klinkenberg (1992) found a correlation of 0.92 between γ and the local slope of a digital terrain model. Following Fox and Hayes (1985), Klinkenberg and Goodchild (1992) conclude that a combination of D and γ would capture all essential characteristics of the land surface.

In recent years fractal analysis have been applied in snow studies (Deems et al., 2006, 2008; Kuchment and Gelfan, 2001; Mott et al., 2011b; Schirmer and Lehning, 2011; Shook and Gray, 1996; Trujillo et al., 2007, 2009; Lehning et al., 2011; Helfricht et al., accepted for publication). It has been shown that snow depth in general is self-similar over a certain range of scales (Kuchment and Gelfan, 2001) and that scale breaks typically occur in the range of tens of metres (Deems et al., 2006; Schirmer and Lehning, 2011; Shook and Gray, 1996; Trujillo et al., 2007). Scale breaks have been identified as indicator for a change of the dominating process at a respective scale. Deems et al. (2006) and Trujillo et al. (2007) related the change of the scaling behaviour of snow to vegetation patterns which showed similar scaling

4

characteristics. The scale breaks of snow depth also appear to be influenced by the wind (Deems et al., 2006; Mott et al., 2011b; Schirmer and Lehning, 2011; Trujillo et al., 2007, 2009) and by the roughness of the local topography (Schirmer and Lehning, 2011).

1.3.2.2 State of the art in statisticall modelling

There are numerous studies which use the terrain parameters described above in order to model the snow cover statistically. Nevertheless most of these studies are limited by the small amount and quality of data available for the analysis. Most studies analysed manual snow-depth measurements and only tens to few hundreds of samples could be used for the modelling.

For example, several studies have successfully applied binary regression-tree modelling for snow-cover variables (Anderton et al., 2004; Balk and Elder, 2000; Elder et al., 1998; Erxleben et al., 2002; Litaor et al., 2008; Lopez-Moreno and Nogues-Bravo, 2006; Molotch et al., 2005; Winstral et al., 2002). By minimizing the sum of the residuals, the response data (e.g. snow depth or SWE) are split along a predictor (e.g. terrain parameter) into subgroups. 18 to 90 % (Litaor et al., 2008) of the snow-cover variability could be explained by such regression trees. The combination of the number of explaining parameters included in the model, the number of splits and the quality, complexity and spatial resolution of the input data influence the performance of such models.

Multiple linear regression analysis is a second statistical approach that has frequently been applied for modelling the spatial variability of snow (Golding, 1974; Chang and Li, 2000; Grünewald et al., 2010; Jost et al., 2007; Lehning et al., 2011; Revuelto et al., 2014). Again, terrain characteristics are applied as explanatory variables for the regression models: Golding (1974) applied multivariate linear regression modelling to explain 48 % of the SWE variability in Marmot Creek, Alberta. Elevation, topographic position, aspect, slope and forest density were selected as model parameters. Marchand and Killingtveit (2005) aggregated a large number snow depths, gathered by georadar and hand probing, to the km-scale and modelled snow depth in open areas of a large Norwegian basin. Different measures, such as elevation, aspect, curvature and slope could account for 5 to 48 % of the snow-depth variability. Based on some tens of manual measurements, up to 90 % of the large-scale variability in SWE could be explained by elevation, aspect and forest cover in a 17 km^2 watershed in Canada (Jost et al., 2007). Hosang and Dettwiler (1991) presented a model which applied elevation, potential radiation and forest cover to reproduce 66 % of the spatial variability of SWE in a small Swiss catchment. Only 33 manual snow samples were used as input for the model. From few hundred snow depth measurements Elder et al. (1991) built a regression model with elevation, slope and radiation for a three year data set for the Emerald Lake basin (California) ($R^2 = 0.27$ to 0.40) and (Chang and Li, 2000) applied measurements from few snow courses to build a model with the parameters elevation, slope, aspect and a relative position that could represent 60 to 90 % of the SWE in Idaho. Lopez-Moreno and Nogues-Bravo (2006) could explain more than 50 % of the snow-depth variability over the Pyrenees. Measurements from 106 snow poles were used as input and elevation, elevation range, radiation and two location parameters served as explanatory variables. Note that all these studies are limited by number and quality of their input data. The studies of Lopez-Moreno and Nogues-Bravo (2006) and (Chang and Li, 2000) are even based on measurements obtained at typical "index sites". Chapter 2 of this thesis shows that such measurements are usually not representative for larger areas.

The increasing application of high-resolution and high-quality snow-depth measurements obtained from terrestrial (Grünewald et al., 2010; Prokop et al., 2008; Schaffhauser et al., 2008) and airborne laser scanning (Deems and Painter, 2006; Deems et al., 2013; Lehning et al., 2011) opened new prospects for studying the snow cover. The tremendous number of data points and the high quality of the measurements provides a much more accurate and detailed picture of the snow-cover variability. In the Wannengrat area (Davos, CH), Grünewald et al. (2010) obtained snow-depth data from repeated terrestrial laser-scanning surveys to explain 30 to 40 % of the variability in melt rates. Elevation, slope, aspect, radiation and elevation, slope, maximum SWE, and wind speed, respectively were selected as explanatory parameters. Based on terrestrial laser-scanning data, Revuelto et al. (2014) investigated the topographic control on snow depth for a small mountain catchment in the Spanish Pyrenees. From the analysis of linear regression models and binary regression trees they found that a topographic position index derived from slope curvature was the best predictor for snow depth in a 5 m grid resolution. They also state that similar topographic parameters were the best predictors for different times in a season and between two

climatically different winters but that the importance of the parameters and the amount of variance explained by the models varied considerably. More than 70 % of the snow-depth variability could be explained by a two-parameter model with elevation and a fractal roughness parameter (Lehning et al., 2011) . The study applied airborne LiDAR measurements for two small catchments in Switzerland. However, the data had to be aggregated to homogenous sub-areas with a length scales of about 500 m.

Such an aggregation is required to average out the extremely large spatial variability which is especially present at small scales (Shook and Gray, 1996; Watson et al., 2006; Schirmer and Lehning, 2011). Aggregation to sub-areas was also performed by Elder et al. (1991) who used elevation, slope and solar radiation as criteria to cluster regions of homogeneous snow depth. Jost et al. (2007) averaged their measurements to the plot scale in order reveal the larger scale dependencies. Such an aggregation is similar to the concept of hydrological response units that has been applied in several hydrological models (Rinaldo et al., 2006; Kite and Kouwen, 1992; Pomeroy et al., 2007).

1.3.3 Airborne laser scanning

Airborne (ALS) and terrestical (TLS) laser scanning, also commonly referred as LiDAR (Light detection and ranging) is a remote sensing technology which has seen wide application in both, science and environmental management in the recent decades. The range of applications is large and besides high precision digital terrain mapping also includes fields like glaciology, forest management, hazard mapping, infrastructure surveys or archaeology. In the last decade, multi-temporal LiDAR surveys have also become prominent for mapping of snow-cover properties, especially snow depth and snow-depth change.

1.3.3.1 Technical background

LiDAR is an active remote sensing technology, where a laser pulse is emitted by the measurement platform. The signal is backscattered by the surface of the target and the distances between the target and the sensor is then obtained based on the principle of the time of flight measurement of the laser pulse. Knowledge on the scanner geometry (angular direction of the pulse) and the position of the sensor enable to calculate spatial coordinates of the measured targets.

In ALS, the sensor is mounted on an aeroplane or helicopter and records the elevation of the earth surface below its flight path. Positioning is usually performed from differential GPS and an inertial measurement unit (IMU) which measures the orientation of the sensor. Both, GPS and IMU measure permanently and are directly coupled to the scanner.

The spatial resolution (point density) that can be reached by LiDAR depends on the combination of the technical properties (pulse repetition frequency, scan rate, measurement angle resolution, beam divergence) of the scanner with the type of operation (target distance, flying speed (ALS), swath with) and the geometry of the terrain (slope, roughness). Modern systems have typical pulse frequencies of several hundreds of kHz and the beam divergence, which determines the size of the laser beam at the target surface, is in the range of 0.1 to 1 mrad. The accuracy of ALS systems is on the decimetre-scale (Deems et al., 2013; Vallet, 2011). The accuracy is mainly affected by potential geo-location errors, errors induced by the terrain (roughness, slope) and vegetation. Interactions of the laser pulse with the surface (especially snow), such as scattering, penetration and attenuation of the beam (in total $\tilde{1}$ cm for snow) only have a relatively small portion relative to the other error sources (Deems et al., 2013). Baltsavias (1999), Wehr and Lohr (1999), Geist et al. (2009) and Deems et al. (2013) provide comprehensive reviews on the LiDAR measurement principle, data aquisition and processing.

1.3.3.2 Applications for snow-cover mapping

The introduction of laser scanning to the snow science community was an important improvement for the collection of area-wide snow-depth data. Due to its high spatial resolution, high accuracy and large spatial coverage, LiDAR has a very high potential for snow-cover studies related to snow depth and snow-depth change. Snow depth is calculated by subtracting two digital surface models, one with snow and the other obtained in snow-free conditions.

Several studies showed that ALS was an appropriate and accurate method for collecting area-wide snow-depth measurements in high spatial resolution and accuracy (Deems and Painter, 2006; Hopkinson

et al., 2001). The accuracy of the data measured by ALS depends on the measurement platform. Most data sets were gathered from aeroplanes which is very effective in terms of the area that can be surveyed. Larger flight height of the plane and lower impact angles of the laser beam in steep terrain lead to reduced accuracy of the data. Nevertheless, the error is usually below 30 cm for snow depth (Moreno Baños et al., 2009; DeBeer and Pomeroy, 2010; Tinkham et al., 2014). Alternatively, ALS campaigns have been performed with helicopter based systems (Skaloud et al., 2006; Vallet and Skaloud, 2005; Vallet, 2011). The reduced terrain-following flying height and the potential of the system to be tilted in direction of the target (improved incident angle) results in a higher accuracy, especially in steep terrain. For snow depth, the accuracy of the data was found to be below 10 cm in comparison to terrestrial laser scanning and tachymeter surveys (Grünewald et al., 2010).

LiDAR data have seen wide application in snow studies in the recent years. Snow-depth maps calculated from ALS or TLS have been used for model validation (Dadic et al., 2010b; Melvold and Skaugen, 2013; Mott et al., 2011a,b; Schirmer et al., 2011), as input surface for models (Dadic et al., 2010b; DeBeer and Pomeroy, 2010; Egli et al., 2012; Melvold and Skaugen, 2013; Mott et al., 2011a,b; Schirmer et al., 2011) or as validation data for precipitation (Scipion et al., 2013) or different snow-depth sensors (Cavalieri et al., 2012). Many studies have used ALS (Cavalieri et al., 2012; Deems et al., 2006, 2008; Trujillo et al., 2007, 2009) or TLS (Grünewald et al., 2010; Mott et al., 2010; Schirmer et al., 2011; Schirmer and Lehning, 2011; Revuelto et al., 2014) data to study the spatial variability of snow depth and snow-depth change. Moreover LiDAR data were used to develop statistical models to explain the spatial variability of snow depth (Moreno Baños et al., 2009; Lehning et al., 2011) and ablation rates (Grünewald et al., 2010) in relation to the terrain. Sovilla et al. (2010) applied ALS data to map the volume of avalanche depositions and Veitinger et al. (2014) applied ALS and TLS data to characterise the change in surface roughness during the snow season.

1.3.3.3 Airborne digital photogrammetry

In recent years airborne digital photogrammetry (ADP) has shown up as a cost effective alternative to ALS. Digital surface models are calculated from digital images taken from an aeroplane, based on photrogrammetric image correlation techniques (Maune, 2001). Identical to LiDAR, snow-depth maps are calculated by subtraction of elevation models obtained in summer and winter. The applicability of the sensor for snow surfaces has been demonstrated by Bühler et al. (2009) who monitored avalanche deposits. Spatial resolution and accuracy are similar to aeroplane based ALS (Bühler et al., 2012).

1.4 Outline

This thesis is divided into four main chapters that accord to four papers. The overall topic of this dissertation is the developement and application of simple statistical and descriptive approaches in order to model and to explain a substantial portion of the snow-depth variability, typically present at mountain sites.

To date, the common approach to assess this spatial variability is still based on spatially sparse snow-depth measurements. The highly relevant question of the representativeness of such point observations for larger areas is systematically assessed in the first paper of this dissertation (Chapter 2).

If reliable input data are available, a second step to model snow-depth distribution is to build statistical models. Such models usually exploit the relationship between terrain and snow cover. In the second study (Chapter 3), our comprehensive data set was used to develop such robust statistical models. Amongst other things, this study confirmed the prominent role of elevation, found in previous studies. Therefore a special focus was set on a detailed assessment of the elevation – snow-depth relationship (Chapters 4 and 5). The first of the two studies addresses the elevation – snow depth relationship for two small study domains and focuses on the question if climatological elevation gradients or gradients obtained from meteorological stations are capable to picture real elevation gradients of snow depth. This approach is strongly related to the questions posed in Chapter 2. The latter study aims to identify typical shapes of the elevation – snow-depth relationship (Chapter 5). The study applies an even larger data set to classify shapes of elevation gradients and to relate them to the general topographic settings.

The dissertation is finally completed by a overall conclusion (Chapeter 6) that merges the results of the four papers and by an outlook (Chapeter 7), highlighting the limitation of the studies and picturing possible future directions of research in the topic.

Are flat-field snow depth measurements representative? A comparison of selected index sites with areal snow depth measurements at the small catchment scale.

2.1 Introduction

Appropriate information on the amount of snow stored on a slope, in a catchment or an entire mountain range is crucial for many applications ranging from hydrological modelling and stream flow management to natural hazards, climate studies, winter tourism or mountain ecology. Area-wide measurements of snow depth in a suitable spatial and temporal resolution are usually not available as they are costly and difficult to obtain. It is therefore a common practice to interpolate snow depths or snow water equivalent (SWE) from a few selected locations, like meteorological stations or snow courses to a larger areas (Balk and Elder, 2000; Carroll and Cressie, 1996; Daly et al., 2000; Erxleben et al., 2002) and to assume that few index sites represent the snow cover of their vicinity(e.g., Egli, 2008). Such index stations are usually set up in flat, often sheltered locations that are characterised by a relatively homogenous snow cover. When considering the well-known large spatial heterogeneity of the snow cover, especially in mountain regions, and particularly at small scales (metres to hundreds of metres), one can expect that snow depths measured at these sites might deviate from the spatial mean of the area. Most studies, which assessed diverse kinds of representativeness confirmed this hypothesis as discussed in more detail below and found that measurements of snow depth or SWE obtained at index stations are not necessarily representing their surrounding (Chang et al., 2005; Lopez-Moreno et al., 2011; Meromy et al., 2013; Neumann et al., 2006; Rice and Bales, 2010; Watson et al., 2006; Yang and Woo, 1999).

Investigations on the representativeness of snow cover properties have been obtained for different landscapes and on scales ranging from metres to kilometres: Lopez-Moreno et al. (2011) analysed snow depth measurements from open and forested terrain in the Pyrenees and found that more than five measurements would be required to represent the spatial mean at the plot scale (10 m). In a study obtained in boreal forests of northern Saskachewan (CA), Neumann et al. (2006) found that single point measurements of snow depth were not able to characterise the snow cover of 100 m transects in their vicinity. In a similar investigation of a stratified sampling design for snow depths in the Yellowstone (US) region, Watson et al. (2006) concluded that more than 50 measurements per stratum would be required to represent SWE at scales of up to 300 m. Yang and Woo (1999) showed that two index stations in the Canadian High Arctic were not capable to represent the snow cover of their surrounding at the kilometre-scale. For three different geographic region in the Western United States, Meromy et al. (2013) analysed the representativeness of snowpack telemetry (SNOTEL) stations for their surrounding at the kilometre-scale. They conclude that about half of the stations deviate less than 10 % from the mean of their neighbourhood (1 km^2 cell) whereas other stations either over- or underestimated their vicinity by up to 77 %. However, due to the very similar criteria applied for their set up, all these stations might be affected by a similar bias, relative to the real snow cover. When developing a sensor network for snow depth observations at the scale of 1 to 16 km^2 for the Yosemite National Park in the Sierra Nevada of California, Rice and Bales (2010) discovered that a single point measurement was a poor estimator for the spatial mean of the area. Chang et al. (2005) compared snow depths obtained from passive microwave satellite data at a cell size of 25 m to point measurements from the Northern Great Planes (USA) and concluded that the differences are significant for most of the stations.

However, all these studies are limited by the amount or quality of the snow depth data they are using to assess the representativeness: Rice and Bales (2010) and Meromy et al. (2013) interpolated snow depth from snow courses by applying binary regression trees and compared it to the measurements of the stations. The other studies directly compared selected measurement stations with spatial means calculated from tens to hundreds of manually obtained snow depth measurements (Lopez-Moreno et al., 2011; Neumann et al., 2006; Watson et al., 2006; Yang and Woo, 1999) or to coarse snow-depth maps obtained from remote sensing (Chang et al., 2005).

In this study we analyse a large data set of area-wide snow depth maps obtained from air-borne laser scanning (ALS) in different mountain regions of the world. The accuracy and very high spatial resolution (1 m) of the data enables for the first time to compare potential index sites with the real snow cover distribution in their vicinity. After a brief description of the study sites and the data analysed in the study, we present the methods and results of two different but complementary approaches: The first approach identifies locations for potential index stations, dependent on the topographic settings and snow cover information and systematically compares the snow depth at these locations with its surrounding. The second method is to analyse the topography of cells that contain a "representative" snow cover.

2.2 Data and Methods

2.2.1 Airborne Laser scanning

ALS has shown to be powerful method for mapping snow depths for large areas (Deems and Painter, 2006; Deems et al., 2013; Hopkinson et al., 2004). ALS is an active remote sensing technology, where a measurement platform emits laser pulses in very high frequency. The distances to the target surface, where the signal is reflected can be obtained based on time of flight measurement of the laser pulse. Knowledge on the scanner geometry and the position of the sensor enable to calculate spatial coordinates of the measured targets and hence to obtain digital surface models. High resolution snow depth maps can then be calculated by subtracting two digital surface models, one obtained in winter and the other one in summer. The mean vertical accuracy of snow depths obtained by ALS is 10 to 30 m (DeBeer and Pomeroy, 2010; Geist et al., 2009; Grünewald et al., 2010; Moreno Baños et al., 2009). For the data sets applied in this study, details on the data acquisition, the post-processing and the respective references can be found in Grünewald et al. (2013). Baltsavias (1999), Wehr and Lohr (1999) and Geist et al. (2009) provide general descriptions on the ALS measurement principle and its application.

2.2.2 Study sites and data

The data sets analysed in this study is the same as in Grünewald et al. (2013). We therefore only give a brief characterisation of the study sites. An overview map of the locations of the study sites is presented in Fig. 2.1. For detailed maps and comprehensive descriptions of the data-sets we refer to Grünewald et al. (2013) and the references therein. In total we analyse ALS data from six different mountain regions.

The Wannengrat (WAN) (Fig. 2.2a) and the Piz Lagrev (LAG) are two small (4 and 3 km^2 respectively) mountain catchments located in the eastern Swiss Alps (Grünewald and Lehning, 2011). WAN consists of the head waters of the Albertibach that drain towards the Landwasser valley in the East and Hinter Latschüel, a smaller section at the western side of the mountain ridge. Both sites are characterised by a mixture of steep and gentle slopes with some rock faces, especially in the summit regions. LAG is much steeper and larger flat areas are completely missing. The ALS winter surveys were performed at 26 April 2009 (WAN) and 7 April 2008 (LAG) respectively. Analysis of snow stations in the vicinity indicate that these dates concur with the peak of the seasonal snow accumulation.

The Haut Glacier d'Arolla (ARO) (Fig. 2.2b) is a glacier catchment situated at the main Alpine divide in southwestern Switzerland. The winter data set was obtained at 1 May 2008 which was near of the peak of the winter accumulation (Dadic et al., 2010b). It covers an area of 10 km^2 including a 4.4 km^2 valley glacier and several small cirque glaciers, surrounded by steep rock faces (Dadic et al., 2010b).

The Hintereisferner (HEF) is a large 25 km^2 data set obtained during the OMEGA project (provided by Institute of Geography of the University of Innsbruck). The study domain is located in the Ötztal Alps at the border between Austria and Italy (Geist and Stötter, 2008). Similar as at ARO, the catchment
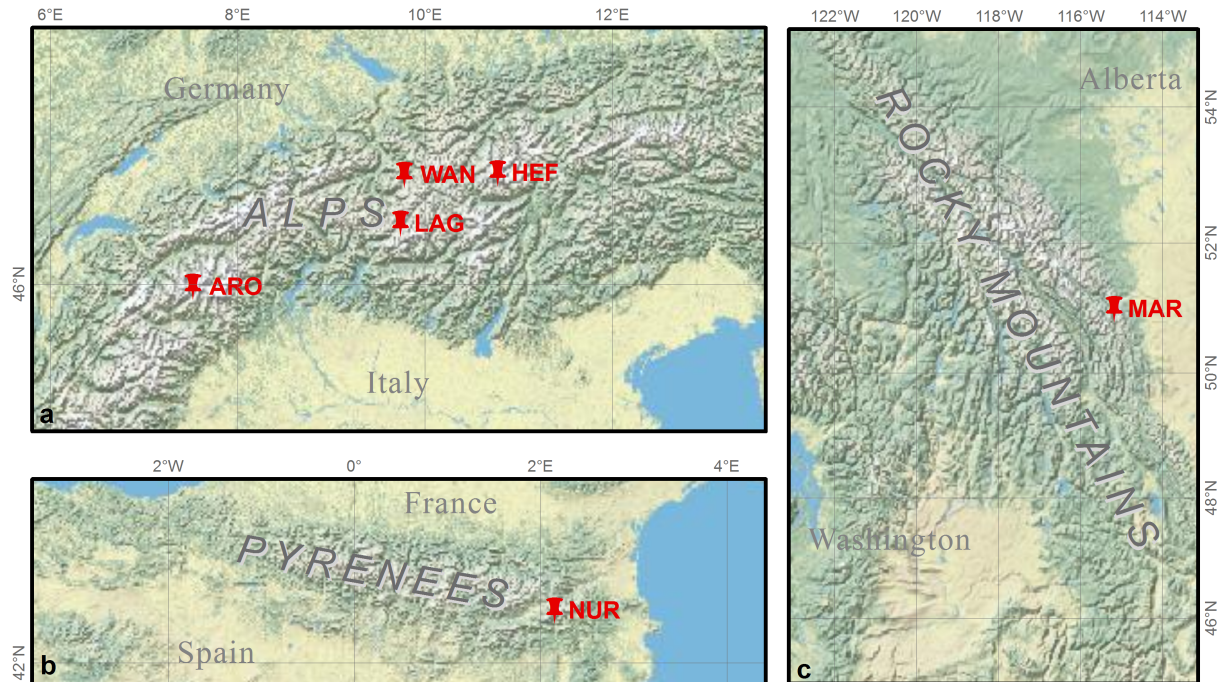
Figure 2.1: Overview maps on the locations of the data-sets Wannengrat (WAN), Piz Lagrev (LAG), Hintereis-ferner (HEF) and Haut Glacier d'Arolla (ARO) in the European Alps **(a)**, Vall de Núria (NUR) in the Spanish Pyrenees **(b)** and Marmot Creek (MAR) in the Canadian Rocky Mountains **(c)**. Basemap: U.S. National Park Service (NPS) Natural Earth physical map, reproduced with permission of Esri.

HEF is dominated by rock faces and large glaciers that covered a little less than half of the 25 km^2 domain in 2002. In this study we are focusing on the snow depth data obtained at HEF in May 2002. According to Helfricht et al. (accepted for publication) the survey concurs with the maximum of the snow accumulation of that year.

The study domain Vall de Núria (NUR) covers an area of 28 km^2 and is located at the main divide of the Spanish Pyrenees. Besides the basin of the Vall de Núria, which is the head water of the Núria river, the domain also includes the outer, northern slopes of the basin (Moreno Baños et al., 2009). A mixture of gentle slopes and steeper, rocky areas are characteristic for the topography of NUR. The winter flight was carried out at 9 March 2009 which is approximately the time of the maximal snow cover in that season (Moreno Baños et al., 2009).

The last study site is the Marmot Creek Research Basin (MAR) in the Kananaskis Valley, situated in the front range of the Canadian Rocky Mountains (DeBeer and Pomeroy, 2010). For our analysis, we selected the alpine areas surrounding Mount Allan which are a mixture of gentle and steep, rocky slopes. The respective snow depth map results from an ALS survey carried out at 29 March 2009 which was several weeks before the maximum of the seasonal snow accumulation. At that point of time, the snow cover had been characterised by low accumulations due to snow scouring by wind (DeBeer and Pomeroy, 2010).

Note that, strictly speaking, only the extents ARO, HEF and LAG are defined by their hydrological discharge area. The remaining study sites also include some slopes outside of the drainage area of the respective streams. However, all study sites are referred to catchments in the following. Moreover we restrict our analysis to the alpine areas of the study domains that are not covered by higher vegetation such as bushes and trees. Areas with significant vegetation have therefore been masked.
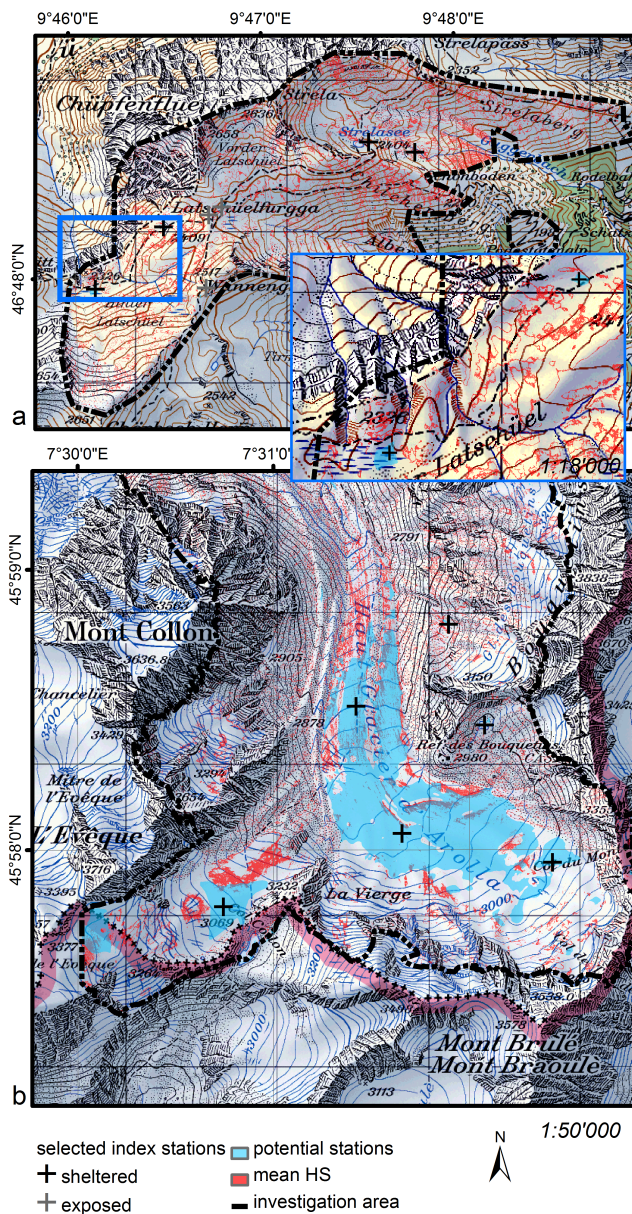
Figure 2.2: Potential index stations (blue), selected stations (crosses) and cells with mean snow depth (red) for Wannengrat **(a)** and Haut Glacier d'Arolla **(b)**. Maps reproduced with permission (Swisstopo, JA100118).

2.2.3 Identification of index stations

A typical location for an index station, as set up for snow cover observations, should be flat, unaffected by the wind and represent the snow conditions in its surrounding. When the Swiss avalanche warning service set up its operational station network (IMIS) in the late 1990s (Egli, 2008; Grünewald and Lehning, 2011; Lehning et al., 1999, 1998), locations were evaluated as appropriate index sites if a 20 m-circle surrounding the station fulfilled the following criteria: (i) the mean slope of the terrain in the circle should be below 10°, (ii) the snow depth should be homogenous and (iii) the snow cover must not show signs of wind redistribution when inspecting the site in winter (H. Gubler, L. Egli, personal communication). Note that the IMIS station network was originally designed to characterise the snow cover characteristics of avalanche release zones and not for applications like hydrological modelling. Nevertheless, the location

12

criteria are very similar to stations defined for hydrological monitoring. In recent years the IMIS data have seen wide application as input for snow cover modelling (Bavay et al., 2013, 2009; Egli et al., 2011; Grünewald and Lehning, 2011; Magnusson et al., 2010).

In order to automatically identify potential index sites in our data sets, we redefined the first two criteria as:

$$SL_{R=20} < 10° \tag{2.1}$$

where $SL_{R=20}$ is the mean slope of all raster cells within a circle with a radius of 20 m.

$$\sigma(HS_{R=20}) > 0.2\,m \tag{2.2}$$

where $\sigma(HS_{R=20})$ is the standard deviation of the snow depths HS within the circle.

From the ALS data we produced snow depth maps and digital surface models of the summer terrain as described by Grünewald et al. (2013). Additionally, a map of the local slope of the summer terrain was derived with a standard ArcGIS operation. We then applied a circular moving window with a radius of 20 m. For each cell, the algorithm calculated the slope and the standard deviation of the snow depth of all cells within the kernel. The combination of the cells that meet both criteria (Eq. 2.1 and Eq. 2.2) are defined as potential sites for index stations. From all cells identified by the algorithm, we then manually selected a limited number of stations for our analysis: In most instances, the approach detected spatial clusters of multiple index cells. From each cluster or if several neighbouring clusters were similar in terms of snow cover and topographic settings, we only selected one single index station. A second criterion was that a sufficient number of neighbouring cells needs to be available for the analysis of the representativeness of the vicinity of the stations. We therefore excluded stations which were close to the edge of the study domains.

Finally we qualitatively evaluated the exposure of the index stations to the wind by visual inspection of the topographic settings (maps and digital elevation models) and, if available, by analysing wind fields of the domains (Dadic et al., 2010a; Mott et al., 2010). Considering information on predominant wind directions that are available from weather stations in the areas, we detected topographically exposed index stations. Such stations were removed from the analysis as significant influence of the wind on the snow cover (erosion) could be expected. This fairly rigorous selection process leaves us with only three to ten index stations per study domain.

2.2.4 Definition of reference areas

The aim of this study is to assess the representativeness of index stations for their surrounding areas from the metre to the catchment scales. Similar as earlier studies (Lopez-Moreno et al., 2011; Meromy et al., 2013; Rice and Bales, 2010) we define a deviation of less than 10 % from the aerial mean as representative. To analyse this representativeness, each point measurement is compared to the mean of all snow depths within its vicinity as defined in the following. The radius of the circle is first set to 20 m, then 50 m and afterwards increased by 50 m steps to 400 m. Moreover the standard deviations of snow depth are calculated for each circle. If the radius is larger than the smallest distance of the index station to the edge of the domain, the representativeness of respective station is not assessed for this scale. Finally, the point values are compared to the mean of the entire catchment.

2.2.5 Identification of cells with mean snow depths

The identification of index sites as described above can be seen as an approach that selects candidate sites on the basis of their topographic characteristics. The inverse procedure would be to detect locations that are representative for the catchment on the basis of their snow depths. In this study snow depths which deviate less than 10 % from the catchment mean are considered as being representative for the complete area. We automatically identified those cells and analysed if their topographic characteristics, namely elevation, slope and Northing (deviation of the aspect from North), deviate from the topography of cells with above- and below-average snow depths. This is performed with box-plots of the distributions of the parameters (Fig. 2.5 – 2.7).

2.3   Results and Discussion

2.3.1   Location of index stations

Examples for potential index sites as defined in this study are shown in Fig. 2.2 for WAN (a) and ARO (b). Blue colours indicate cells which satisfy the criteria for index stations as defined in Eqs. 2.1 and 2.2. For WAN these cells are extremely rare: Table 2.1 indicates that only 0.1 % of the cells came into consideration and for the locations that are suitable as index stations, only single or few neighbouring pixels meet the criteria. The crosses are marking the locations that were then manually selected as index sites. For WAN nearly all suitable locations were selected. Stations used for the further analysis are indicated in black, stations that were removed due to their presumed exposure to the wind are shown in brown.

Table 2.1: Ratio of cells that fulfil the criteria for potential index sites (% of catchment area) and ratio of cells with '"representative" snow depth (deviate from catchment mean ¡ 10 %).

Area	pot. index stations [%]	repr. HS [%]
WAN	0.1	16
LAG	0.2*	25
NUR	0.5	23
MAR	1	20
ARO	11	8
HEF	13	21

*R=5 m

In contrast to the WAN area, at ARO large coherent areas exist, and many index sites would be possible (Table 2.1: 11 % of all cells), especially located at the glacier and in the forefront of the glacier (Fig. 2.2b). This is due to the large, flat surface of the glacier and the relatively homogeneous snow cover in these areas. From these large areas, we only selected few index stations as example sites and supplemented them with potential locations from the rougher, ice-free terrain in the surrounding of the glacier.

Similar patterns can be reported for the remaining study sites (not shown). While many sites, especially at the glaciers, would be possible for HEF, only relatively few and discontinuous locations were selected for NUR and MAR (Table 2.1). No potential index sites where identified for LAG when applying the criteria with a radius of 20 m. The reason is that no flat areas of that size are present at LAG. For this site we therefore reduced the radius to 5 m, which enabled to identify several potential sites of which we selected four for the analysis. It can be concluded that potential index sites are rare (less than 1 %) for all study sites which are not glaciated. On the flat glaciers, numerous sites would be possible (Table 2.1).

2.3.2   Representativeness of index stations

In Fig. 2.3, the mean and the standard deviation of snow depth for the circular areas, surrounding the respective index station, are plotted against its radius. Hence, each single line indicates the representativeness of one index station and the black dashed line represents the overall catchment mean (HS_c).

Mean
At the scale of a single point (Radius=0), all stations clearly overestimate the mean of the catchments for WAN (Fig. 2.3a left panel) and LAG (Fig 2.3b left panel). For WAN the overestimation is between 13 and 53 %, for LAG even 89 to 200 %. The larger the support-area the lower the difference between HS_c and the mean of the respective circular area. At distances of 200 to 300 m, the means of some of the circular areas coincide with HS_c. This trend is valid for all stations at LAG and two stations at WAN. Three of the stations at WAN exhibit a slightly increasing trend for radii between 20 and 100 m which is then followed by a marked decrease. The presence of an increasing trend for the smaller support areas
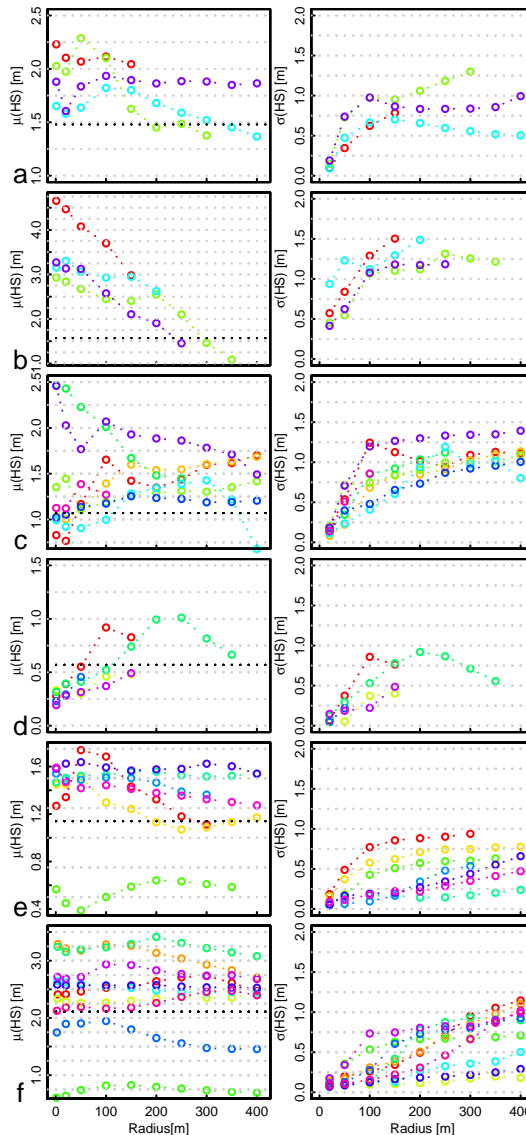
Figure 2.3: Mean and standard deviation of snow depth versus Radius of the support area **(a)** WAN, **(b)** LAG, **(c)** NUR, **(d)** MAR, **(e)** ARO, **(f)** HEF. The dotted black line indicates the catchment mean.

can be explained by the influence of local accumulation zones in the vicinity of the stations, like cornices and drifts (Fig 2.3a: blue, dark blue), or a deposition zone at the foot of a rock face (Fig. 2.3a: green). As long as the support area of the circles is little, extreme values as present in such small-scale features can have a significant influence on the aerial mean. When the circles get larger, the impact of the - then relatively rare extremes - is smoothed out by the larger number of cells with unexceptional values.

Not surprisingly, most of the index stations in the glaciated catchments (Fig. 2.3e, f) are also characterised by a clear overestimation of the catchment mean. For ARO 29 to 39 % more snow than average has been measured at stations located at the glaciers. From the stations that are outside of the glacier, two stations also overestimate HS_c (2.3e: red, yellow). Only the single station that is located in the forefront of the glacier (Fig. 2.2b), measured lower snow depth (half of the catchment mean). At HEF the picture is similar (Fig. 2.3f): Eight of nine stations on the glacier overestimate HS_c (up to 70 %). The station on the glacier tongue (-10 %) and the one in the forefront (-216 %) are underestimating the catchment mean. The reason for the very clear underestimation of the stations in the forefront of the two

glaciers is their situation in the lowest parts of the catchments. These areas are generally characterised by lower snow depth and it can also be expected that the snow cover at these elevations had already been affected by surface melt at the time of the ALS surveys (Dadic et al., 2010b; Grünewald et al., 2013). Unlike for WAN and LAG, no distinctive trends of decreasing underestimation with increasing support area can be determined for ARO and HEF. While the stations located outside of the glacier in ARO indicated a trend (also partly increasing overestimation at low radii), which can again be attributed to local accumulation zones, the stations on the glacier do not show a significant trend. This is attributed to the large areas with relatively homogeneous snow cover in the surrounding of the stations on the glacier and consistent with the large clusters of potential index sites.

Table 2.2: Mean wind speed of weather stations in or near the investigation areas averaged over a one (1 M), three (3 M) and six months (6 M) period before the ALS winter survey.

Area	Station	vw [m/s]			Data source
		1 M	3 M	6 M	
WAN	WAN1	3.8	3.8	4.4	SLF
LAG	LAG1	3.3	3.5	3.3	SLF (IMIS)
NUR	FNUR2	6.8	5.8	-	www.isaw.ch
MAR	Nakiska Alpine	5.8	6.3	7.0	Pomeroy et al. (2011)
ARO	ARO1	1.0	1.9	2.5	SLF (IMIS)
HEF	Vernagt Schwarzkögele	3.9	4.8	5.3	Kommission für Erdvermessung und Glaziologie

In contrast to the investigation areas described above, a clear tendency to overestimate HS_c does not exist for NUR (Fig. 2.3c) and MAR (Fig. 2.3d). While the snow depths at half of the index stations was similar or smaller than HS_c at NUR, all five stations clearly underestimate HS_c at MAR at the point scale. We associate this with higher wind speeds that affected the snow cover of the two areas. Especially the snow cover at MAR had been shaped by strong storms in the period before the ALS survey was performed (Grünewald et al., 2013; MacDonald et al., 2010). A comparison of mean wind speeds, measured at meteorological stations in or near to the investigation areas (Table 2.2) showed clearly higher wind speeds for MAR and NUR and therefore supports this hypothesis. In these wind-swept landscapes, the snow is likely to end up in gullies and other depressions. When analysing mean snow depths of the circular subareas, Fig. 2.3c indicates reverse trends for overestimating and underestimating index stations: All index stations, such with above and such with below average snow depth, show a clear trend towards HS_c which means that the curves decrease for the stations with high snow depths and increase for the stations with low snow depths. Similarly, the underestimation of the stations at MAR decreases with increasing radius (Fig. 2.3d) and even exceeds HS_c for two of the stations.

Fig. 2.4 shows the relationship between snow depth and elevation for the index station and relates it to measured elevation gradient of the respective catchment. Identical to Grünewald and Lehning (2011), the elevation gradient was calculated as the mean snow depth of the respective 100 m elevation band. Fig. 2.4 indicates predominantly positive elevation gradients for the means of the elevation bands. In contrast, no clear increase in snow depth with elevation appears evident for the index stations. Furthermore, snow depth at the majority of stations strongly deviates from the mean snow depth of the respective elevation band. This means that single index stations are not only incapable to represent entire catchments (with potentially large elevation ranges), but also to reproduce snow depth for regions of identical elevation.

It can be summarized that the majority of the index stations tend to overestimate HS_c for most catchments and elevation bands. Principally, the larger snow depths at index sites are not surprising: By definition the locations of these sites are flat and not wind-swept. This favours the accumulation of a deeper snow covers than on slopes that are rather exposed to wind erosion and to removal of snow by gravitational forces. On the contrary, some of index sites - especially those located in windy regions - underestimated HS_c. However, at the point scale, a huge variation is present between the stations of each investigation area. This variation decreases with an increasing radius of the support.
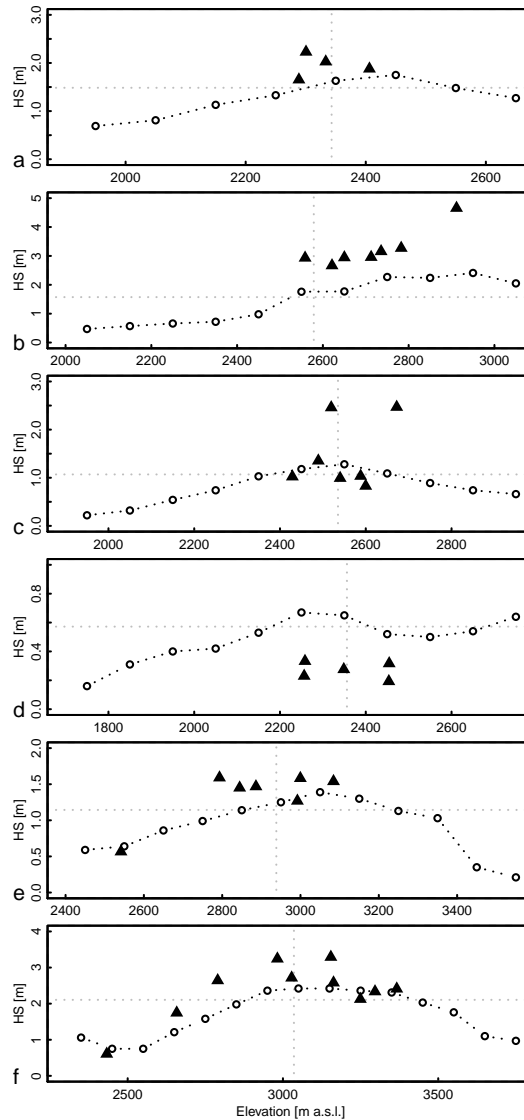
Figure 2.4: Elevation dependency of snow depth for the index stations (triangles) and the mean of 100m elevation bands (black lines) for **(a)**) WAN, **(b)**) LAG, **(c)**) NUR, **(d)**) MAR, **(e)**) ARO, **(f)**) HEF. The grey dotted lines indicate the mean snow depth (vertical) and elevation (horizontal) of the respective catchment.

Standard deviation

The standard deviations of snow depths are shown in the right panels of Fig. 2.3. All plots are characterised by an increase of the standard deviation with larger areas of interest. The increase rate is largest at small distances and flattens at distances of about 100 m. This indicates that the largest variability of snow depths is present at short distances. This is in accordance with the findings of Shook and Gray (1996), Watson et al. (2006) and Schirmer and Lehning (2011) who report the highest variability of snow depth at scales of metres to tens of metres.

2.3.3 What places feature representative snow cover?

As mentioned before, we defined cells where the snow depth deviated less than 10 % from HS_c as having representative snow cover for the catchment. Dependent of the investigation area 8 to 25 % of all cells have been classified as representative (2nd column of Table 2.1). Examples for such cells are indicated
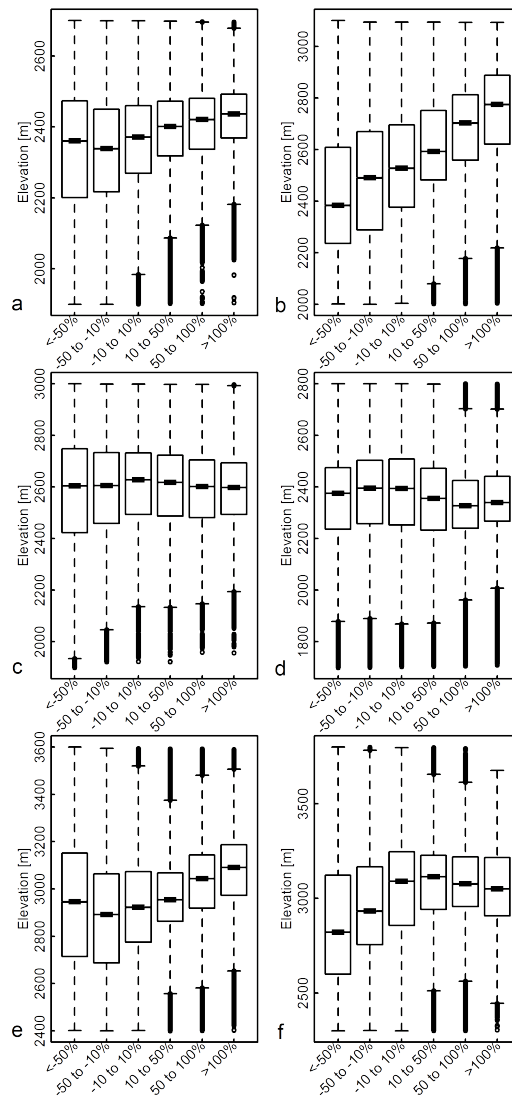
Figure 2.5: Boxplots of classified snow depths (relative deviation from the catchment mean) versus elevation for the investigation areas WAN (**(a)**), LAG (**(b)**), NUR (**(c)**), MAR (**(d)**), ARO (**(e)**) and HEF (**(f)**). The boxes indicate the inter-quantile range of the 1st and 3rd quantile and the black line in the box is the median (with notches). The length of the whiskers is three times the length of the boxes.

by red colours in Fig. 2.2a for WAN and 2.2b for ARO. Fig. 2.2a does not demonstrate clear spatial patterns. Representative snow depths appear to be randomly distributed across the entire catchment. Similar conclusions can be drawn from the maps for LAG, NUR and MAR (not shown). At the glaciated areas (Fig. 2.2b and HEF – not shown) representative cells can also be found in the complete area but larger clusters of representative cells appear on some sections of the glaciers, especially in the lower elevations and on wind exposed areas. This is consistent with the observation discussed above that the majority of cells on the glacier overestimate snow depth of the catchment.

To evaluate this visual impression, we calculated boxplots that compare the classified distributions of snow depth in dependence of the topographic parameters elevation (Fig. 2.5), slope (Fig. 2.6) and Northing (Fig. 2.7). We grouped all cells into six bins according to their snow depth value relative to the catchment mean HS_c. The classes range from -50 % (half of catchment mean) to >100 % (exceeding double of catchment mean). Each of the boxes in Fig. 2.5 to 2.7 represents one of these classes and relates
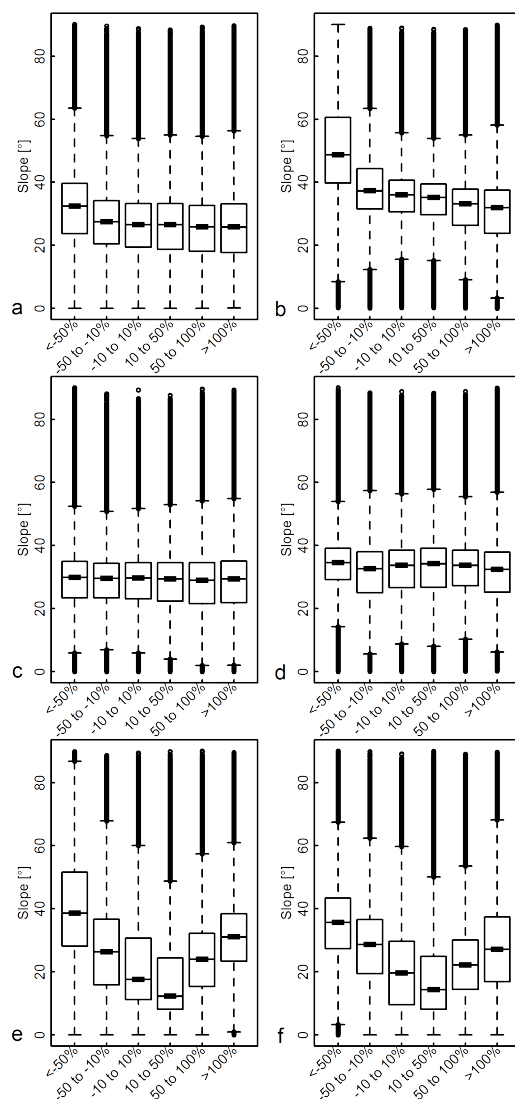
Figure 2.6: Boxplots of classified snow depths (relative deviation from the catchment mean) versus slope for the investigation areas WAN (**(a)**), LAG (**(b)**), NUR (**(c)**), MAR (**(d)**), ARO (**(e)**) and HEF (**(f)**). The boxes indicate the inter-quantile range of the 1st and 3rd quantile and the black line in the box is the median (with notches). The length of the whiskers is three times the length of the boxes.

it to the distribution of its respective topographic parameter. This analysis aims to assess if the location of representative snow depth is related to simple topographic parameters.

Four of the data sets (WAN, LAG, ARO, HEF) are characterised by a slight increase of snow depth with elevation (Fig. 2.5a,b,e,f). Mean snow depths can mainly be found in the middle elevations but appear to be rare in very high and very low altitudes. No trend is evident for MAR and NUR (Fig. 2.5c,d). Neither the slope appears to be connected to the snow depth classes at MAR and NUR (Fig. 2.5c,d). Contrary, negative dependencies of snow depth and slope are evident at LAG (Fig. 2.6b) and WAN (Fig. 2.6a). The trend is most pronounced for LAG. At WAN only a slight decrease of snow depth at steeper slopes is visible. For HEF (Fig. 2.6e) and ARO (Fig. 2.6f) most representative snow depths are found in the flatter sections and both, above and below average snow depths exist in steeper slopes.

For Northing, slight negative trends can be reported for LAG, WAN and MAR (Fig. 2.7a,b,d). This means that cells with high snow depths tend to be in the North sector. No overall trend can be identified
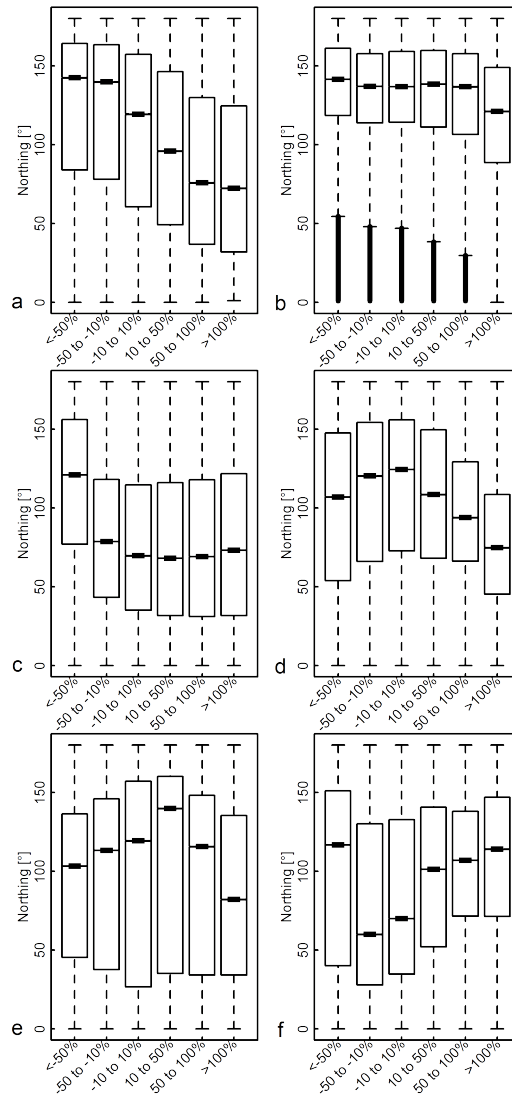
Figure 2.7: Boxplots of classified snow depths (relative deviation from the catchment mean) versus Northing (deviation of aspect from North) for the investigation areas WAN (**(a)**), LAG (**(b)**), NUR (**(c)**), MAR (**(d)**), ARO (**(e)**) and HEF (**(f)**). The boxes indicate the inter-quantile range of the 1st and 3rd quantile and the black line in the box is the median (with notches). The length of the whiskers is three times the length of the boxes.

for NUR, HEF and ARO (Fig. 2.7c,e,f).

When interpreting the plots, one needs to be aware that the classes do neither have equal intervals nor equal numbers of observations. Note that the number of observations is still very large for each class. Moreover, some of the parameters, especially Northing, are not equally distributed for some of the investigation areas (e.g. Southern aspects are nearly missing at ARO). Finally it must be noted that the resulting boxes heavily overlap for all parameters and all investigation areas. Consequently a specific location cannot be assigned to a snow depth class, solely based on its topographic settings. This is consistent with earlier investigations showing a limited predictive power of terrain parameters for snow depth, especially for small scale (pixel) based attempts (Grünewald et al., 2013).

We must therefore conclude that it appears implausible to define typical topographic settings for areas with representative snow depths. This means that it is not feasible to state that a representative snow cover will be found, e.g. in a flat place in the middle of the elevation spectrum of a catchment, at least

not if the judgement is purely based on topographic and snow depth criteria as presented above.

2.4 Summary and conclusions

High-resolution snow depth and terrain maps obtained by ALS in different mountain regions enabled for the first time to compare point observations with aerial mean values of the real snow depth distribution. It was therefore possible to systematically check the often-reported hypothesis of non-representativeness of typical flat-field snow stations. Our data set allowed a quantification of the representativeness for a range of scales i.e. support areas. We have presented two complementary approaches in order to assess the representativeness of point observations of snow depth for their surrounding area.

The first approach, that identifies potential index stations based on topographic characteristics as commonly applied when setting up monitoring stations for snow depth, indicated that most of the potential index stations strongly overestimate the mean of their surrounding area. Nevertheless, we also found some stations with snow depths below the areal mean, especially when they are exposed to wind or at locations that generally experience high winds. It can be stated that the difference between point value and reference area increases with the size of the reference area. Our findings are in general agreement with earlier studies that addressed the representativeness of point measurements of snow. All these studies showed that single point measurements are usually not capable to represent the snow cover of their surroundings (Chang et al., 2005; Meromy et al., 2013; Moreno Baños et al., 2009; Neumann et al., 2006; Rice and Bales, 2010; Watson et al., 2006; Yang and Woo, 1999). As discussed in the Introduction, these studies have had a limited aerial data basis. Our analysis supports these earlier findings with quantitative data and for a range of scales. Contrary to their expectations Winstral and Marks (2014) found that an index site in a wind-sheltered forest opening of a small mountain catchment in Canada provided a good representation of the mean SWE for most of 21 surveys. Winstral and Marks (2014) explain this good relationship as "merely a product of a chance balancing of all aspects of snow accumulation and melt".

The second approach aimed to explore the topographic characteristics of those cells where the snow depths did not deviate much from the catchment mean at the time of the observation. We were not able to identify distinct topographic patterns that could be used for a priori selection of representative points.

We finally conclude that typical index sites appear unable to reliably represent the snow depth of their surrounding at scales ranging from metres to the catchment scale. Neither exist distinct topographic characteristics for representative locations, at least not for the data analysed in this study. The consequence of these findings is that extreme caution is required whenever working with point measurements of snow depth as model input or for interpolation to larger areas. One should be aware that the available input data might inadequately represent the snow cover of the area of investigation. Detailed knowledge of the relationship between point observation and areal snow depth distribution of the specific area would be required to enable a plausible correction of the data. Such information is usually not available. Site independent correction methods are currently not existing and a development based on simple terrain characteristics will be difficult, if not impossible.

In this study we could only analyse snow conditions as present near the peak of the local accumulation season. It would be interesting to investigate the development of the relationships between index station and aerial mean for an entire season or for multiple years. However, such data sets are presently not available but are currently being collected by a number of groups worldwide.

Statistical Modelling of the Snow Depth Distribution on the Catchment Scale

3.1 Introduction

One of the most apparent characteristics of mountain snow cover is its spatial heterogeneity (e.g. Seligman, 1936; McKay and Gray, 1981; Pomeroy and Gray, 1995). This spatial variability is present at a large range of scales, ranging from the sub-metre scale to hundreds of kilometres. The heterogeneity of the mountain snow cover has a significant influence on avalanche formation (Schweizer et al., 2003), local ecology (Litaor et al., 2008) and especially on hydrology (Balk and Elder, 2000; Lundquist and Dettinger, 2005; Bavay et al., 2013). The amount of water stored in the snow cover and its spatial distribution has an important impact on the timing, magnitude and duration of run-off related to the melt of snow (Pomeroy et al., 1998; Lundquist and Dettinger, 2005; Lehning et al., 2006) and ice (Dadic et al., 2008). Many human activities, including agriculture (e.g. irrigation), hydropower or water resources management, depend on information on the spatio-temporal variability of snow cover and melt. In order to capture the temporally varying run-off caused by snowmelt, hydrological models need to account for the spatial distribution of snow.

Recent years have seen advances in modelling snow distributions by applying sophisticated physically based snow cover redistribution models (Pomeroy and Li, 2000; Liston and Elder, 2006; Lehning et al., 2008; Schneiderbauer and Prokop, 2011). Such models have been operated at grid resolutions of a few metres (e.g. Essery et al., 1999; Liston and Elder, 2006; Mott and Lehning, 2010; Mott et al., 2010; Schneiderbauer and Prokop, 2011) to hundreds of meters (e.g. Bernhardt et al., 2009; Bavay et al., 2009, 2013; MacDonald et al., 2010; Magnusson et al., 2010). These models require high level input, including meteorological data, sometimes detailed flow fields (Raderschall et al., 2008) and sometimes high-resolution digital elevation models. They are therefore very expensive in terms of required information and calculation resources, and have not been applied for larger areas or longer time frames. In general, there is a trade-off between model complexity and generality on the one hand and computation time on the other hand although reasonable compromises have been achieved using the hydrological response unit concept (MacDonald et al., 2009; Fang and Pomeroy, 2009) which derives from that of landscape units for stratified snow sampling (e.g. Steppuhn and Dyck, 1974).

Topography strongly influences snow distribution but is not a causative factor in itself (e.g. McKay and Gray, 1981; Pomeroy and Gray, 1995). The spatial heterogeneity of the snow cover is attributed to a number of different processes which act on different scales: local precipitation amounts are strongly affected by the interaction of the terrain with the local weather and climate (Choularton and Perry, 1986; Daly et al., 1994; Beniston et al., 2003; Mott et al., 2014). Wind plays a major role for the deposition and redistribution of snow (e.g. McKay and Gray, 1981; Pomeroy and Gray, 1995; Essery et al., 1999; Trujillo et al., 2007; Lehning et al., 2008). Moreover, snow can be relocated by avalanches and sloughing (Blöschl and Kirnbauer, 1992; Gruber, 2007; Bernhardt and Schulz, 2010), and the local radiation and energy balance influence the spatially varying ablation processes (Cline et al., 1998; Pomeroy et al., 1998, 2004; Pohl et al., 2006; Mott et al., 2011a).

Many studies have attempted to exploit the relationship between topography and snow in statistical models. Topographic parameters serve as explanatory variables for explaining the spatial heterogeneity of snow depth, snow water equivalent (SWE) or melt rates. Several studies have successfully developed

binary regression tree models (e.g. Elder et al., 1998; Balk and Elder, 2000; Erxleben et al., 2002; Winstral et al., 2002; Anderton et al., 2004; Molotch et al., 2005; Lopez-Moreno and Nogues-Bravo, 2006; Litaor et al., 2008), where the response data (e.g. snow depth) are repeatedly split along a predictor (e.g. terrain parameter) into sub-groups by minimising the sum of the residuals. Such regression tree models were capable of explaining 18 to 90 % of the snow-cover variability. The performance of the models depends on both the complexity of the tree (number of explanatory parameters and number of splits), and on the quality and complexity of the data that are analyzed.

A second very common statistical approach is multiple linear regression. As in the regression tree models, terrain parameters serve as explanatory variables. An early example is the multivariate regression model developed by Golding (1974) and applied to Marmot Creek Research Basin, Alberta. Golding (1974) found that elevation, topographic position, aspect, slope, and forest density were the most important variables for predicting snow accumulation but together these could only explain 48 % of the variation of SWE. Based on 106 snow poles Lopez-Moreno and Nogues-Bravo (2006) were able to explain more than 50 % of the large scale snow depth variability over the Pyrenees with elevation, elevation range, radiation and two location parameters. Chang and Li (2000) used monthly SWE data averaged from 13 to 36 snow courses in Idaho to build regression models with a combination of elevation, slope, aspect and a relative position. The models could explain 60 to 90 % of the monthly SWE variability for different regions and large catchments. Marchand and Killingtveit (2005) found that it was possible to model snow depth in open and forested areas of a large ($849\,\mathrm{km}^2$) Norwegian catchment with different measures of elevation, aspect, curvature and slope ($R^2 = 5$–$48\,\%$). For their analysis, they aggregated a very large number of snow depth measurements, obtained by georadar and hand probing to a grid of $1000\,\mathrm{m}$. Pomeroy et al. (2002) used a parametric model derived from a physically based snow interception model to explain snow accumulation in the boreal forest of Saskatchewan and Yukon, Canada, as a function of winter plant area index with an R^2 of 79 %; the parametric model had almost identical form to a regression model using canopy cover developed by Ku'zmin (1960) for snow accumulation in Russian boreal forests, suggesting commonality in the relationship of snow accumulation to forest structure in circumpolar boreal forests.

Beside such applications for very large areas, several studies have applied linear regression for smaller catchments: for each of 19 topographic sub-units, Jost et al. (2007) averaged 60 manual snow depth and 12 density measurements of a $17\,\mathrm{km}^2$ catchment in Canada. A linear regression model with elevation, aspect and forest cover could explain up to 89 % of the large scale variability in SWE. In order to apply universal kriging of SWE for a $8\,\mathrm{km}^2$ glacier in Austria, Plattner et al. (2006) built a linear regression model with elevation, curvature, distance from ridge and a shelter index ($R^2 = 41\,\%$). The SWE measurements were obtained from the average of three snow depth measurements at 165 sample sites and snow densities from five snow pits. Elevation, potential radiation and forest cover were good for representing 66 % of the spatial variability of SWE, obtained from 33 snow cores in a small Swiss catchment (Hosang and Dettwiler, 1991). In order to optimise a snow depth sampling scheme, Elder et al. (1991) applied regression models with elevation, slope and radiation, which explained 27 to 40 % of the SWE variability of a three year data set for the Emerald Lake basin (California). SWE was calculated from density measurements and 86 to 354 manual snow depths taken by manual probing.

Nonetheless, in evaluating such results the sample density, data quality, and scale of the investigation must be considered. All the studies listed up to now in this paper were limited by the small amount and spatial coverage of snow depth observations available for the analysis. Most are based on manual snow depth measurements and only tens to a few hundreds of samples could be used for the regression modelling.

In the recent years, high-resolution and high-quality snow depth data from terrestrial (e.g. Prokop et al., 2008; Grünewald et al., 2010) and airborne laser scanning (ALS) (Hopkinson et al., 2004; Deems et al., 2006; Grünewald and Lehning, 2011) have become available. Grünewald et al. (2010) used snow depth data obtained by terrestrial laser scanning and built linear regression models (elevation, slope, aspect, radiation/elevation, slope, maximum SWE, wind speed) which could explain 30 and 40 % of the spatial variability of daily ablation rates in the Wannangrat area (Davos, CH). In a recent study, Lehning et al. (2011) analyzed airborne Lidar measurements for two small catchments in Switzerland, and showed that a two-parameter model with elevation and a fractal roughness parameter can explain more than 70 % of the snow depth distribution when clustering data to sub-areas. Even though restricted to two small catchments, Lehning et al. (2011) speculate that it might be possible to transfer their findings to other

Table 3.1: Data sets. "Date" is the date of the winter survey, "Area" the area of the data set, "Mean acc." the mean accuracy in vertical direction as quoted in the reference column and "Platform" the measurement plaform.

Name	Date	Area [km^2]	Mean acc. [m]	Platform	Reference
Wannengrat (WAN)	26 Apr 2008	4	0.1	Riegl LMS Q240i-60	Grünewald et al. (2010); Lehning et al. (2011); Grünewald and Lehning (2011)
	9 Apr 2009	1.5			
Piz Lagrev (LAG)	7 Apr 2009	3	0.1	Riegl LMS Q240i-60	Grünewald and Lehning (2011); Lehning et al. (2011)
Haut Glacier d'Arolla (ARO)	1 May 2007	10	0.15	Riegl LMS Q240i-60	Dadic et al. (2010b,a)
Hintereisferner (HEF)	7 May 2002	25	0.3	Optech ALTM1225	Geist and Stötter (2008); Bollmann et al. (2011)
	15 Jun 2002			Optech ALTM1225	
	4 May 2003			Optech ALTM2050	
	7 May 2009			Optech ALTM3100	
Val de Nuria (NUR)	9 Mar 2009	28	0.3	Optech ALTM3025	Moreno Baños et al. (2009)
Marmot Creek (MAR)	29 Mar 2008	9	0.2	Optech ALTM3100C	DeBeer and Pomeroy (2010); Hopkinson et al. (2011)
Skogan Peak (SKO)		8			

mountain areas, and that a universal relationship of snow depth and accessible topography parameters might exist.

In this paper we would like to test this hypothesis using a much larger data set. We assembled high-resolution snow depth data from different mountain regions. For the first time, such high-resolution snow depth data from different areas are combined and compared in a statistical analysis. This permits testing the hypothesis of whether the same or similar topographic parameters dominate the snow depth distribution on the catchment scale (100 to 10 000 m) in different areas. In Sect. 3.2, we describe the climatological and morphological characteristics of each data set and present the methods of data aggregation and linear regression in detail. In the Results section, the models developed for each region are compared with each other and results from model combinations are discussed.

3.2 Data and methods

3.2.1 Airborne laser scanning

Several studies have successfully applied snow depth data obtained by ALS in the recent years (e.g. Deems et al., 2006, 2008; Trujillo et al., 2007, 2009; Grünewald et al., 2010; Grünewald and Lehning, 2011). ALS enables area-wide data to be gathered in a very high spatial resolution and accuracy. Hopkinson et al. (2004) and Deems et al. (2006) showed that ALS was an appropriate and accurate method for gathering snow depth measurements, and since then, a rising number of data sets have become available (Deems et al., 2006; Moreno Baños et al., 2009; Dadic et al., 2010b; DeBeer and Pomeroy, 2010; Grünewald and Lehning, 2011; Schöber et al., 2011; Hopkinson et al., 2012). Detailed descriptions of the ALS measurement principle can be found in Geist et al. (2009), Baltsavias (1999) and Wehr and Lohr (1999).

From the point clouds obtained by ALS, we calculated digital surface models by averaging the points to a regular grid of 1 m cell size. Snow depth maps were then produced by subtracting a digital surface model, obtained by the same technology, in snow-free conditions from a digital surface model that was measured in the winter. Unrealistic data such as negative snow depths or extremely high values are rare but still need to be filtered. Such outliers mainly occur in very steep and rough terrain, which is attributed to larger measurement errors in such terrain (Grünewald et al., 2010; Grünewald and Lehning, 2011; Bollmann et al., 2011; Hopkinson et al., 2012). In this study, we set negative snow depths to zero and excluded extremely high snow depths from the data. The threshold for extremely high snow depth was set by visual inspection of the distribution separately for each data set, and was between 5 and 15 m. As ALS cannot measure snow depth on forested mountain slopes with reasonable accuracy and snow redistribution by interception and accumulation in forests were outside of the scope of this study, areas with forests and high bushes were masked. Most data sets currently available were measured near the peak of the local snow accumulation and represent the maximum of the seasonal snow amounts.

The accuracy of ALS-data depends mostly on the measurement platform. Most data sets mentioned above were gathered from airplanes, which are very effective in terms of the area that can be surveyed. The larger the flight height of the plane, which is typically several hundreds of metres above the surface, and the lower the impact angles of the laser beam in steep terrain, the lower is the accuracy. Nevertheless, the vertical error is usually below 30 cm for snow depth in alpine areas (Geist and Stötter, 2008; Moreno Baños et al., 2009; DeBeer and Pomeroy, 2010) but can be much larger in steep and rough areas. Alternatively, ALS campaigns can be performed with helicopter-based systems (Vallet and Skaloud, 2005; Skaloud et al., 2006; Vallet, 2011). The reduced terrain following flying height and the potential of the system to be tilted in the direction of the target (improved incident angle) results in a higher accuracy. Comparing helicopter-based snow depth maps with terrestrial laser scanning and tachymeter surveys, Grünewald et al. (2010) found that the error of the ALS data was below 10 cm. The typical area covered by ALS data sets obtained for this study is between 1 and 30 km^2 and they all have a spatial resolution close to one metre. Accuracy estimations and references to the data analyzed in this study are given in Table 3.1.

3.2.2 Site description

We assembled a large data set consisting of seven investigation areas located in six different regions, including the Swiss and the Austrian Alps, the Spanish Pyrenees, and the Canadian Rocky Mountains. Two catchments are dominated by glaciers whereas the remaining areas are free of ice. The borders of the investigation areas analysed in this study have been defined manually. This study focuses on the snow depth distribution of alpine areas. Therefore, effects of vegetation, such as interception of snow by trees, were not considered and all parts of the investigation areas which are covered by significant vegetation were masked from the data. Furthermore, it has been shown that ALS snow depth measurements are more accurate over alpine areas than adjacent forest covered areas (Hopkinson et al., 2012). In the following, we give a brief overview of the study sites. For more details, the reader may refer to Table 3.1, Figs. 3.1 to 3.3 and to the references given in the text.

3.2.2.1 Wannengrat, CH

The Wannengrat (WAN) area (Fig. 3.1a) is a small alpine catchment that is located in the eastern part of the Swiss Alps. The site has been an intensive investigation area for snow studies in recent years (Grünewald et al., 2010; Grünewald and Lehning, 2011; Mott et al., 2010, 2011a, 2014; Schirmer et al., 2011; Schirmer and Lehning, 2011; Wirz et al., 2011; Egli et al., 2012). Most of the area is above the local tree line and no tall vegetation is present. Elevations range from 1940 to 2650 m a.s.l. and the lower part is typically characterised by gentle slopes whereas the summit region is formed by talus and steep rock faces. Storms which dominate the snow accumulation in the area usually come from the north-west (Mott et al., 2010; Schirmer et al., 2011). Two helicopter-based (Vallet and Skaloud, 2005; Skaloud et al., 2006; Vallet, 2011) winter ALS data sets were obtained in the area on 26 April 2008 and 9 April 2009, which represent the maximum snow accumulation in the area for the two years. The area of the second flight covers 5 km^2, whereas the first flight only covers a small part of the domain (1.5 km^2, see Grünewald et al., 2010; Grünewald and Lehning, 2011).

3.2.2.2 Piz Lagrev, CH

The Piz Lagrev (LAG) study area (Fig. 3.1b) includes the south face of the Piz Lagrev, which is part of the mountain range defining the northern rim of the Engadin valley in the south-east of the Swiss Alps. The site is above the local tree line, and elevations range from 1800 to 3080 m. The Piz Lagrev is characterised by steep talus slopes which are surrounded by steep rock faces. Two pronounced, sheltered bowls dominate the upper part of the area (Grünewald and Lehning, 2011). ALS measurements were obtained on 7 April 2009 using the same technology as for the Wannengrat, and cover an area of about 5 km^2. Analysis of a nearby weather station indicates that the prevailing wind direction is south-west.

3.2.2.3 Haut Glacier d'Arolla, CH

The study domain Haut Glacier d'Arolla (ARO) is located on the main Alpine divide in the south-west of Switzerland (Fig. 3.2a). Elevations range from 2400 to 3500 m a.s.l. and the area of the domain is about
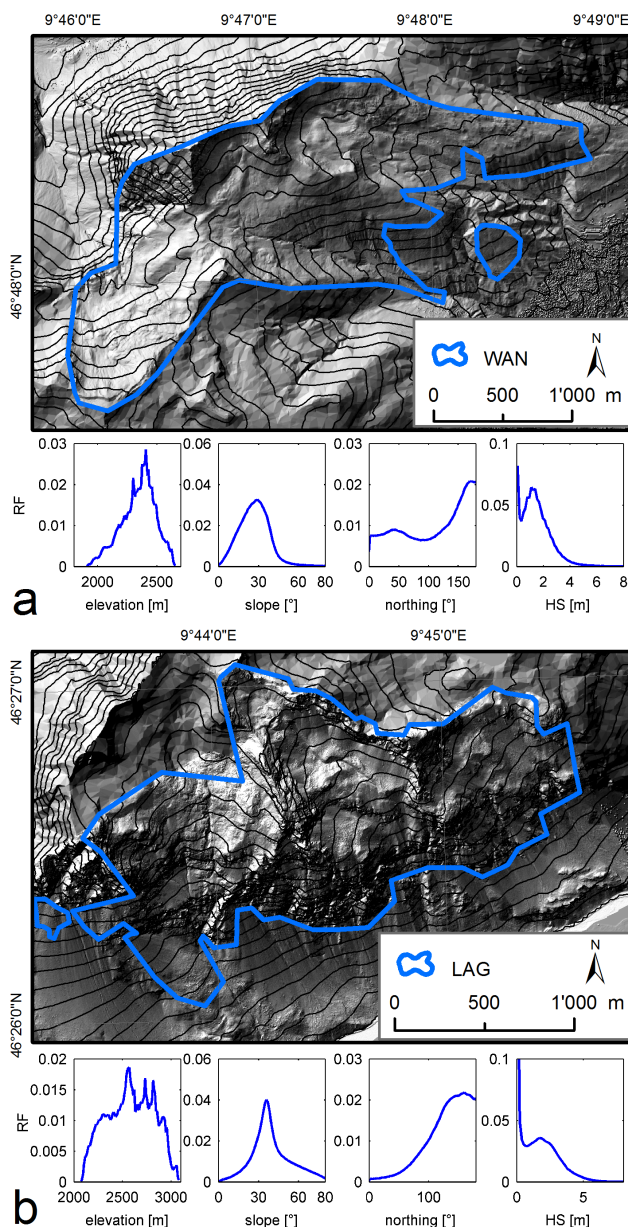
Figure 3.1: Hillshade map of **(a)** the Wannengrat (WAN) and **(b)** the Piz Lagrev (LAG) study areas. The contour lines have an equidistance of 50 m. The right panels show histograms for elevation, slope, northing and the area-wide absolute snow depth obtained from ALS. Data source basemap: **(a, b)** DOM-AV[©]2012 swisstopo (5704 000 000).

10 km^2. The region is dominated by the 4.4 km^2 Haut Glacier d'Arolla and by several smaller cirque glaciers. About 50 % of the area is glaciated and the rest of the domain is characterised by steep slopes and rock faces. Helicopter-based Lidar measurements of the area were obtained in November 2006 and May 2007 (Dadic et al., 2010b,a). The resulting snow depth map represents the time of the maximum snow accumulation for at least the high regions of the catchment. According to Dadic et al. (2010b), at that point of time, elevations below 2700 m a.s.l. had already been affected by surface melt. Note that changes of the surface of the DEM due to glacier dynamics and the settling of firn in the accumulation area were not accounted for when calculating the snow depths. This resulted in a potential underestimation of the true snow depth in the accumulation area of the glacier, and in an overestimation in the ablation
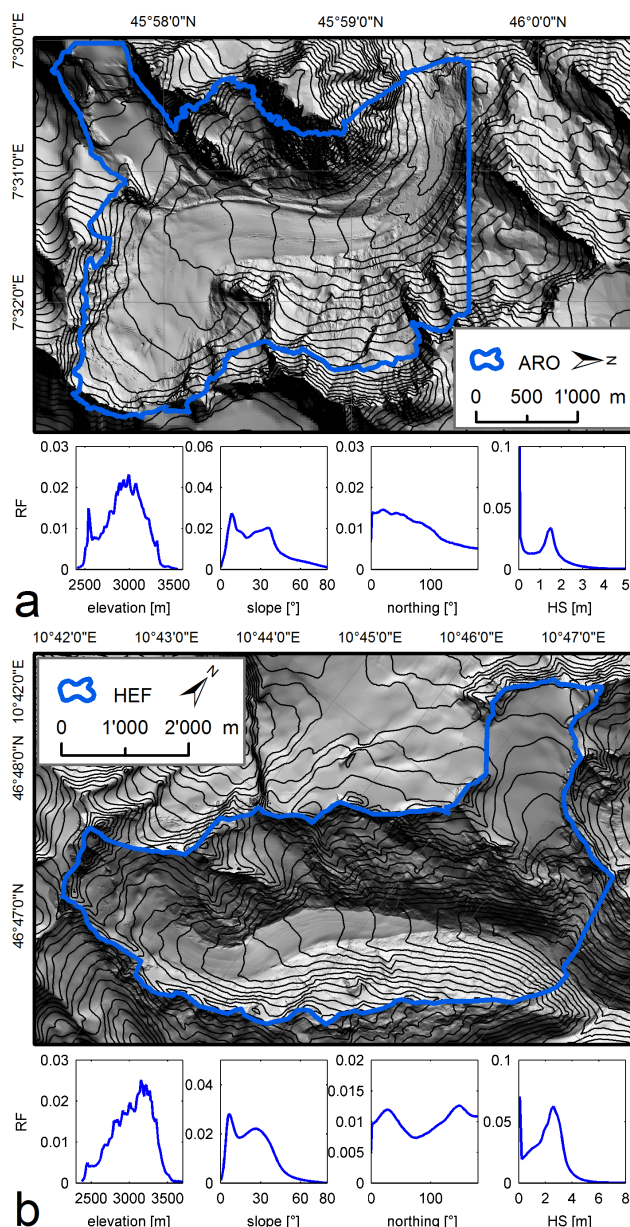
Figure 3.2: Hillshade map of **(a)** Haut Glacier d'Arolla (ARO) and **(b)** the Hintereisferner (HEF) study areas. The contour lines have an equidistance of 50 m. The right panels show histograms for elevation, slope, northing and the area-wide absolute snow depth obtained from ALS (for HEF: Mai 2002). Data source basemap: **(a)** DOM-AV[©]2012 swisstopo (5704 000 000); **(b)** Land Tirol – http://data.tirol.gv.at.

zone, whereas the overestimation in the ablation zone may be countered by the previously mentioned surface melt. An analysis of weather stations in the surrounding area showed that wind directions are variable, but that the synoptic main flow is from the southwest. This is also confirmed by temporary measurements in the catchment (Dadic et al., 2010b,a).

3.2.2.4 Hintereisferner, AT

The investigation area Hintereisferner (HEF) is situated in the upper Rofen valley, which is part of the Ötztal Alps at the Austrian–Italian border (Fig. 3.2b). The catchment, as defined for this study, covers

an area of $25\,km^2$ and is characterised by glaciers, steep slopes and rock faces. Elevations range from 2300 to 3740 m a.s.l. and the largest glaciers are the valley glacier Hintereisferner (2002: $\sim 6.5\,km^2$) and the Kesselwandferner (2002: $\sim 3.8\,km^2$). On the local scale, wind directions are very variable, but the main direction is northwest. In this study, we analyze data obtained in three measurement campaigns in the beginning of May 2002, 2003 and 2009, and one data set acquired in June 2002 (Geist and Stötter, 2008, Table 3.1). The first three flights were near the end of the seasonal snow accumulation in the area, whereas snowmelt clearly had an effect on the lower parts of the catchment in June 2002. To calculate snow depth, each of the winter DSMs was subtracted from a summer DEM obtained in the previous autumn of the respective year. As for ARO, glacier dynamics were neglected in the calculations. More details on the investigation area and the ALS campaigns can be found in Geist and Stötter (2008) and Bollmann et al. (2011).

3.2.2.5   Vall de Núria, ES

Vall de Núria (NUR) (Fig. 3.3a) is located at the main divide in the Eastern part of the Spanish Pyrenees. An ALS campaign covering an area of $38\,km^2$ was performed on 9 March 2009, which is near the time of the peak of the seasonal accumulation for the area (Moreno Baños et al., 2009). After masking significant vegetation and human infrastructure $28\,km^2$ of the area remained. Elevations range from 2000 to 2900 m a.s.l. and the mean slope is $28°$. The area is characterised by a mixture of gentle slopes and some steeper, rocky areas in the summit region. The most frequent synoptic wind direction in the area is from the northwest, even though a large variability of the wind direction is present on the local scale.

3.2.2.6   Marmot Creek, CA

Marmot Creek Research Basin in the Kananaskis Valley, Alberta is located within the Front Range of the Canadian Rocky Mountains. For our analysis we selected two small domains (Fig. 3.3b). The investigation area named Marmot Creek (MAR) in this study is the alpine zone surrounding Mount Allan and includes the Marmot Creek basin in the East. The $9\,km^2$ area is above the local tree line (about 2200 m) and covers elevations from 1760 to 2765 m a.s.l. MAR is characterised by a mixture of gentle and steep slopes (average slope $31°$), covered by alpine tundra with some small bands of rock on the steepest slopes. The second study area is the summit region of Skogan Peak (SKO), which is 4 km to the east from Marmot Creek, above Skogan Pass and near Mount Lorette. The size of the domain is $8\,km^2$ and the elevation range is 1660 to 2660 m a.s.l. SKO is characterised by very rough topography with steep slopes and rock faces (average slope $40°$). Only small areas have gentle terrain. Airborne Lidar surveys of the snow cover were obtained at 29 March 2008. The time of the flight did not coincide with the maximum of the seasonal snow accumulation in the area, which was reached in mid-May (DeBeer and Pomeroy, 2010; Hopkinson et al., 2012). The snow cover in the complete area is strongly affected by winds, which mainly come from the northwest to Fisera Ridge in MAR but generally come from the southwest (MacDonald et al., 2010). Further information on the area and the climatic conditions can be found in DeBeer and Pomeroy (2010), MacDonald et al. (2010), Marsh et al. (2012) and Pomeroy et al. (2012).

3.2.3   Aggregation of sub-areas

The aim of this study is to explain the spatial variability of snow depth on the catchment scale. With high-resolution snow depth measurements at hand, a statistical assessment considering snow depth and topography at the highest possible resolution is not meaningful. The difficulty becomes obvious if one thinks about cornices or other drift features. Maximum snow depth in a cornice is not the result of topographic features (e.g. slope) directly at this point but is shaped by the upwind topography interacting with the wind. Therefore, a systematic correlation between snow depth and terrain parameters will not be found at very small scales. Regression models of snow depth of the different investigation areas (not shown) confirmed that and showed that at the highest resolution (metre scale without aggregation), only 2 to 37 % of the variability could be explained by the terrain. Because of the large spatial variability at scales of metres (Shook and Gray, 1996; Watson et al., 2006), we define subareas in order to smooth
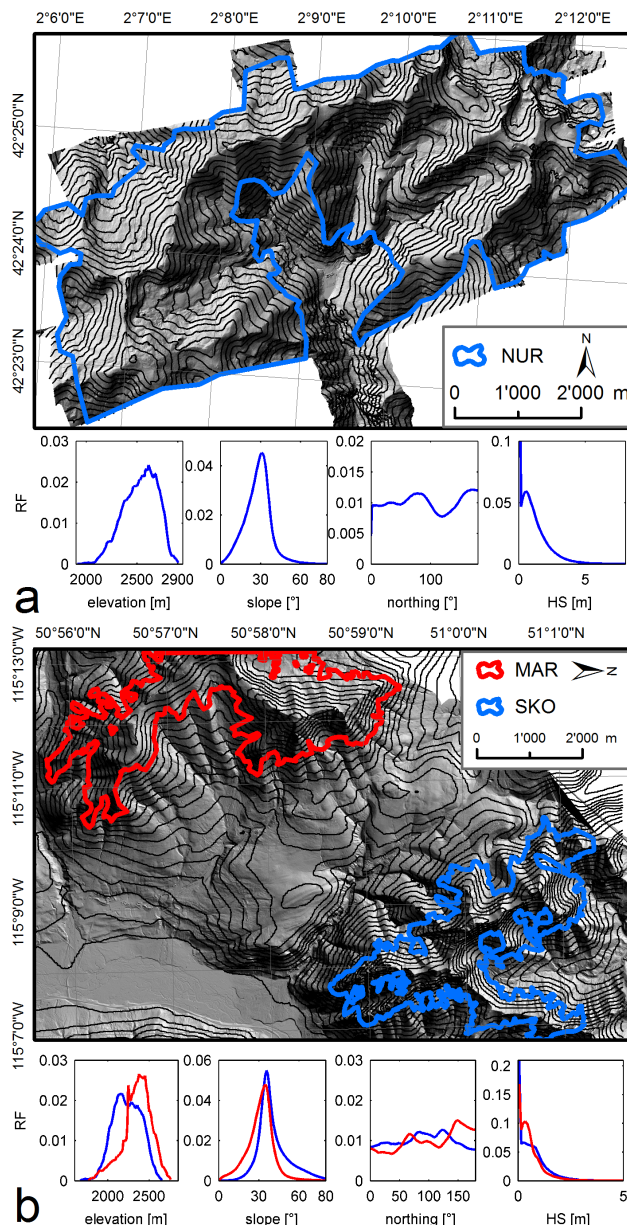
Figure 3.3: Hillshade map of **(a)** the Val de Núria (NUR) and **(b)** Marmot Creek Research Basin area with the study areas Marmot Creek (MAR) and Skogan Peak (SKO). The contour lines have an equidistance of 50 m. The panels below show histograms for elevation, slope, northing and the area-wide absolute snow depth obtained from ALS.

this small-scale variability. We aggregated the data to spatially continuous subareas with length scales of some hundreds of metres.

Two different methods for the aggregation are applied. The first is the same as performed by Lehning et al. (2011), who manually defined sub-areas from a subjective impression of the terrain (Fig. 3.4). The length scale of these subareas was approximately 500 m. Such an aggregation follows the concept of hydrological response units (HRU), which has successfully been applied for semi-distributed hydrological models (Kite and Kouwen, 1992; Rinaldo et al., 2006; Pomeroy et al., 2007) and is consistent with the concept of stratified snow sampling (Steppuhn and Dyck, 1974) where landscape units were defined to minimise within-unit variance of SWE and maximise difference in SWE between units. The facets applied
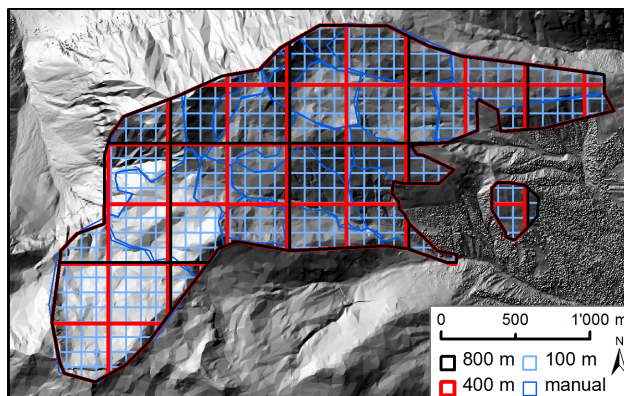
Figure 3.4: Aggregation of sub-aras for the Wannengrat area by the manual and the automatic method (grids of different cell size).

by Daly et al. (1994) for the calculation of precipitation gradients or to the concept of snow accumulation units outlined by Hopkinson et al. (2012) are also similar approaches. The second method is a simple automatic approach which divides the domain into quadratic subareas. This approach is very similar to a simple resample of the data to larger cell sizes. We have tested different grid sizes ranging from 100 to 800 m. An example which illustrates the aggregation is shown in Fig. 3.4. The criteria which were applied to select the cell size appropriate for the study are: (i) the small scale variability should be smoothed out to an extent that the remaining variability can be reasonably explained by the topographic parameters, and (ii) the number of sub-areas must be large enough to be able to fit robust regression models ($N \gtrsim 30$). In order to avoid small clusters which do not represent a significant footprint of the catchment, very small sub-areas ($< 10\,000\,\mathrm{m}^2$) were automatically excluded from the aggregated data. The approach is similar to the concept of representative elementary area (Wood et al., 1988; Blöschl et al., 1995), which aims to identify ideal scales for hydrological modelling applications.

As the second method is a straightforward and fully automated approach, it is possible to compose multiple statistical models by randomly shifting the origin of the grid. This approach helps to identify the range of model performance and if a selected grid results in a representative model. The impact of random effects, which might be caused by a single grid or by subjective classification of the sub-areas, can therefore be assessed.

3.2.4   Statistical models

We use multiple linear regression to model the spatial variability of snow depth. The dependent variable is the relative snow depth dHS (deviation from the catchment mean). Simple parameters that describe the surface topography and that can be derived from a summer digital elevation model serve as explanatory variables. Elevation reflects the effect of decreasing air temperatures with altitude and can therefore be used as a proxy for parameters such as freezing level or the amount of energy available for melt (Clark et al., 2011), and for orographic effects of precipitation (Frei and Schär, 1998; Grünewald and Lehning, 2011) though it is recognized that there are substantial differences in orographic effects between windward and leeward slopes (Pomeroy and Brun, 2001). In order to be able to combine data sets from different areas, elevation was changed to relative elevation (dE), which is the difference between the absolute and the minimum elevation of the area. This mapping respects the fact that all data sets are from the alpine zone at or above tree line but that this corresponds to different absolute elevation in the different areas. The slope (SL) represents gravitational processes such as sloughing and avalanching, which can have a significant effect on the snow distribution (Blöschl and Kirnbauer, 1992; Gruber, 2007; Sovilla et al., 2010; Bernhardt and Schulz, 2010). In combination with northing (NO), the slope also describes the amount of solar energy which is available for the ablation and settling of snow. NO is also important for the deposition and redistribution of snow by wind (Seyfried and Wilcox, 1995; Lehning et al., 2008), as more snow is usually accumulated in the leeward sides of slopes and mountains. An additional parameter,

which represents the effect of the wind, is the mean sheltering index SX (Winstral et al., 2002), which has been calculated for the direction of the main flow (see site descriptions) and for a maximum distance of 100 m. Several studies showed that SX is a good measure for sheltering and exposure of the local terrain, which gives a simple but reasonable representation of the local flow field and therefore of the redistribution of snow by wind (e.g. Winstral and Marks, 2002; Winstral et al., 2002; Anderton et al., 2004; Erickson et al., 2005; Molotch et al., 2005; Litaor et al., 2008; Schirmer et al., 2011). Finally, different measures for the surface roughness are applied. The standard deviation of the elevation ($\sigma(E)$) and slope ($\sigma(\mathrm{SL})$) represent classical morphometric roughness measures (Evans, 1972; Speight, 1974; Shepard et al., 2001). The surface roughness strongly affects the redistribution of snow by wind and gravitational processes (Jost et al., 2007), and can be seen as the capability of the surface to trap snow. As suggested by Lehning et al. (2011), we also tested the fractal dimension D and the ordinal intercept γ of the semi-variogram, which have been identified as good measures for the surface roughness (Goodchild and Mark, 1987; Power and Tullis, 1991; Klinkenberg, 1992; Klinkenberg and Goodchild, 1992; Xu et al., 1993; Sun et al., 2006; Taud and Parrot, 2006).

For each of the aggregated data sets, we separately calculated all possible two- and three-parameter regression models and selected the most significant models (p value < 0.001). Further selection criteria are the explanatory power (R^2) of the model and – if the R^2 was similar – the number of parameters included in the model. For data sets with a two-parameter model, which had a similar performance as the best three-parameter-model, the two-parameter-model was selected. To account for possible interactions of the parameters included in the models, factor combinations (multiplication of parameters) have been tested and included where appropriate. The preconditions of linear regression (normal distribution and constant variance of residuals) were examined by analyzing the Quantil–Quantil plots and the Tukey–Anscombe plots of the model residuals (not shown). Additionally, the physical meaningfulness of the models (e.g. sign of the coefficients) has been examined, and models have not been selected if the sign of the coefficient was counter-intuitive. As mentioned before, the automatic aggregation to quadratic sub-areas allows the calculation of multiple random grids. This in turn can be used to analyse whether the best models are consistent (same explanatory variables) and show a small standard deviation of the coefficients when calculated for different grid realizations. Note that the fractal parameters D and γ could not be included in the multiple model runs, as their computation is computationally very demanding. D and γ were therefore only applied for the models with manually defined sub-areas and for few selected quadratic models.

To assess the transferability of the results, we also built a "global" model by combining all data sets. In addition, sub-sets of the data were combined based on their morphological characteristics. The two morphological models discussed here are "Glacier", which includes the two sites which are currently glaciated, and "No glacier", which combines all remaining, non-glaciated data sets from alpine terrain.

The multiple-year data sets for HEF and WAN allow a validation in order to investigate the inter-annual consistency of the models. For HEF, models calculated from data sets containing three of the snow depth surveys in the area are validated with the remaining years. We repeated this procedure for each combination. Scatter plots and the coefficients of determination (R^2_{det}) are used to assess the performance of the validation. As the extent of the 2008 data set for WAN is very small it could not be used to compose an own regression model. Nonetheless it could be used to validate the model obtained from the 2009 data set.

3.3 Results and Discussion

3.3.1 Aggregation of sub-areas

In order to find the appropriate level of aggregation for the automatic approach, we calculated models for different grid sizes and compared the results in terms of model performance. Figure 3.5 illustrates such a result for the Wannengrat area. The explanatory parameters of the model are dE, SL and NO. The figure illustrates a strong decrease in the snow depth variability with increasing grid size (Fig. 3.5a), which is negatively correlated to an increased model performance (Fig. 3.5b). This relationship is not surprising since an increasing portion of the variability is smoothed out by the aggregation. Nevertheless, at cell sizes of about 400 m the effect of additional smoothing appears very limited. Based on the analysis
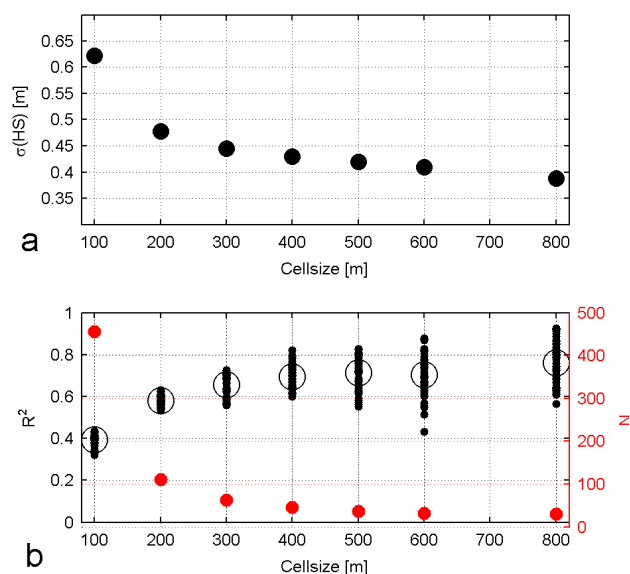
Figure 3.5: Relationship between the level of aggregation (cell size) and snow depth variability expressed by **(a)** the standard deviation σ(HS), and **(b)** model performance (R^2) for the Wannengrat area (model with dE, SL, NO). The black circles indicate the mean of 50 random model runs. The R^2 of each run is induced by a small black dot. The red dots show the average number of sub-areas (N) at each aggregation level.

shown in Fig. 3.5, this level therefore appears to be a good choice. It can explain much of the remaining larger scale spatial variability, while the number of sub-areas still remains large enough to calculate robust statistical models. For the other investigation areas, similar results (not shown) were obtained. Cell sizes between 200 and 500 m showed to perform best. This is consistent with the length scale of > 100 m found by Shook and Gray (1996) for minimal autocorrelation in snow depth data. We therefore decided to apply a grid size of 400 m to all areas. Choosing a 200 m grid instead of the 400 m would result in very similar models but with lower performance: while the model parameters remain the same, the modelled R^2 would be reduced by 0.01 to 0.14 for the different data sets. For example for WAN R^2 would decrease from 73 to 59 % (Fig. 3.5b). Moreover, a 400 m grid is a similar level of aggregation as for the manually defined sub-areas. A comparison of models, calculated with sub-areas identified by the manual and the automatic (400 m) approach, showed that the results are very similar in terms of the best parameters selected for the final models, and in terms of model performance. As it is an objective and fully automatic method, we only show results from the automatic procedure in the following.

3.3.2 Statistical models

The model assumptions for linear regressions (see above) were fulfilled satisfactorily for all data. Nevertheless, small deviations from the normal distribution of residuals for very large positive and negative residuals have to be reported for ARO, HEF and SKO. Logarithmic transformation of the variables has been tested. As this did not yield improvements, the original, non-transformed variables were used.

3.3.2.1 Single catchment models

Table 3.2 summarises the best models for each of the single investigation areas. The table indicates that similar parameter combinations dominate most areas. Such, dE, NO and SL are included in almost all models. SX is included for NUR and for MAR. A roughness index is only present in the model for NUR (σ(SL)) and SKO (γ). Nevertheless substituting γ by, for example, (σ(SL)) would result in a model with a similar performance. For some areas, different parameter combinations than the ones presented have

Table 3.2: Best two- to three-parameter model for each single investigation area, where dHS and dE are in metres and SL and NO in degree. Column 3 to 5 show the R^2, the adjusted R^2 (R^2_{Adj}) and the number of sub-areas for each model. For HEF all data (four points of time) were combined to one single model.

Area	Model							R^2	R^2_{Adj}	N
WAN	dHS =	$0.00153 \cdot \mathrm{d}E$	$-0.0240 \cdot \mathrm{SL}$	$-0.0043 \cdot \mathrm{NO}$			$+0.60$	0.76	0.73	35
LAG	dHS =	$0.00202 \cdot \mathrm{d}E$	$-0.0574 \cdot \mathrm{SL}$				$+1.39$	0.91	0.90	29
NUR	dHS =		$-0.0005 \cdot \mathrm{NO}$	$+0.56 \cdot \mathrm{SX}$	$+0.1715 \cdot \sigma(\mathrm{SL})$	$-0.0012 \cdot \mathrm{NO} \cdot \sigma(\mathrm{SL})$	-0.49	0.50	0.49	222
MAR	dHS =		$-0.0115 \cdot \mathrm{SL}$	$-0.0025 \cdot \mathrm{NO}$	$+0.77 \cdot \mathrm{SX}$	$-0.0049 \cdot \mathrm{NO} \cdot \mathrm{SX}$	$+0.61$	0.30	0.27	66
SKO	dHS =		$-0.0363 \cdot \mathrm{SL}$	$-0.0074 \cdot \mathrm{NO}$	$+0.59 \cdot \gamma$		$+1.84$	0.41	0.38	66
ARO	dHS =	$0.00246 \cdot \mathrm{d}E$	$-0.0009 \cdot \mathrm{SL}$	$-0.0032 \cdot \mathrm{NO}$		$-4.054 \times 10^{-5} \, \mathrm{d}E \cdot \mathrm{SL}$	-0.26	0.53	0.50	82
HEF*	dHS =	$0.00182 \cdot \mathrm{d}E$	$-0.0385 \cdot \mathrm{SL}$	$-0.0024 \cdot \mathrm{NO}$			$+0.05$	0.51	0.50	720

* includes HEF(05-2002), HEF(06-2002), HEF(05-2003), HEF(05-2009)

only a slightly lower performance (not shown). Factor combination significantly improved the model for NUR, MAR and ARO. Adding an additional parameter would further improve the models for some of the areas (NUR, MAR, SKO). In order to keep the models as simple as possible and to avoid an over-parameterization of the small areas, we do not include such additional variables.

As an example, we now focus on the Wannengrat area (first row in Table 3.2). The model represents a positive elevation gradient of the snow depth which is 15 cm per 100 m, a decrease of dHS with the slope angle ($2\,\mathrm{cm}\,(^\circ\,\mathrm{SL})^{-1}$) and a decrease of dHS toward southerly aspects ($4\,\mathrm{cm}\,(10^\circ\,\mathrm{NO})^{-1}$). Figure 3.6 compares a dHS map resulting from the model with measured dHS, aggregated to the model resolution. The upper image shows the snow depth distribution as aggregated from the ALS measurements, while the lower image presents the snow cover as calculated with the model. The figure illustrates that the statistical approach seems suitable to characterise the general spatial patterns of the snow depth distribution. Deviations occur especially in regions of extreme dHS, for example, in single cells in the northwest, the southeast or the southwest. This indicates that the model does not properly capture the extremes of the distribution. Nevertheless, the deviations are only small.

Returning to Table 3.2 and focussing on the different areas, it appears that both the parameters and the model coefficients are varying between the data sets. It is also obvious that the performance of the models (R^2) is quite different. While the model for LAG can explain more than 90 % of the snow depth variability, only 30 % could be explained for MAR and 41 % for SKO. For most areas, the R^2 is between 50 and 70 % which is a very good score in comparison to published results obtained at similar scales. The large range in the model performance might be attributed to the topographic diversity within the single catchments. Smaller, less heterogeneous catchments, such as LAG or WAN perform much better than the very large (HEF, ARO, NUR) or very complex (MAR, SKO) areas. Reasons for the relatively low R^2 for MAR and SKO can be found in the characteristics of the data sets, where the topography in the summit region of the two areas is dominated by extremely steep rock faces (Fig. 3.3b), which are exposed to wind and avalanches. In the period before the snow depth data had been acquired, several heavy storms occurred in the area. The heavy winds eroded and sublimated much of the snow cover in the summit region and, as a result, the major portion of the summit region was nearly free of snow. This is a common characteristic of alpine snow in the relatively windy Canadian Rockies (MacDonald et al., 2010). A further possible reason for the lower performance of some of the models could be the accuracy of some parts of the ALS data. As mentioned before, it must be expected that biases are larger in steep and rough terrain, especially for the data obtained from airplanes. Such terrain-based errors will also influence the models on resolutions as presented here and must be considered when interpreting results from such areas, especially when slope serves as an explanatory variable.

In general, the results confirm that topography dominates the snow depth distribution at that scale. The deviations between the models indicate that the influences on the snow depth distribution are variable in the different areas. For example, the magnitude of the elevation gradient is between 6 and 25 cm/100 m, and the coefficient for slope varies by a factor of four (ARO not included because of factor combinations). For NUR and MAR, the elevation gradient dE seems not to be relevant at all. Instead, the sheltering effect of the terrain (SX) is more important.
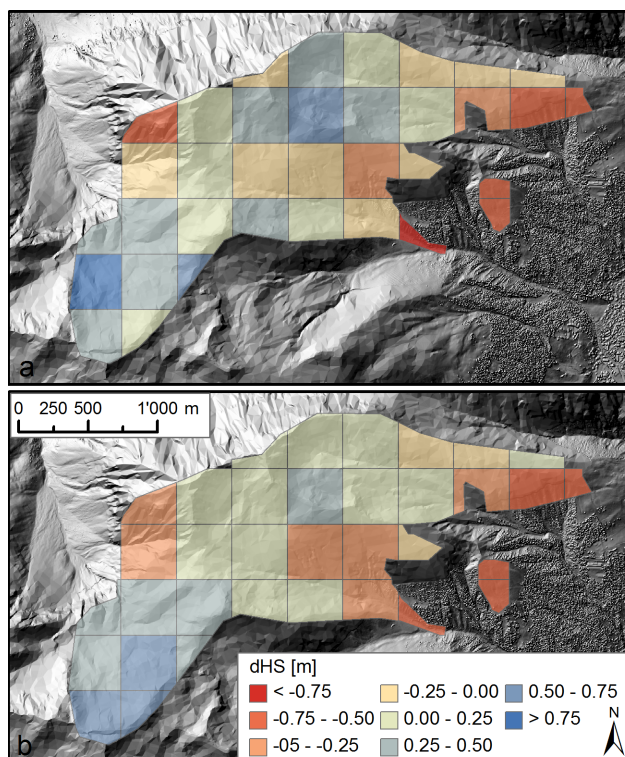
Figure 3.6: Comparison of dHS for the Wannengrat in April 2009, aggregated to **(a)** a 400 m grid form ALS-measurements, and **(b)** modelled with a regression model with dE, SL and NO.

The representativeness of the results obtained from the selected grid (Table 3.2, Fig. 3.4) was assessed by calculating multiple model runs, for which the origins of the grid were shifted randomly. Results are summarised in Table 3.3. Fifty runs were performed for the best model, as identified in Table 3.2 (but without factor combinations), for each investigation area. The table shows the sample space (25 to 75 % quantiles) for all model parameters and for the model performance. The last column indicates the R^2 of the model run that is based on the same grid as the models presented in Table 3.2.

Generally the table indicates relatively small interquantile ranges for most models and parameters. For example for WAN (first line) the difference between the upper and lower quantile and the median of α_i is only 6 to 10 % of the median. Similar ranges are characteristic for most parameters in the other data sets. Only α_1 and α_3 for SKO and α_3 for ARO show larger deviation of the quantiles and the median. For R^2, interquantile ranges between 0.01 and 0.12 (Table 3.3) were calculated. Nevertheless, it is still necessary to note that for a few data sets outliers with much larger or much smaller R^2 values were observed. It is therefore an important finding from these ensemble calculations that the scatter between the single runs is only moderate. Taken as a whole, Table 3.3 shows that most of the models represent the total average well. Moreover, we can conclude that the absolute position of the subareas only has a minor effect on the models. The spatial averaging procedure appears to result in relatively stable statistical relations, at least at the scale of the 400 m grid.

Table 3.3: Comparison of the model performance of the multiple random runs and the single selected model as presented in Table 3.2 (R^2_{sel}). α_i are the factors of the respective model parameters as listed in column 2. The 50 model runs obtained for each data set resulted in a distribution for each of the factors (α_i, β) and R^2. Column 3 to 7 show the 25, 50 and 75 % quantiles of these distributions.

Area	Model	Quantiles α_1			Quantiles α_2			Quantiles α_3			Quantiles β			Quantiles R^2			R^2_{sel}
		0.25	0.5	0.75	0.25	0.5	0.75	0.25	0.5	0.75	0.25	0.5	0.75	0.25	0.5	0.75	
WAN	$\alpha_1 \cdot dE + \alpha_2 \cdot SL + \alpha_3 \cdot NO + \beta$	0.00131	0.00140	0.00151	−0.0046	−0.0042	−0.0039	−0.0260	−0.0240	−0.0224	0.58	0.62	0.68	0.67	0.73	0.77	0.76
LAG	$\alpha_1 \cdot dE + \alpha_2 \cdot SL + \beta$	0.00218	0.00226	0.00232	−0.04764	−0.04579	−0.04317				0.74	0.86	1.02	0.90	0.91	0.92	0.91
NUR	$\alpha_1 \cdot NO + \alpha_2 \cdot SX + \alpha_3 \cdot \sigma(SL) + \beta$	−0.0101	−0.0099	−0.0096	0.52	0.58	0.61	0.0691	0.0726	0.0752	0.21	0.28	0.31	0.47	0.49	0.50	0.46
MAR	$\alpha_1 \cdot SL + \alpha_2 \cdot NO + \alpha_3 \cdot SX + \beta$	−0.0129	−0.0124	−0.0118	−0.0038	−0.0037	−0.0035	0.32	0.38	0.43	0.69	0.71	0.72	0.28	0.30	0.32	0.28
SKO	$\alpha_1 \cdot SL + \alpha_2 \cdot NO + \alpha_3 \cdot \sigma(SL) + \beta$	−0.0114	−0.0074	−0.0052	−0.0061	−0.0059	−0.0057	0.009	0.0165	0.0221	0.68	0.73	0.85	0.31	0.33	0.35	0.37
ARO	$\alpha_1 \cdot dE + \alpha_2 \cdot SL + \alpha_3 \cdot NO + \beta$	0.00119	0.00128	0.00136	−0.01981	−0.01902	−0.01813	−0.0040	−0.0030	−0.0027	0.16	0.23	0.26	0.50	0.56	0.61	0.49
HEF*	$\alpha_1 \cdot dE + \alpha_2 \cdot SL + \beta$	0.00126	0.00127	0.00130	−0.03934	−0.03863	−0.03801				0.14	0.18	0.21	0.41	0.42	0.42	0.43

* includes HEF(05-2002), HEF(06-2002), HEF(05-2003), HEF(05-2009)

Table 3.4: Best models, R^2, R^2_{Adj} and number of subareas (N) for different combinations of the investigation areas.

Area	Model					R^2	R^2_{Adj}	N
All[a]	dHS =	$0.00079 \cdot dE$	$-0.0145 \cdot SL$	$-0.0028 \cdot NO$	$+0.28$	0.23	0.22	682
No Glacier[b]	dHS =	$-0.0133 \cdot SL$	$-0.00528 \cdot NO$	$+0.0454 \cdot \sigma(SL)$	$+0.53$	0.30	0.29	423
Glacier[c]	dHS =	$0.00021 \cdot dE$	$-0.0686 \cdot SL$	$+5.329 \times 10^{-5} \, dE \cdot SL$	$+0.79$	0.48	0.48	802

included data sets: [a] WAN, LAG, NUR, MAR, SKO, ARO, HEF(05-2001); [b] WAN, LAG, NUR, MAR, SKO

[c] ARO, HEF(05-2002), HEF(06-2002), HEF(05-2003), HEF(05-2009)

Table 3.5: Inter-annual consistency for HEF and WAN. The first column lists the data which were used to fit the model (model parameters dE, SL, NO). The second column shows the data set used for the validation. R^2_{Model} is the R^2 of the model, and R^2_{det} the coefficient of determination.

Data in model	Validation data	R^2_{Model}	R^2_{det}
HEF 5/2002, 6/2002, 5/2003	HEF 5/2009	0.51	0.48
HEF 5/2002, 6/2002, 5/2009	HEF 5/2003	0.50	0.53
HEF 5/2002, 5/2003, 5/2009	HEF 6/2002	0.48	0.59
HEF 6/2002, 5/2003, 5/2009	HEF 5/2002	0.54	0.35
WAN 2009	WAN 2008	0.76	0.40

3.3.2.2 Combined models

For practical applications on a large scale, it would be very beneficial if it were possible to find a "global" model, which would be able to predict a large portion of the spatial variability for all data sets. We therefore combined all data to one large data set and built a new model, following the same procedure described above. However, the resulting model (Table 3.4), which selected dE and SL as explanatory variables, was only able to explain 23 % of the total snow depth variability of the aggregated data. Additional model parameters or factor combinations could not significantly improve the model. A model that only includes data from the alpine areas, which are presently not glaciated, is capable of explaining 30 % of the variability. This is clearly worse than the models for most of the single data sets (Table 3.2). It appears that as suggested by Pomeroy and Gray (1995), the interaction between topography and snow depth is not the same at different sites, and that a statistical relationship, developed for one area, cannot directly be transferred to a different site. In contrast, the "glacier" model features a similar performance to the models for the single glaciers (ARO and HEF). This could indicate that similar characteristics are important for the snow cover on glaciated catchments or that the sample size is too small to show substantial variability in glaciated sites. However, since the model consists of the same data as the HEF model presented in Table 3.2, only supplemented by the comparably small ARO data, the ARO data will only have a minor effect on the model and its R^2 value.

Finally, when combining data sets from different sources, one needs to be aware of possible differences in the platforms and sensors applied for the data acquisition. Sensors of different manufacturers can be very diverse in their design, operational envelope and laser pulse specifications which might result in different levels of performance and error propagation. Nevertheless, the influence on statistical relationships should be marginal.

3.3.2.3 Inter-annual consistency

Results of the analysis of the inter-annual consistency, as described in Sect. 3.2.1, are shown in Table 3.5. Figure 3.7 illustrates the scatter plots for the validation, as shown in lines two (a) and five (b) of Table 3.5. The table emphasizes that the R^2_{det} values are around 50 %, which is similar to the R^2 values of the full models. Only WAN and the fourth HEF model have a lower R^2_{det}. Nevertheless, Fig. 3.7b shows that for the WAN data the model is appropriate for both years for most sub-areas.
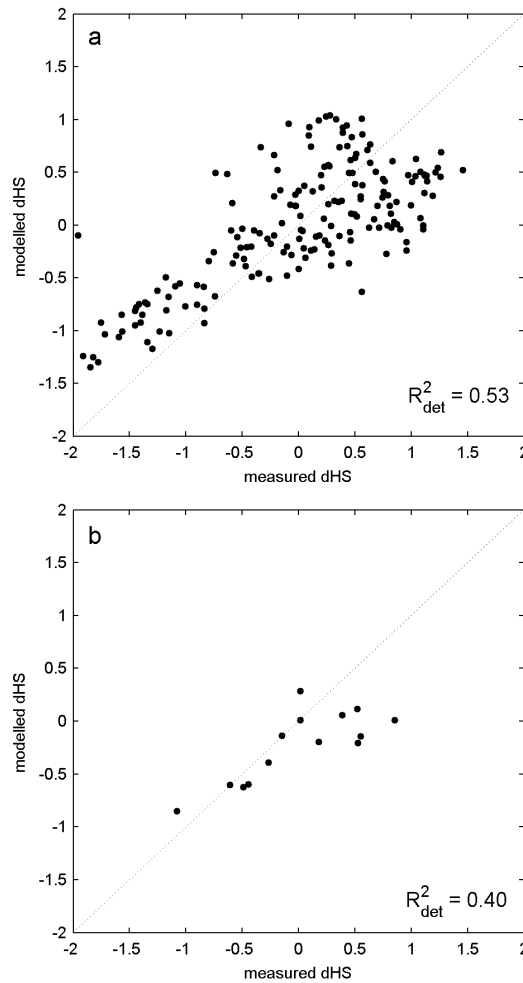
Figure 3.7: Measured vs. modelled (parameters: dE, SL and NO) dHS for **(a)** HEF and **(b)** WAN. For HEF, the snow depth data obtained in May 2003 are validated in a model calculated with the data from May 2002, June 2002 and May 2009. For WAN, the model from 2009 is validated with data from 2008.

From these findings, we conclude that the models can be transferred between various years, at least for the points of time at which maximum snow accumulation occurred. This confirms a finding of Schirmer et al. (2011), who detected a large consistency in the snow depth distribution at the Wannengrat between two years. A high inter-annual correlation was also reported by Deems et al. (2008) for two mountain sites in Colorado. However, at Wolf Creek Research Basin in Yukon, Canada, Pomeroy et al. (2004) and MacDonald et al. (2009) found substantially different snow accumulation distributions from year to year as primary wind directions of the major storms shifted between southerly and westerly. From our data, we cannot verify if the models can also be applied for earlier periods in the season. As the snow cover present at the end of the winter is the result of many individual snow fall events which are all affected by the topography, we speculate that the models, at least at a scale as presented in this paper, might also have explanatory power if applied to the accumulation season. The study of Schirmer et al. (2011), who concluded that few major storms shape the snow depth distribution at the end of the winter, supports that hypothesis.

3.4 Conclusions

In this paper, we have applied linear multiple-regression modelling of snow depth distributions with topographic parameters for several small and medium size catchments in different mountain regions of the world. We showed that statistical modelling is capable of explaining large parts of the spatial distribution of snow depth on the catchment scale. This is only achieved if the data is aggregated to length scales of some hundreds of metres, in order to smooth out the very large heterogeneity caused by drifting snow at small scales. After arbitrary clustering of the data to quadratic cells with a grid size of 400 m, 30 to 91 % of the variability could be explained by including only three explanatory parameters. For the first time, a systematic investigation of the explanatory power as a function of scale has been made. The parameters which are most frequent in the models are the elevation gradient (dE), the slope (SL), a substitute for the aspect (NO), and a wind-sheltering index (SX). These results are typically better than those obtained by other studies because of the systematic aggregation. It is important to notice that owing to the high resolution of the original data applied in our study, the full small-scale variability of the snow cover is captured. This is not the case for most earlier studies, which had to rely on a limited number of point observations, such as snow stakes or SNOTEL sites. This means that not only is it likely that the full variability is not represented in these data sets, but also that there is a potential bias in the data, e.g. if only flatter portions of a catchment are sampled (Wirz et al., 2011).

Studies which compare data from different regions are also rare. Our analysis showed that there are clear differences between the models for the specific regions, but that a global model still explains a significant fraction of the variability (23 or 30 % without glaciers). This indicates that the relationship between snow and topography is less universal than hypothesized by Lehning et al. (2011) and the application of a "global" model is limited. On the contrary, it could be shown that statistical models, developed for one year, can be well applied to other years, at least for the points of time of the maximum seasonal accumulation. This is an important finding for applications in hydrology or glaciology. A method, as presented here, can serve as a straightforward approach to characterise the spatial distribution of the snow cover. Applications from year to year should be applied with caution in some areas which have been reported to show high inter-annual changes in wind regimes that transport blowing snow.

We expect that more area-wide snow depth data sets will become available in the coming years. It might soon be possible to cover a larger spectrum of mountain regions for all over the world.

It will be interesting to see if the main topographic parameters that provided some explanation of snow depth distributions here for a limited section of climatic and physiographic environments are also important in other environments. Combining statistical with parametric or physically based methods might also yield more robust, yet still simple, models of snow accumulation. Another question which needs to be addressed is if such statistical relations are also valid for different points of time during the snow season, and how the statistical relationships change with time. This would require area-wide snow depth data for a larger area from different points of time during a season.

It should also be possible to extend similar models to vegetated areas. This would lead to the introduction of additional explanatory parameters which represent the influence of trees and vegetation, for example, a measure of winter plant-area index as used by Pomeroy et al. (2002).

Altitudinal dependency of snow amounts in two small alpine catchments: Can catchment wide snow amounts be estimated via single snow or precipitation stations?

4.1   Introduction

Mountain snow cover is characterized by a high spatial heterogeneity. The amount of snow stored within an alpine catchment and its spatial distribution strongly influence avalanche risk, water storage or mountain ecology.

The spatial variability of the snow cover is governed by different processes which interact with the local topography. Precipitation–altitude relationships (e.g. Sevruk, 1997; Pipp, 1998; Wastl and Zängl, 2008) or preferential deposition of precipitation (Lehning et al., 2008; Mott and Lehning, 2010; Mott et al., 2010) result in spatial variable accumulation patterns of snow. Wind drift (e.g. Gauer, 2001; Liston et al., 2007; Lehning et al., 2008) or avalanches (e.g. Schweizer et al., 2003) further redistribute the snow. Another important effect is the altitude dependency of temperature, which affects the solid and liquid portions of precipitation.

Mountains strongly affect precipitation amounts. This effect usually accounts for an increase in precipitation with altitude (e.g. Lauscher, 1976; Lang, 1985; Kirchhofer and Sveruk, 1992; Zängl, 2008). Nevertheless, owing to the large effect of topography and climatology, precipitation gradients are known to vary on a regional scale (e.g. Sevruk, 1997; Schwarb et al., 2001; Wastl and Zängl, 2008). In general, similar gradients are found for mean and extreme precipitation events (Blanchet et al., 2009). Annual precipitation gradients, ranging from 0 to 200 mm per 100 m height difference have been published (e.g. Baumgartner et al., 1983; Schwarb et al., 2001). Baumgartner et al. (1983) and Schwarb et al. (2001) even report slightly negative gradients for some inner alpine regions. As snow distribution is strongly affected by precipitation, the increase in precipitation is reflected in an increase in snow amounts with altitude as confirmed by several studies (e.g. Rohrer et al., 1994; Pipp, 1998; Foppa et al., 2005; Lopez-Moreno and Stähli, 2008; Bavay et al., 2009; Bavera and De Michele, 2009; Jonas et al., 2009). From snow water equivalent (SWE) measurements, Keller et al. (1984) found significant mean annual altitudinal gradients of SWE, ranging from 50 to 100 mm per 100 m elevation change which varied strongly over the years. Witmer (1986) reports similar results obtained from snow depth data.

However, all existing studies established altitudinal gradients on the basis of data obtained from a very limited number of meteorological stations or field surveys with point measurements. The aim of this study is to analyse high-resolution snow depth observations to assess altitudinal gradients of the snow cover with respect to topographical and process-related deviations. Peak winter snow depths were collected using airborne laser scanning (ALS) technology for two high-alpine catchments located in eastern Switzerland. This allowed us not only to calculate robust mean altitudinal gradients of snow stored in the catchment but also to focus on different sub-areas, characterized by distinct topography and governed by different processes. We also examine the interannual persistence of the altitudinal gradients for one catchment by comparing data from two consecutive years. Additionally, meteorological stations located in and near the study areas permit a comparison with gradients obtained from these stations and those predicted by climatological altitudinal gradients.
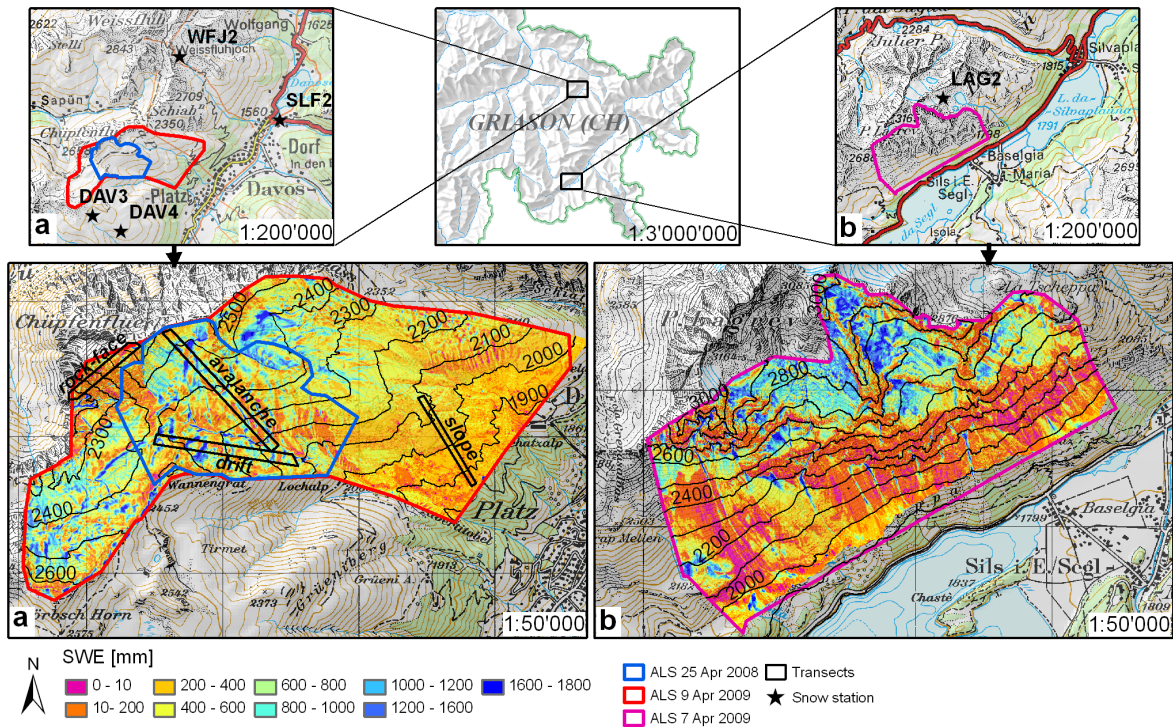
Figure 4.1: Location of the Wannengrat **(a)** and Lagrev (**(b)** test sites. The areas covered by ALS surveys are outlined with coloured lines, and flatfield snow stations are shown with black stars. The black lines show the sub-areas. SWEs shown in (a) and (b) refer to the 2009 ALS surveys. (Base map: Pixelkarte PK25[©]2009 swisstopo (dv033492).)

4.2 Methods and Data

4.2.1 Site description

We studied two small mountain catchments, located in the eastern part of the Swiss Alps (Fig. 4.1). The Wannengrat area (Fig. 4.1a) is near the city of Davos. The study area includes the Albertibach and Guggerbach basins, the Hintere Latschüel and the Chüpfenflue rock face. Elevations range from 1800 to 2658 m a.s.l. and are characterized by gentle slopes surrounded by steep mountain ridges.

The Lagrev area (Fig. 4.1b) includes the steep south-facing slopes of Piz Lagrev, which is located on the northern rim of the upper Engadin valley. Elevations range from 1800 to 3085 m a.s.l., and the site is characterized by steep slopes in the lower parts, followed by a band of rock faces and two pronounced bowls in the upper section. Each site has a total area of about $5\,km^2$. A small part ($1.5\,km^2$) of the Wannengrat area was also monitored in 2008.

As one variant of the analysis, we defined several subareas, shown by the 50–75 m wide transect strips indicated in Figure 4.1a. The sub-areas are characterized by distinct topography or by a dominant process which shapes the snow cover in the sub-area (i.e. drift, avalanche). The first sub-area (slope) is located on a gentle wind-protected slope just above the treeline. The second transect strip (avalanche) covers the southeast-facing slopes of the Albertibach catchment. This transect is characterized by a huge avalanche that was released at the upper slopes of Chüpfenflue in March 2009. No avalanche occurred in the 2007/08 season. Moreover we defined a sub-area which covers the northeastern slopes of Wannengrat (drift). This strip cuts two pronounced cornice-like drifts formed by wind (Grünewald et al., 2010; Mott et al., 2010; Schirmer et al., 2011). The last sub-area selected for detailed analysis crosses the steep southeast-facing rock face of Chüpfenflue (rock face). Similar sub-areas were analysed for Lagrev but are not discussed in detail as they are based on the same processes and produced similar results. The sites are equipped with

meteorological stations, which provide continuous snow depth measurements (Fig. 4.1). For Wannengrat there are four stations: one in the valley and three at higher elevations up to 2540 m a.s.l. (Fig. 4.1a). For Lagrev, only one station is available, at 2730 m a.s.l. (Fig. 4.1b). For the valley floor, manual snow pole readings of two local avalanche observers are used.

4.2.2 Snow depth measurements and calculation of altitudinal gradients

4.2.2.1 Areal snow depths obtained from ALS

Area-wide snow depth measurements were obtained from three ALS campaigns using a helicopter-based technology (Vallet and Skaloud, 2005; Skaloud et al., 2006). ALS measures the distances from the scanner to the surface (snow cover) with high spatial resolution and accuracy. To obtain absolute snow depths, the scans must be subtracted from a digital elevation model. Digital elevation models were created in summer surveys for each study area using the same technology. The winter flights were operated on 26 April 2008 and 9 April 2009 for the Wannengrat area and on 7 April 2009 for Lagrev (Fig. 4.1). These dates are close to the time of peak accumulation and therefore represent most of the annual precipitation which fell as snow. For this interpretation, we need to neglect evaporation and occasional minor melt in our analysis.

The accuracy of the ALS was checked by comparing the data to a tachymeter survey which was performed simultaneously on the first flight across Wannengrat. The analysis showed that the difference between ALS and tachymeter data had a mean deviation of about 5 cm and a standard deviation of 6 cm. More details on the accuracy of the ALS are provided by Grünewald et al. (2010). No such quality checks could be performed for the two other datasets. Analysis of histogram representations of the snow depth distributions suggested that the data appear to be accurate for most areas with the exception of the rock faces at Lagrev. These areas showed very long-tailed distributions with a significant number of negative or extremely high snow depths. These unrealistic snow depths were excluded from the analysis. Since precipitation and accumulation gradients are usually given in mm w.e., we had to transform the snow depth data to SWE. To achieve this, an estimation of the snow density is required. For this purpose we used the method of Jonas et al. (2009), who provided a formula to directly calculate SWE from snow depth and the additional parameters: site altitude, site location and season.

Altitudinal gradients were calculated by dividing the study area into 100 m elevation bands. For each belt the mean SWE value and the standard deviation were determined. We calculated such gradients for the two overall sites and for each of the sub-areas defined above. We thus gained high-resolution altitude–SWE relationships as shown in Figure 4.2. Mean altitudinal gradients were calculated with linear regression analysis of altitude against SWE, giving R^2 values between 0.7 and 0.8 for the two study areas.

4.2.2.2 Single-point snow depths obtained from snow stations

To assess the quality of gradients obtained from single-point measurements, separate gradients were calculated from the snow stations located in the investigation areas (Fig. 4.1). The stations are part of the operational snow station network (International Measurement and Information System (IMIS)) operated by the Swiss avalanche warning service (Lehning et al., 1999). The flat-field snow stations are located at different altitudinal levels and provide automatic snow depth measurements. Since for Lagrev no automatic station was available at the valley floor, the average of two manual flat-field snow pole readings performed by two local avalanche observers in St Moritz (1890 m a.s.l.) and Maloja (1800 m a.s.l.) was used instead. SWE for each of the investigation dates was calculated from the snow depth measurements of the stations and observers applying the method described above. Altitudinal gradients were defined from the difference of SWE between the stations at different altitudes as indicated in Figure 4.2. Mean gradients were calculated using linear regression as described above.

4.2.2.3 Climatological gradient (*Hydrological atlas*)

For our analysis we chose a climatological gradient calculated from the annual precipitation gradient which was published in the *Hydrological atlas of Switzerland* (Kirchhofer and Sveruk, 1992). In this study an altitudinal gradient of 80 mm/100 m was established to calculate a mean annual precipitation map of
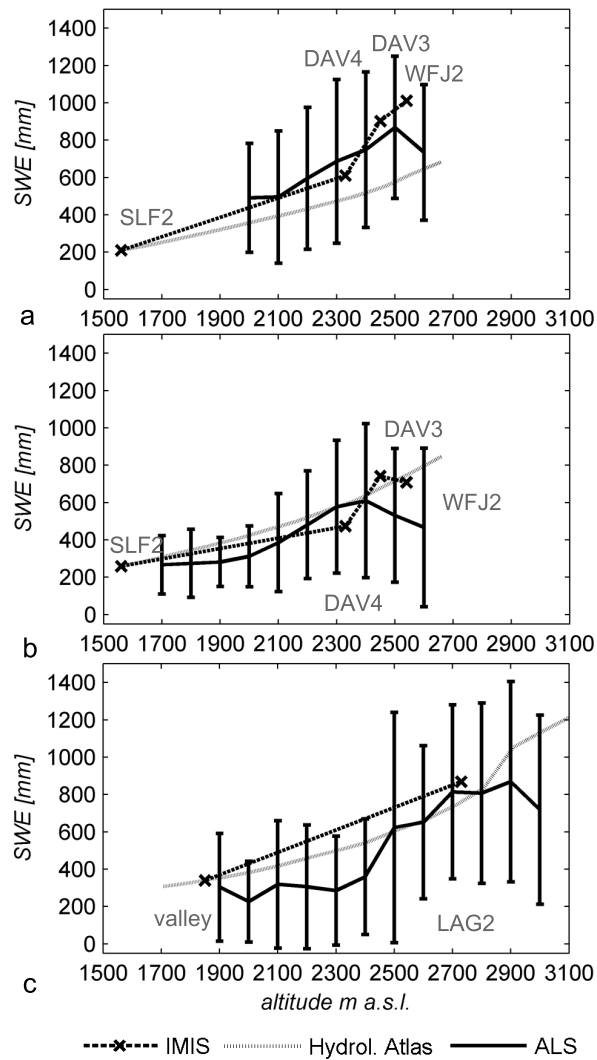
Figure 4.2: Altitudinal dependencies of SWE derived from IMIS flat-field snow stations, the *Hydrological atlas of Switzerland* and ALS data for **(a,b)** Wannengrat on **(a)** 26 April 2008 and **(b)** 9 April 2009 and **(c)** Lagrev on 7 April 2009. SWEs obtained from ALS were averaged to 100 m elevation bands. The x-axis label refers to the lower boundary of each band. The standard deviations from the ALS data are indicated by the black error bars. Locations of the snow stations are indicated by crosses and labelled with the station names.

Switzerland. As this altitudinal gradient refers to an increase in precipitation relating to the total annual precipitation, the fraction of snow in the total amount of precipitation has to be taken into account. The solid portion of precipitation (pp_{snow}) was calculated using precipitation and temperature data measured at gauged stations located in the two valley floors. To account for the increase in the portion of snow with altitude due to decreasing temperatures, the solid portion of precipitation should be calculated separately for each elevation band ($pp_{snow}(h)$). We thus determined temperature gradients between the valley stations and the mountain stations (WFJ2/LAG2) for each time-step. We then calculated the solid portion of precipitation for each band with the simplified assumption that precipitation at temperatures below 0°C falls as snow. Note that the gradient will not be very sensitive to the temperature threshold chosen to distinguish between liquid and solid precipitation. The formula for the gradient is

$$SWE(h) = SWE_0 + \frac{80\,mm}{100\,m} pp_{snow}(h) * \Delta h \qquad (4.1)$$

where SWE_0 is SWE at the snow station in the valley and h is elevation (m a.s.l.). For the complete Wannengrat area, in 2007/08 43 % and in 2008/09 51 % of the annual precipitation was calculated to be snow. For Lagrev the portion was 59 %. Measurement accuracy of the gauges and effects of catch loss were not taken into account in these simplified calculations.

4.3 Results and Discussion

4.3.1 Representativeness of "simple" gradients and climatological gradients

All altitudinal SWE gradients for the time of peak accumulation are shown in Figure 4.2a and b (Wannengrat) and Figure 4.2c (Lagrev). All curves show a distinct increase in SWE with altitude and thus confirm earlier findings (e.g. Keller et al., 1984; Witmer, 1986; Rohrer et al., 1994; Pipp, 1998). Nevertheless SWE does not increase linearly but is characterized by changing gradients for different elevation bands. Some segments even show negative gradients, which means that snow decreased with altitude for that section. These anomalies are attributed to the small-scale variability induced by topography and the snow redistribution, described in more detail below. The climatological gradients show different trends. For the Wannengrat site, the climatological gradient greatly underestimates the measured altitudinal gradient of snow distribution in 2007/08 (Fig. 4.2a), but shows a small overestimation of the gradient in 2008/09 (Fig. 4.2b). For Lagrev, the climatological gradient is similar to the measured gradient (Fig. 4.2c).

This difference was confirmed by comparing mean gradients calculated from linear regression analysis. At Wannengrat the gradient interpreted from the Hydrological atlas was 42 mm SWE/100 m in 2007/08 and 52 mm SWE/100 m in 2008/09. From the ALS data, mean gradients of 58 mm SWE/100 m in 2007/08 and 37 mm SWE/100 m in 2008/09 were obtained. At Lagrev a climatological gradient of 64 mm SWE/100 m versus a very similar measured gradient of 62 mm SWE/100 m was found. The spatial variability in the measured data, given by the error bars in Figure 4.2, was quite high for all elevations. The gradients obtained from snow stations overestimate the real snow distribution. The station gradient for Wannengrat was too high in 2007/08 (76 mm SWE/100 m and 2008/09 (46 mm SWE/100 m). For Lagrev, the station gradient (60 mm SWE/100 m) was similar to the measured and climatological gradients.

There are strong deviations between SWE measured at flat-field stations and mean values calculated from the ALS data for the respective elevation bands. At Wannengrat, the flat-field station DAV3 was characterized by below elevation- band average SWE, whereas SWEs were much too high at DAV4 and WFJ2 for both years. The general overestimation can be explained by the fact that the flat-field measurements obtained at the stations do not represent the steep slopes and rock faces which characterize the topography at higher elevations of Wannengrat. In contrast, at Lagrev the highaltitude station LAG2 and the valley observations seem to reproduce the snow amount accurately.

4.3.2 Influence of topography and processes

Measured altitudinal gradients for selected sub-areas at Wannengrat are shown in Figure 4.3. The variation of the gradients reflects the different accumulation processes that characterize these sub-areas.

The slope sub-area is distinguished by a very regular gentle altitudinal gradient. The slope seems to be characterized by very homogeneous accumulation patterns which show a small but distinct effect of the altitude (Fig. 4.3). In contrast, the other three transects do not feature such regular gradients. The rock face shows a curve which first decreases and then increases slightly. This trend can be explained by the topography of the rock face. Flatter areas, where snow can accumulate, are located at the bottom and the top. Furthermore snow might have been redistributed by wind and avalanches from steeper to flatter sections.

A very distinct peak is obvious in the curve of the drift sub-area. This peak represents two large cornice-like drifts which developed owing to wind-induced redistribution of snow (Mott et al., 2010). The leeward side contributes to the higher snow amounts accumulated in this area. Both gradients for 2008 and 2009 show this distinct peak (Fig. 4.3). A different pattern dominates the two curves for the avalanche sub-area for 2007/08 and 2008/09. Both curves are similar up to the 2400 m elevation band. Here a strong decrease was present in 2009 while the curve for 2008 still increased to 2500 m. This
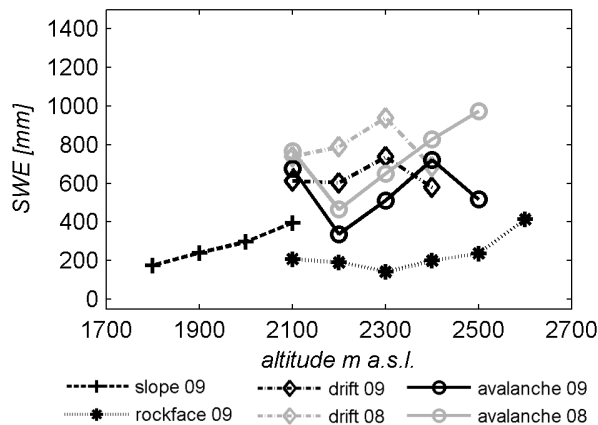
Figure 4.3: Altitudinal dependencies of SWE for the sub-areas of Wannengrat indicated in Figure 4.1. Black lines refer to 9 April 2009 and grey lines to 26 April 2008.

difference demonstrates the effect of a large avalanche which occurred in March 2008 and which relocated most of the snow from the upper slopes. The accumulation area of the avalanche is not captured by the transect. The peak in the 2100 m elevation band is explained by a snow-filled ditch.

The local topography and the processes acting on the snow cover have a strong influence on the altitudinaldependent distribution of SWE. Previous studies demonstrated that the upper areas are dominated by wind-induced redistribution processes (Mott et al., 2010) whereas the lower parts of the investigation area are more sheltered, and redistribution of snow due to wind might therefore have a minor effect in these areas. A comparison of the slope and drift sub-areas reflects the spatially varying influence of the wind on snow accumulation (Fig. 4.3). Moreover, the relocation of snow by avalanches could be demonstrated in the avalanche transect and the influence of very steep and rough terrain by analysing the rock-face sub-area.

4.3.3   Inter-annual persistence

Even though only two sets of data were available for analysis, some observations on the interannual persistence (Schirmer and others, in press) of the snow distributions can be derived by analysing the Wannengrat data. Both curves (Fig. 4.3a and b) are characterized by a similar shape for elevations ranging up to 2400 m. The absence of the pronounced peak in the 2500 m elevation band for 2009 is explained by the large avalanche that occurred in that season (see above).

It is worth noting that SWE was much higher at all elevations in 2008. The 2007/08 winter was characterized by exceptionally high snow depths while the 2008/09 winter only showed average snow accumulation. Nevertheless, the total snow amount does not significantly influence the altitudinal gradient of the snow cover. This strong similarity of altitudinal gradients for both years confirms the findings of Schirmer et al. (2011) and Schirmer and Lehning (2011), who studied snow-depth distributions and their scaling behaviour for three sub-areas at Wannengrat and found very strong interannual correlations.

4.4   Conclusion

A set of high-resolution SWE data obtained from ALS campaigns was used to analyse the altitudinal characteristics of the snow distribution at the time of peak accumulation. We investigated data from the two alpine catchments, Wannengrat and Lagrev. For Lagrev, only data from one ALS campaign were available whereas 2 years of observations were available for Wannengrat. Clear altitudinal gradients for SWE could be detected from the measurements. This confirms previous studies on altitudinal dependencies of snow and precipitation amounts.

A good interannual consistency of measured SWE altitudinal gradients was found, while total snow amounts were clearly different. This finding is in agreement with the studies of (Mott et al., 2010)

and (Schirmer et al., 2011) who report a strong interannual correlation of the snow-depth distributions. However, investigating sub-areas we found a strong influence of the local topography and of local snow redistribution processes due to wind or avalanches. On small scales, these local effects clearly override the regional accumulation patterns. From comparison with the climatological gradient published in the *Hydrological atlas of Switzerland* (Kirchhofer and Sveruk, 1992) we found that this gradient did not show a consistent relationship with the measured ALS gradients. For Wannengrat the climatological gradient underestimated snow amounts in 2007/08 but overestimated them in 2008/09. For Lagrev the gradient seemed to be a good estimation for the real snow distribution. An investigation of altitudinal gradients obtained from flat-field snow stations located in the area indicated that these gradients tend to overestimate the snow-elevation dependency found in reality. This may be attributed to the fact that flat-field sites, which are usually used for snow stations, become biased towards "more than average snow" at higher altitudes, where snow redistribution becomes more important. Furthermore, detailed analysis of specific elevation bands showed strong deviations from average snow amounts, depending on local characteristics of the terrain or on the occurrence of an avalanche.

Future work on altitudinal characteristics would strongly benefit from larger datasets. On the one hand, high-resolution measurements of more study sites, spread over different regions, would be important to allow for general conclusions on regional deviation and characteristics. On the other hand, for a more accurate assessment of interannual persistence, a larger dataset covering several seasons would be required. One important aspect is whether the altitudinal gradient changes over the winter and for individual storms. This could not be addressed in the analysis presented here and would require repeated measurements at high temporal resolution over a winter. Finally, analysis of such area-wide datasets using more advanced methods like geostatistics or physically based model approaches (Lehning et al., 2008; Mott and Lehning, 2010) would provide more complete knowledge on spatial snow-cover distributions.

Acknowledgements

Elevation dependency of mountain snow depth

5.1 Introduction

Complex orography is the main driving factor for the spatial heterogeneity of precipitation. When advecting moist air masses are blocked by mountains they are forced to ascent at the mountain slopes. Declining air temperatures result in a cooling and a decrease of the saturation pressure of the lifted air parcels. Once the saturation level is reached moisture condensation leads to clouds formation and finally to the onset of precipitation. These processes are enhanced by further lifting which finally results in an increase of precipitation with elevation. However, the interaction of clouds and precipitation particles with the local wind can strongly modify the precipitation patterns at the ground (Mott et al., 2014).

Orographic precipitation effects have been studied at a large range of scales for mountain regions all around the world. Most studies identified a distinctive increase of precipitation with altitude (e.g. Spreen, 1947; Peck and Brown, 1962; Frei and Schär, 1998; Blumer, 1994; Johnson and Hanson, 1995; Liu et al., 2011; Asaoka and Kominami, 2012). This positive correlation is also reflected in a general increase of snow depth or snow water equivalent (SWE) as reported by many studies (e.g. Rohrer et al., 1994; Bavera and De Michele, 2009; Lopez-Moreno and Stähli, 2008; Durand et al., 2009; Lehning et al., 2011; Grünewald and Lehning, 2011; Grünewald et al., 2013). Contrary, some studies also report on no or even negative dependencies of elevation and precipitation: For a study site in New Zealand, Kerr et al. 2013 could not identify elevation gradients of SWE and no clear correlations between elevation and SWE were found for some inner-alpine regions in Switzerland (Rohrer et al., 1994). Blumer (1994), Basist et al. (1994) and Arakawa and Kitoh (2011) even reported on negative elevation gradients of precipitation.

Consequently the shape of the elevation – precipitation relation can vary strongly even over small distances (e.g. Lauscher, 1976; Rohrer et al., 1994; Basist et al., 1994; Sevruk, 1997; Wastl and Zängl, 2008). This strong variability is attributed to the highly complex interaction of the weather patterns with the local topography. Sevruk (1997) speculates that "in a series of inner-alpine valleys following each other and having different orientation, slopes and altitude, the redistribution of precipitation by wind can be the dominant factor of its spatial distribution suppressing any other effects including the altitude". Other studies postulate an advective leeward shift of the local precipitation maximum, favoured by specific topographical and meteorological conditions (Carruthers and Choularton, 1983; Robichaud and Austin, 1988; Zängl, 2008; Zängl et al., 2008; Mott et al., 2014). Due to its lower fall speed, this shift is more pronounced for snow fall than for rain (Colle, 2004; Zängl, 2008). On a smaller scale, Mott et al. (2014) showed that orographically modified patterns of mean horizontal and vertical wind velocities affect particle trajectories inducing reduced snow deposition rates on windward slopes and enhanced deposition on leeward slopes. Small-scale snowfall patterns over single inner-alpine mountain peaks can, thus, differ significantly from those observed on a larger scale for large mountain ranges, where cloud formation processes tend to make the leeward slopes drier than windward slopes (Houze, 2012; Mott et al., 2014). The thickness of the snow cover at the end of the winter season can serve as a proxy for the seasonally accumulated precipitation on the ground. However, Scipion et al. (2013) identified large differences between precipitation patterns obtained by a high resolution Doppler X-band radar and the final seasonal snow accumulation. These differences are attributed to several processes that affect the snow once on the ground: Due to gravitational forces snowflakes might immediately glide downslope if they land on sufficiently sloped surfaces. Furthermore the wind can redistribute the snow

from exposed to sheltered locations (Gauer, 2001; Mott et al., 2010). The erosion by the wind is largest at higher altitudes as wind speeds and exposure tend to increase with elevation. Moreover, driven by gravitation, snow is potentially moved downward by creeping, sloughing and avalanching (Bernhardt and Schulz, 2010; Gruber, 2007). Finally snow melt, sublimation and phase transitions from snow to rain, especially in spring might affect the snow amount, particular in lower elevations (Elder et al., 1991). In combination, these processes modify the elevation driven precipitation signal stored in the snow cover. As a rough summary, reduced snow amounts at the crest level, in steep slopes and the lowest elevations are contrasted by enhanced accumulation in flat and protected areas at the slope toes.

As most of the studies mentioned before are based on a limited number of gauges or weather stations, the potential bias of the results appears relatively large (Havlik, 1969; Sevruk, 1997). Inadequate spatial station coverage, especially in high altitudes (Blanchet et al., 2009; Daly et al., 2008; Sevruk, 1997; Wastl and Zängl, 2008) and the large potential measurement error of precipitation, especially in exposed areas (Rasmussen et al., 2001, 2011; Sevruk, 1997; Yang et al., 1998) are important factors that might have an impact on the results of these studies. In contrast, owing to the rapid development of remote sensing techniques such as laser scanning (LiDAR), high spatial resolution data sets have recently become available for the snow cover (e.g. Deems et al., 2013; Grünewald et al., 2010, 2013). Furthermore, significant advances in the development and application of Doppler radars for precipitation quantification have been reported (Scipion et al., 2013; Mott et al., 2014). However, the resolution of these systems is still insufficient to reflect the small scale variability of precipitation and snow fall close to the surface.

To our knowledge the only systematic study on elevation gradients of snow that is based on such area-wide data has been presented by Grünewald and Lehning (2011). They compared elevation gradients calculated from airborne LiDAR surveys with simple climatological and snow station based gradients for two small study sites in the Eastern Swiss Alps. Principally Grünewald and Lehning (2011) identified a positive correlation of SWE and elevation but they also recognised strong deviations between the two sites, two consecutive years and between the three different approaches. For the LiDAR gradients they found that the relation between elevation and snow depth levelled at a certain altitude and finally even decreased. From this finding the question arose, if such a shape is generally characteristic for the snow depth elevation relationship.

The availability of a large data set consisting of area-wide high resolution snow depth data from different mountain regions (Grünewald et al., 2013) now allows us to test this hypothesis. Based on Grünewald and Lehning (2011) we systematically analyse snow depth elevation gradients for different scales ranging from slope transects to the entire catchments or mountain sites. In addition to the identification of typical shapes we also aim to explain the location of the previously mentioned maximum of the relation between elevation and snow depth.

5.2 Data

5.2.1 Airborne laser scanning (ALS)

Recent years have seen an increasing number of applications of airborne laser altimetry (ALS or LiDAR) for snow studies (e.g. Deems et al., 2006, 2008; Grünewald et al., 2013; Grünewald and Lehning, 2011; Lehning et al., 2011; Trujillo et al., 2007, 2009). High resolution snow depth maps are calculated by subtracting two digital surface models (DSM), one obtained in snow-covered and one in snow-free conditions. It has been shown that ALS is a valid method for gathering area-wide snow depth data (e.g. Hopkinson et al., 2004; Deems and Painter, 2006; Deems et al., 2013) and that vertical accuracies are in the range centimetres to few decimetres (Grünewald et al., 2010; Bollmann et al., 2011; Hopkinson et al., 2012; Deems et al., 2013). In principal, data sets obtained by helicopter-based LiDAR appear to be more accurate than data sets gathered from airplanes (Grünewald et al., 2013). This is attributed to reduced flying height, terrain-following flight line of the helicopter and a better footprint in steep terrain due to the tilting sensor. A detailed review on ALS for snow cover observations has recently been published by Deems et al. (2013). Additionally, more general information can be found in Baltsavias (1999) and Wehr and Lohr (1999). The ALS data sets analysed in this study and how they were processed is comprehensively described in Grünewald et al. (2013).
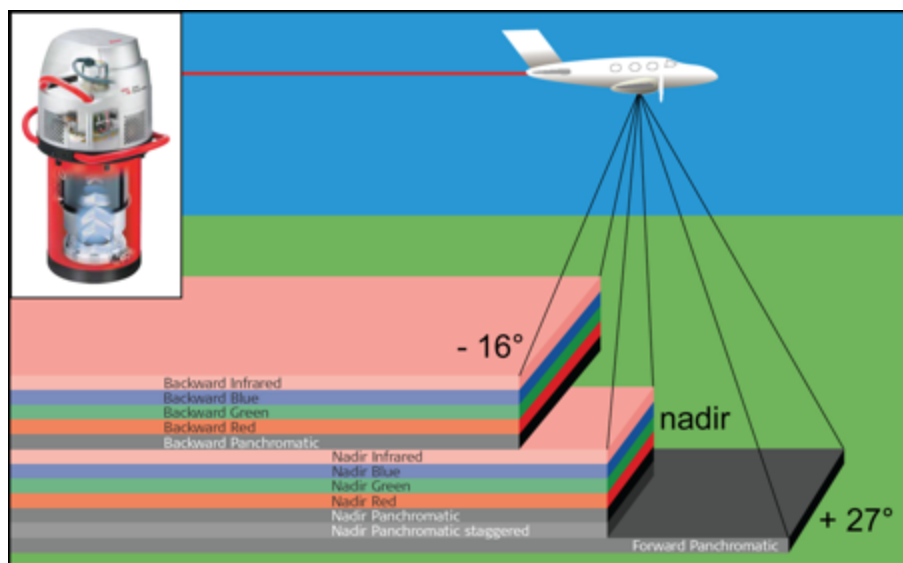
Figure 5.1: ADS80 sensor (top left) and data acquisition scheme with spectral bands and viewing angles (Source: (Bühler et al., 2009).

5.2.2 Airborne digital photogrammetry (ADP)

Digital photogrammetry (ADP) is a remote sensing technology that is applied to acquire high resolution DSMs by exploiting photogrammetric image correlation techniques (Maune, 2001). Identical to ALS, snow depth maps can be calculated by subtracting a summer DSM from a winter DSM.

The Leica Geosystems Airborne Digital Sensor ADS80 (Fig. 5.1) is an opto-electronic line scanner mounted on an airplane, that is able to simultaneously acquire four spectral bands (red, green, blue and near infrared) with a radiometric resolution of 12 bits from three different viewing angles. GNSS/IMU supported orientation of the image strips supplemented by the use of ground control points achieved a horizontal accuracy of 1-2 ground sampling distances (0.25-0.5 m). The sensor had already been successfully used to detect avalanche deposits in the area of Davos (Bühler et al., 2009) and is more economic for large-scale data aquisition than ALS due to higher flight altitude and therefore reduced flight time. More detailed information on the Leica ADS opto-electronic scanner can be found in Sandau (2010).

In this study we apply snow depth maps in 2 m resolution produced by Bühler et al. (2014). Areas covered by forests, bushes and buildings as well as identified outliers are masked out prior to the snow depth map generation because the reliability of the DSM is substantially reduced in those areas. Bühler et al. (2014) compared the ADS snow depth maps with different independent snow depth measurements. They find RMSE values of less than 30 cm in areas above tree line. The RMSE values strongly depend on the distance of the sensor to the ground which reduces the accuracy of snow depth to less than 50 cm at the valley bottom (highest distances). Moreover Bühler et al. (2012) found that the quality of the data is limited by the steepness of the terrain. They state that data gathered in slopes steeper than 50° might be affected by large potential biases.

5.3 Study sites

Basic descriptions and some summary statistics on topography and snow cover of the investigation areas are provided in Table 5.2. Apart from the ADS-data, the data sets analysed in this study are the same as in Grünewald et al. (2013). We are therefore only proving a very short overview on each of the study sites.

A large data set has been collected by ADS for the district of Davos in the eastern part of the Swiss Alps at 3 September 2013 and 20 March 2012 (Fig. 5.2). In total an area of 124 km^2 consisting of 12 overlapping image strips (approx. 70 % overlap across track) has been covered in the surveys. The ground
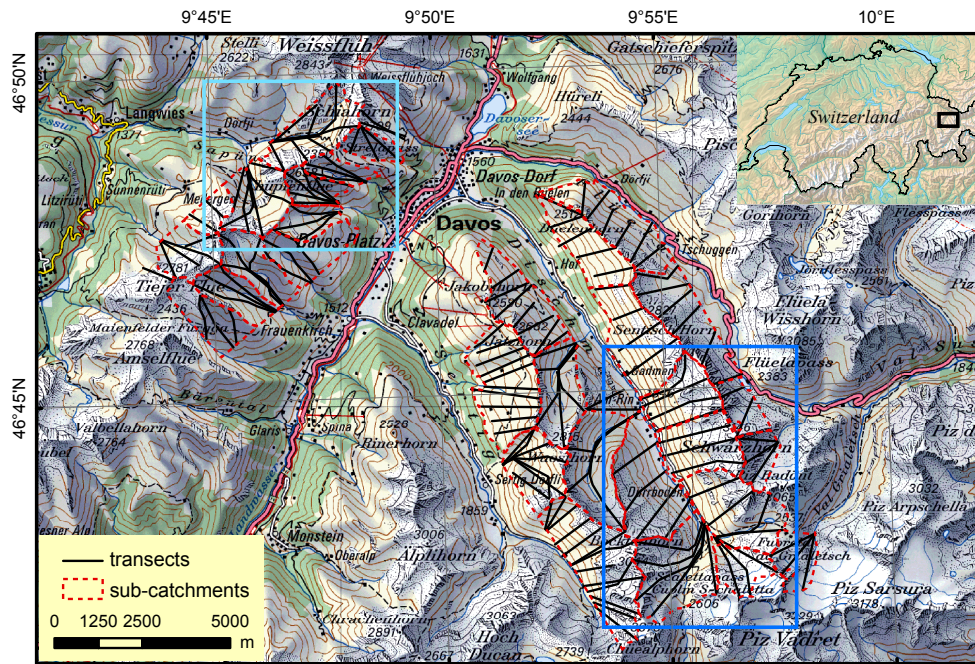
Figure 5.2: Overview map on the study region DIS and STRE. The upper left panel indicates the position in the East of Switzerland. Detailed views for parts of the domains are shown in Fig. 5.3. Maps reproduced with permission (Swisstopo, JA100118).

Table 5.1: Data sets analysed in the study where "Date" refers to the date of the winter survey, "Mean acc." to the mean accuracy in vertical direction as denoted in the reference column and "Platform" to the measurement platform.

Name	Date	Mean acc. [m]	Platform	Reference
Dischma valley (DIS)	20 Mar 2012	0.3-0.5	Leica ADS80	(Bühler et al., 2009, 2014)
Strela (STRE)				
Val de Núria (NUR)	9 Mar 2009	0.3	Optech ALTM3025	Moreno Baños et al. (2009)
Hintereisferner (HEF)	7 Mai 2002	0.3	Optech ALTM1225	Geist and Stötter (2008); Bollmann et al. (2011)
Haut Glacier d'Arolla (ARO)	1 Mai 2007	0.1	Riegl LMS Q240i-60	Dadic et al. (2010b,a)
Wannengrat (WAN)	26 Apr 2008	0.1	Riegl LMS Q240i-60	Grünewald and Lehning (2011); Lehning et al. (2011)

sampling distance of the imagery is about 25 cm, limited through the minimal flying height for high alpine terrain (Bühler et al., 2012).

The data set has been split into two study sites: The Strela data set (STRE) covers a large section of the mountain range located in the Northwest of the Landwasser valley (Fig. 5.2, 5.3c). The mountain range spans from Southwest to Northeast and is perpendicular to the main wind that is typically from the Northwest (Schirmer et al., 2011). Northern and southern aspects are dominant in the data. The terrain is a mixture of alpine slopes with varying steepness. Rocky outcrops and some larger rock faces are present, especially in the summit regions. Note that the Wannengrat data set (WAN) is a small subsection in the centre of STRE. However the year of the survey and the sensor obtained for the data collection differ (Table 5.1).

The second study site in the region of Davos is the Dischma valley (DIS) in the East of the town of Davos (Fig. 5.2, 5.3a). The 13 km long valley extends parallel to the main flow from the Northwest to the Southeast. The data set is not only consisting of the eastern and western slopes of the Dischma valley but also includes the upper flanks of the two neighbouring valleys. The land cover is similar to STRE but easterly and westerly aspects are dominating. Two summer season were between the summer (Sept 2013) and the winter survey (Mar 2012) applied for the snow depth calculation. As we cannot account
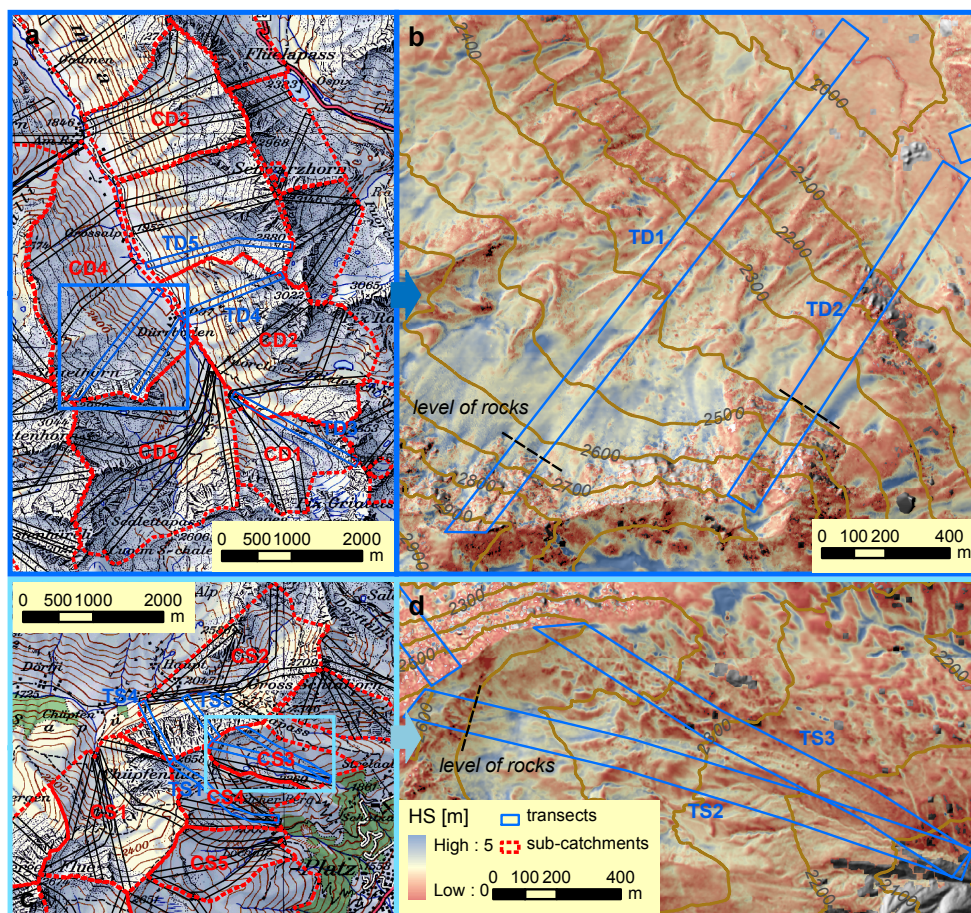
Figure 5.3: Detailed maps of catchment (CD1-5 and CS1-5 see Fig. 5.6), and transects (CT1-5 and CS 1-5 see Fig.,5.7) and discussed in the text. Maps reproduced with permission (Swisstopo, JA100118).

for potential changes of the glacier surface in summer, that could bias the snow depth on the glaciers, we removed the two small glaciers in the highest elevation of the site.

This large data set is supplemented by the smaller, ALS based data sets presented by Grünewald et al. (2013) (Table 5.1, 5.2). The Piz Lagrev (LAG) is a steep, south-facing mountain slope in the Engadine valley in the Southeast of Switzerland. The area is dominated by steep rock-faces and two rather flat bowls where most of the snow accumulates. The Haut Glacier d'Arolla (ARO) is located in the western part of the Swiss Alps. About half of the site is covered by glaciers. The remaining areas are rather steep talus slope and rock-faces. The characteristics of the Hintereisferner (HEF) study domain in the Öztal Alps of southwestern Austria are similar to ARO. Steep talus slopes and rock-faces dominate the valley flanks and about 50 % of the domain is glaciated. The last study site analysed in this paper is the Vall de Núria located at the main divide of the eastern Spanish Pyrenees. Slopes of diverse steepness with some rocky outcrops near the summit level are typical of this $28\,\mathrm{km}^2$ data set.

5.4 Methods

This study analyses elevation dependencies of snow depth at three different scales. First regional characteristics are assessed by calculating gradients for the complete data sets listed in Table 5.2. Secondly, we subdivided the data into smaller sub-catchments ($1\,\mathrm{to}\,5\,\mathrm{km}^2$) as shown in Fig. 5.2 and 5.3a,c. This gives a measure of the variability. To assess the scale of single mountain slopes, we manually defined $100\,\mathrm{m}$ wide transects (Fig. 5.3). These transects extend perpendicular to the slope and span the entire difference in

Table 5.2: Summary statistics and main characteristics of the investigation areas: "Area" is given in km^2, elevation range (EL) in $m\ a.s.l.$, mean slope (SL) in $°$, mean and standard deviation (std) of snow depth (HS) in m. Areas with trees and larger vegetation were masked from the data sets.

Name	Location	Area	Elev	SL	Asp	mean HS	std HS	Description
DIS	Davos, Eastern Swiss Alps	78	1760-3146	29	All	1.37	0.95	Mixture of steep and gentle slopes, some rock faces
STRE	Davos, Eastern Swiss Alps	26	1850-2781	29	All	1.77	1.46	Mixture of steep and gentle slopes, some rock faces
NUR	Southeastern Spanish Pyrenees	28	2000-2900	28	All	1.05	1.06	Mixture of gentle slopes and some rock outcrops
HEF	Rofen valley, South-western Austrian Alps	25	2300-3740	24	All	2.09	1.2	50% glaciers, steep talus and rock-faces
ARO	Valais, Southwestern Swiss Alps	10	2400-3500	28	SW to SE	1.14	0.9	50% glaciers, steep talus and rock-faces
WAN	Davos, Eastern Swiss Alps	4	1940-2650	27	All	1.48	1.07	Mainly talus slopes, some rocky outcrops and rock-faces in summit region
LAG	Engadine, Southeastern Swiss Alps	3	1800-3080	40	SE to SW	1.56	1.41	Steep talus slopes surrounded by rock-faces

altitude of the respective mountain slopes.

Similar as in Grünewald and Lehning (2011) the subareas were subdivided into 100 m elevation bands and the mean snow depth was calculated for each subarea and each elevation zone. To avoid values that are based on a very small number of cells, elevation zones that had less than 0.5 % of the total number of cells of the specific sub-catchment or transect were removed. The mean snow depths were then plotted against their respective elevation level and classified according to their general shape. Based on a first visual analysis we identified a set of typical shapes of gradients as indicated in Fig. 5.4 and discussed below. For all curves that were characterised by a distinctive peak (Fig. 5.4 shape A and B), that reflects a local maximum of the elevation – snow-depth relationship, the elevation level of this peak was detected.

A visual examination of the location of the peak in relation to the topography of the subarea suggests a possible correlation with the elevation level of distinctive rocky outcrops (level of rocks). The lower elevation levels of such rocky sections were therefore, where present, manually identified from topographic maps or hillshade-images and rounded to the nearest 50 m contour line. This procedure works well for transects but is rather vague at the scales, where large areas are included in each elevation zone. This leads to large potential scatter of the level of rocks. While relatively clear levels could be detected for most slope transects, the rocky sections already varied strongly for the sub-catchments. At the scale of entire valleys or mountain ranges (data sets) the even larger diversity fully prevents an identification of a single rock level. Finally, it needs to be noted that such rocky sections were not present for all subareas. For the subareas that featured both, a peak and a clear level of rock, we finally created scatter plots and correlation analysis. This was on the one hand performed for each of the study areas separately and on the other hand for the comprehensive data set.

5.5 Results

5.5.1 General shape of gradients

Figure 5.4 indicates idealised shapes of the elevation – snow-depth relationships as qualitatively detected from the data (Fig. 5.5, 5.6, 5.7). The most prominent shape is shown in panel A of Fig. 5.4: The curve increases up to a specific elevation level where it peaks and finally decreases in the remaining elevation bands. Note that this shape is an oversimplification that only aims to picture the main characteristics of the general shapes. The slope is not necessarily steady, several smaller spikes and peaks might be present and the peak of the gradient can be flat and span several elevation bands. Figures 5.5 to 5.7 are examples for the variability of the single shapes.
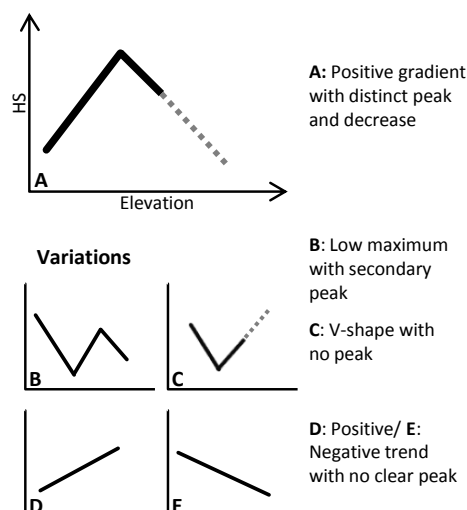
Figure 5.4: Idealised shape of elevation gradients and variations as identified from the data sets.

Panels B to E of Fig. 5.4 illustrate variations of type A. Type B is principally identical to A but is additionally characterised by a dominant snow depth maximum in the lowest elevations. Such maxima are caused by local accumulation zones such as snow filled ditches or avalanche depositions. A distinctive secondary maximum is always present in class B. For the analysis presented in 5.5.6, this secondary maximum is treated as peak of the elevation – snow-depth relationship. Gradients classified as type C to E do not show distinctive peaks. C is similar to B but a decrease of snow depth in the higher elevations is missing. Shape D and E present steady positive (D) or negative (E) gradients with no clear maximum. These variations are attributed to processes in the discussion below.

Figure 5.5a presents elevation gradients of snow depth for the entire data sets. For Fig. 5.5b, the curves were normalised according to:

$$\tilde{X} = \frac{X - min(X)}{max(X) - min(X)} \tag{5.1}$$

where $\tilde{X}$ represents the scaled variable (snow depth or elevation).

5.5.2 Gradients: entire data sets

At the scale of the entire data sets, we only detected type A gradients (Fig. 5.5). This shape is evident for the raw data (Fig. 5.5a) and the curves show a fairly nice collapse in the rescaled data (Fig. 5.5b). All data sets show a clear increase of snow depth with elevation followed by a pronounced maximum and a more or less definitive decrease. Even though the general shape appears similar, the location of the maximum and the gradient appear variable between the study sites.

5.5.3 Gradients: sub-catchment

Figure 5.6 presents curves for five selected sub-catchments for STRE (Fig. 5.6a) and DIS (Fig. 5.6b) respectively. The locations of the sub-catchments are indicated in Fig. 5.3. Most of the curves can be classified as type A (CS1, CS3, and CD2 to 5) but the shapes are more variable than on the scale of the entire data sets (Fig. 5.5). Mean snow depths are clearly increasing with elevation and reach pronounced peaks at a certain level.

CS2, CS4, CS5 and CD1 are representative for type B gradients: A maximum in the lowest elevation band is followed by a short negative trend and a steady increase culminating in a distinct peak. The maxima at the low elevation bands are attributed to snow filled ditches that dominate the largest portion

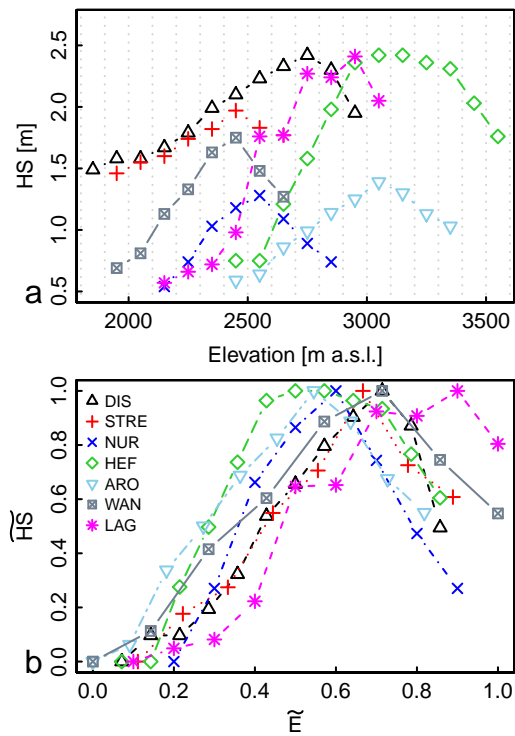Figure 5.5: Elevation gradients on the scale of the complete data sets. In a) snow depths are plotted against Elevation as raw values (a) and rescaled by applying Eq. 5.1 to snow depth and elevation
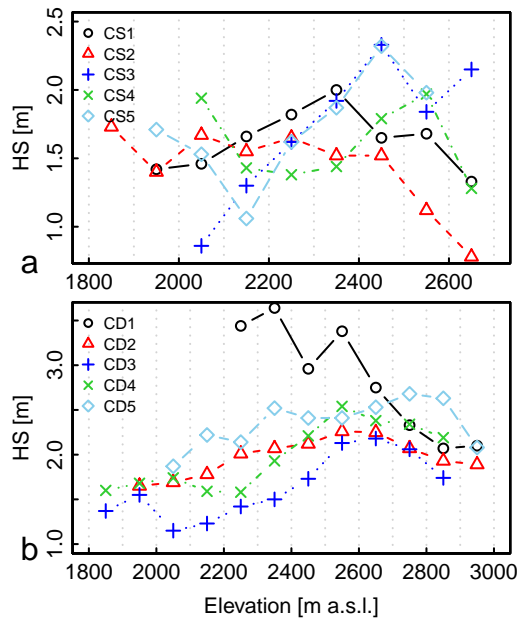

Figure 5.6: Elevation gradients of selected sub-catchments from the Strela mountain range (a) and the Dischma valley (b)
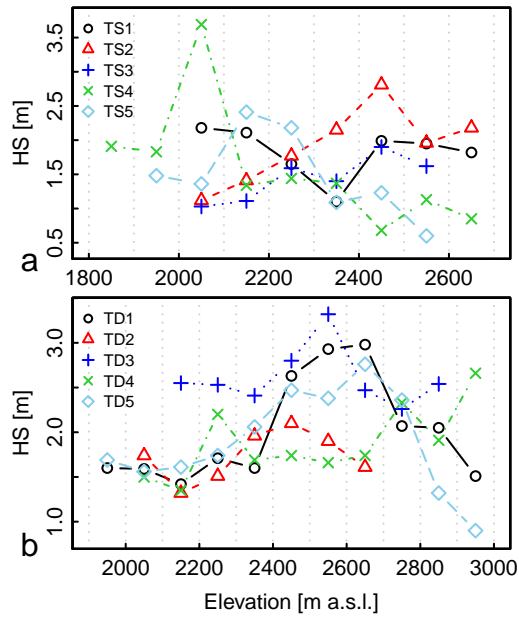
Figure 5.7: Elevation gradients of selected transects from the Strela mountain range (a) and the Dischma valley (b).

of the lowest elevation bands. The combination of a relatively small area of the elevation zone (in comparison to the other zones of the sub-catchments) with snow depths of more than five metres in the gullies explains the low maxima for CS4 and CS5. The accumulation zone in and around a ditch in CS2 with snow depths around 2 m, is clearly less pronounced than those in CS4 and CS5. However, this small area of snow accumulation is still enough for the slight maximum in comparison to the shallower snow depth in the higher elevation zones. The extreme snow depths in CD1 are caused by the deposition of large snow drift in a terrain depression at the foot of the steep northern slopes. This accumulation zone is covering the vast part of the two lower elevation bands and snow depths of more than eight metres could be detected. Depositions of similar dimensions are also present in some of the higher elevation bands. However, they do not cover such large portions of the area as in the lower section. This results in the clearly reduced mean values and in the decreasing trend of the black curve (CD1) in Fig. 5.6b. Above the low-elevation maxima typical type A shapes are evident for CS2, CS4, CS5 and CD1.

5.5.4 Gradients: slope-transects

Figure 5.7 displays identical relations as Fig. 5.6 but for transects instead of sub-catchments. The shapes of the curves show a higher variability in Fig. 5.7 than those in Fig. 5.5 and 5.6. This is because the slighter support areas of each elevation band provoke larger effects of the small scale variability in snow depth on the shape of the curves. In contrast this small scale heterogeneity is rather smoothed out for the sub-catchment (Fig. 5.6) or the complete data sets (Fig. 5.5). However, the principal findings are also visible for the transects. Most of the curves can be classified as type A (TS2, TS3, TS4, TS5, TD1, TD2, TD3, TD5). TS2 displays nearly an ideal type A (Fig. 5.4) curve with a linear increase, followed by a marked snow depth maximum at 2450 m. Contrary, the maximum of TS3 appears less pronounced. The detailed map of the two transects (Fig. 5.3d) provides insight into the snow cover characteristics that cause the respective curves. Little snow in the lower sections, the location of the maxima in the flat bowls and the decrease of snow depth in the steep, rocky slopes at the highest elevations are clearly visible. A second detailed map is illustrated in Fig. 5.3b for TD1 and TD2. Again, the pronounced peaks and the distinct decrease of snow in the steep rock bands at the top levels are well illustrated. The curve with the most extreme maximum is represented by TS4 (Fig. 5.7a). While only little snow had been accumulated

57
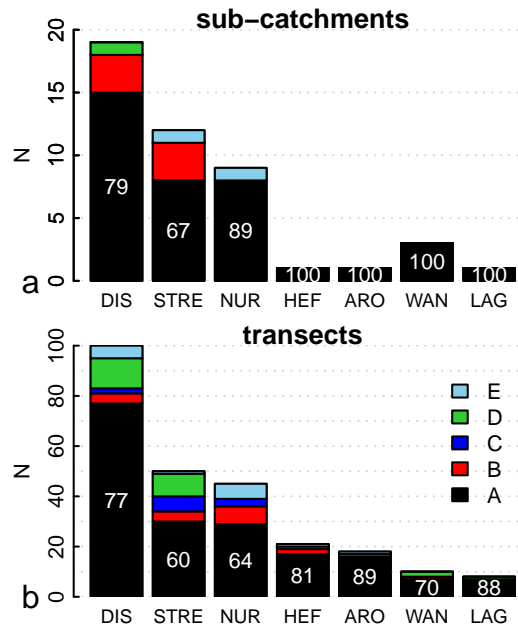
Figure 5.8: Frequency distribution of the types of gradients (A-B as shown in Figure 5.4) for sub-catchments (a) and transects (b) of each data set. White numbers indicate the percentage of subareas classified as type A.

on the rock-face itself, a large deposition zone is evident in the gentle slope at the foot of the rock-face (Fig. 5.3c). Redistribution of snow due to gravitational forces might be the main cause for these extreme snow depth differences.

Different types of shape are only present for TS1 and TD4. TS1 represents a type C curve with a low peak, a distinctive minimum and a slightly denoted secondary peak in the higher elevation. The low maximum is attributed to a snow filled ditch in the lowest elevations and the secondary peak is caused by an accumulation zone in a gentle bowl below steep slopes at the top. TD4 has been classified as type D. The curve is characterised by predominately positive slopes with two smaller peaks and a maximum in the highest elevation zone.

5.5.5 Frequency distribution of gradient types

Figure 5.8 summarises the number of subareas that have been assigned to the specific type of gradient for each data set. 67 to 100 % of all gradients have been classified as type A for the sub-catchments of each specific study site (Fig. 5.8a). In total 79 % of all sub-catchments belong to type A. Merging all gradients with a distinctive peak (type A and B) increases the portion to 93 %. All other types appear to be rare. Only one sub-catchment in DIS has been classified as type C and one in each case for NUR and STRE. A similar picture characterises the distribution of the gradient types at the scale of the transects (Fig. 5.8b). 72 % of all transects (60 to 89 % of each data set) belong to type A. Combining type A and B results in an increase to 79 %. Similar to Fig. 5.8a, the remaining types are very rare. Only type D (positive trend) curves are more frequent, at least for DIS and STRE.

5.5.6 Relation of elevation gradients and topography

In the previous section we have shown that the vast majority of subareas feature distinctive maxima in their elevation – snow-depth relationships. From this finding, the question whether the elevation level of this peak can be explained by the topographical settings of its respective location should be answered. Visual impression suggests that most of the maxima would be found below distinctive terrain breaks such as steep cliffs or slopes. We tried to automatically identify the elevation of the most dominant terrain break for each subarea by calculating the maximum inclination of the relationship between elevation and terrain
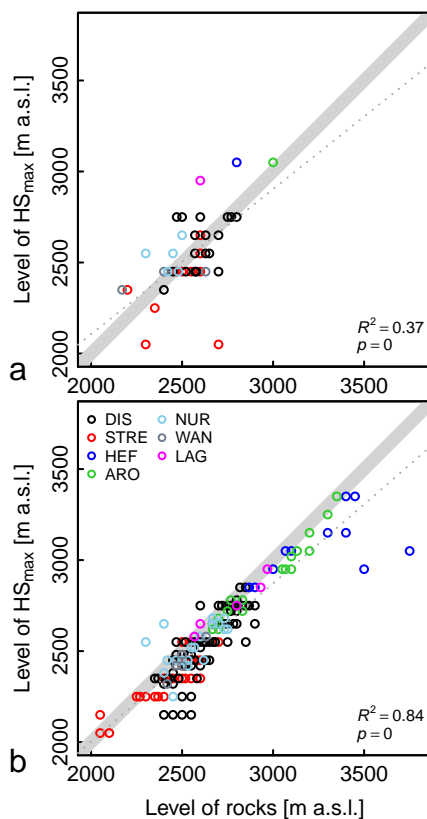
Figure 5.9: Level of rocks versus level of the maximum of the elevation – snow-depth relationship for the transects (a) and the sub-catchments (b). The grey shaded area illustrates the 1-1 line (± 50 m) and the dashed line the linear fit of the merged data.

slope and terrain roughness (expressed by the standard deviation of the slope) respectively. However, the topographical complexity of the terrain prevented an adequate identification of the appropriate elevation level. This is also reflected in the correlation of these measures with the elevation levels of the maxima of the elevation – snow-depth relationships that were relatively low. Following this, we manually identified the predominant level of rocks as described before.

A rock level was present for the majority of the subareas (transects: 70 %, sub-catchments: 71 %). In total 67 % of the sub-catchments and 58 % of the transects feature both, a peak in the elevation – snow depth curves (Fig. 5.8 shape A and B) as well as a level of rocks.

Figure 5.9 illustrates scatter-plots of the level of rocks versus the level of the maximum of the elevation – snow-depth relationship. Especially for the transects (Fig. 5.9b) a clear linear relationship (R^2=0.84) is visible. Such a correlation is present for each single data set and for the merged data. Figure 5.9b also indicates that the vast majority of the points are shifted by about 50 to 200 m below the 1-1 line. Hence, the areas with the peak in the snow depths tend to be located below the level of rocks. This confirms the expectation that more snow tends to accumulate in gentle slopes at the foot of steep slopes and rough terrain due to preferential deposition (Lehning et al., 2008) and redistribution of snow by sloughing, avalanching and wind drift. The two outliners for HEF (dark blue circles at the right side of Fig. 5.9b) are transects that span the entire glacier. Rocks are only present in the highest elevation bands. The snow depth maxima are located at accumulation zones in the middle elevations of the glacier. A secondary, less pronounced peak was found below this rock band but is not visible in Fig. 5.9b. The two positive outlier of NUR (light blue circles at the left side of Fig. 5.9b) can also be explained by their specific topography: A small rock band is present in both transects but the main peak in the elevation – snow depth curve can be found in a flatter section on top of the rock face. Removing these four outliers

would increase R^2 to 0.9.

In contrast to Fig. 5.9b the correlation ($R^2 = 0.37$) for the sub-catchments (Fig. 5.9a) – even though still highly significant – appears much weaker. A downward shift as notified for the transects is not evident. As described before, the reason for this reduced correlation is probably that the level of rock cannot be clearly detected for such large areas. Moreover, the mean snow depths in each elevation band rather reflect the average of large areas with variable topography and not of a clearly differentiated terrain unit as for the transects. In combination, this higher variability counteracts the predictability of the location of the peak.

5.6 Discussion

We have shown that the vast majority of subareas are characterised by positive elevation gradients of snow depth with distinct peaks at a certain level. This finding is valid for all investigation areas and at all scales even though the effect was less universal for smaller subareas (transects). We suggest that this shape is attributed to a principal positive elevation gradient of precipitation that is modified by the interaction of the snow cover with the local terrain. Processes that reshape the precipitation distribution near the surface and the snow accumulation at the ground are first the preferential deposition of precipitation in sheltered areas and secondly the redistribution of snow by wind and gravity. These processes result in a relocation of snow from steep and exposed areas to rather sheltered gentle slopes in lower elevations. Such steep, exposed and frequently rocky areas are usually located in the highest elevations (at least for the data sets analysed in this study). This interpretation is well confirmed by our results. Hence, our results are in agreement with findings of earlier studies. Most of them reported on positive gradients of precipitation (e.g. Spreen, 1947; Peck and Brown, 1962; Frei and Schär, 1998; Blumer, 1994; Johnson and Hanson, 1995; Liu et al., 2011; Asaoka and Kominami, 2012) and snow (e.g. Rohrer et al., 1994; Bavera and De Michele, 2009; Lopez-Moreno and Stähli, 2008; Grünewald and Lehning, 2011; Lehning et al., 2011; Grünewald et al., 2013). Nevertheless, we also show that the elevation – snow depth relation can vary significantly even at small distances and that areas of negative gradients are also existing. Such variability had also been postulated in earlier publications (e.g. Lauscher, 1976; Rohrer et al., 1994; Basist et al., 1994; Sevruk, 1997; Wastl and Zängl, 2008).

We acknowledge the previously mentioned limitation in reliability of the data in extremely steep slopes. This constraint is especially affecting the ADP data (Bühler et al., 2012) but must also be considered for the ALS data, especially for HEF and NUR, that had been obtained on airplane-based platforms (Bollmann et al., 2011; Hopkinson et al., 2012). However, the relatively small portion of such steep slopes in the data strongly limits the influence of such cells on the presented analysis. Only about 5 % of the cells in DIS, STRE and HEF (2 % of NUR) are steeper than 50° and less than 2 % are steeper than 60°. For STRE and HEF about one third of these steep (>50°) cells had already been masked in the post-processing of the data. Following this, the reduced accuracy of extremely steep areas will only have a minor impact on analysis of larger subareas (entire data sets and sub-catchments). Contrary, for transects, large portions of elevation bands that coincide with pronounced rock-faces are present. However, a detailed examination of such sections did not yield any conspicuous outcome. As the results agree with our principal process understanding we are confident that the findings are adequate, especially as the focus of the analysis is rather qualitative.

5.7 Conclusions

We present a detailed assessment of the relationship of snow depth and elevation. The analysis is based on an extensive, spatial continuous data set consisting of high resolution and high quality snow depth data from seven mountain sites in the European Alps and Spanish Pyrenees. All data sets were gathered near to the maximum of the winter accumulation of the respective site and year. The analysis is performed on three different scales that range from basements or mountain ranges (entire data sets) to sub-catchments (km-scale) and individual slope transects.

We show that a characteristic shape of the elevation – snow depth relation was evident for the majority of the subareas at all scales. Typically, snow depth increases with elevation up to a certain level where a distinct peak can be found. Following this maximum, the mean snow depth tends to significantly

decrease for the highest elevations (type A in Fig. 5.4). At the mountain range scale all data sets showed the characteristic type A curve. 79 % of the sub-catchments and 72 % of the transects belong to this type. Merging the two types that are characterised by a distinct peak (A and B) increases the portion to 93 % for the sub-catchments and 79 % for the transects. However, the detailed shapes of the gradients are still variable. Location and shape of the peak and the slope of the curves differ between the subareas. Curves that deviate from this general shape are sparse but present.

We attribute this typical shape to an increase of snow fall with elevation. Snow depths are reshaped by redistribution of snow by wind and gravitational forces. In combination, these processes determine the typical shape of the gradients. In how far already the expected decrease in total precipitation / snow fall with altitude (e.g. Blanchet et al., 2009) is playing a role remains to be investigated in future.

This interpretation is fortified by an examination of the topographical location of these peaks. This analysis showed that a high correlation between the elevation of the peak and – if present – the level of predominant rocks exists. For the transects the maximum of the elevation – snow-depth relationship tends to be located 50 to 200 m below the level of rocks. Note that this study is restricted to a fistful of selected study sites and single dates in a solitary year. The transferability of the results to other years remains limited, even though several studies have identified a high temporal consistency of snow depth between different seasons (Deems et al., 2008; Schirmer et al., 2011; Helfricht et al., accepted for publication). However, it may not be assumed that such a consistency is valid for all mountain sites. Moreover, we analysed snow depth data that reflect a cumulative snow accumulation record of an entire accumulation season. Elevation gradients of single precipitation events might deviate from the patterns averaged for a complete accumulation season.

Acknowledgements

The topic of this dissertation was a detailed assessment of the spatial heterogeneity of snow depth at the small scale, based on descriptive and statistical analyses of an unique high-resolution data set from diverse mountain ranges. Such rather simple advances have a very high relevance for snow-cover modelling, especially in practical applications. The field of application includes hydrology, glaciology, mountain ecology, natural hazards and climate studies and ranges from small catchments to the large mountain areas. In many applications, estimations of the mean state of the snow cover, its distribution, spatial variability and evolution in time are usually based on a limited number of point observations like snow courses or meteorological stations which are extrapolated to larger areas. Alternatively, information based on remote sensing, mainly obtained from satellites, can be applied. However, such space borne products are strongly limited in terms of spatial resolution (usually hundreds of metres to kilometre resolution) and accuracy (Nolin, 2010; Dietz et al., 2011; Frei et al., 2012).

Many studies have developed approaches or models that aim to estimate areal snow-cover information usually restricted by amount and quality of the input data available as input. However, the quality of input data is a fundamental prerequisite. This leads us to the first research question posed in this dissertation:

How representative are snow-depth measurements at typical flat-field sites in comparison to slopes in the surrounding and to entire catchments or mountain sites?

This question is of tremendous importance as large potential biases are incorporated by non representative input data. In most recent applications this large potential source of error could not be adequately assessed and the number of studies that addressed this question is very limited. The availability of a large data set of spatially continuous snow-depth maps from different mountain regions of the world now enabled a systematic evaluation of this question based on highly accurate input data.

The results presented in Chapter 2 of this dissertation indicated that the vast majority of typical index stations defined for the study clearly overestimated snow depth of the respective catchment or mountain site. Such stations appear to be incapable to accurately represent the mean snow cover of large areas, such as catchments or mountain sites. Moreover, they also significantly deviate from the mean of their direct surrounding (tens to hundreds of metres) and from the mean snow depth of their respective elevation zone. The inability to estimate snow depth based on single measurements that are then related to their altitude was also shown in Chapter 4: Elevation gradients of snow depth calculated from meteorological stations clearly overestimated the real snow depth of two small mountain catchments. Moreover, the results of the study (Chapter 2) indicate that locations, which were characterised by a snow cover that did not significantly deviated from the catchment mean, were rather randomly distributed and not characterised by specific topographical settings. Following this, it seems impossible to identify representative locations for snow-cover observations a priori or based on topographical information alone.

As a consequence much care is required when point observations are applied as input for models or for spatial extrapolation. Unfortunately, it appears unfeasible to derive methods that are able to correct these biases. In praxis, an experienced observer might be able to adjust the relationship between snow station and the surrounding area of interest adequately. However, such familiarity requires long term observations and expert experience. Nevertheless, at sites with a high inter-annual consistency of the snow cover (Deems et al., 2008; Schirmer et al., 2011; Helfricht et al., accepted for publication; Winstral and Marks, 2014), relationships between point observation and catchment can be developed based on a detailed survey in one year and then be transferred to other years. On the contrary, Pomeroy et al.

(2004) and MacDonald et al. (2009) identified significant variations between snow cover distributions of different years for Wolf Creek, Yukon,Canada. They attribute these differences to changing directions of the dominant snow storms. This example points out that information on the consistency of climatic characteristics of a specific study site remains mandatory. Similar restrictions apply to statistical models developed for a specific data set when aiming to be assigned to other years or regions. This topic is comprised in the second set of research questions:

Can we explain the small-scale snow-depth variability with simple statistical models?
Which parameters are important? How universal are such relationships and how do they vary between different regions?
To what degree must the data spatially be aggregated to produce meaningful statistical models and how can such an aggregation be performed?

The first question was clearly approved in Chapter 3: Multiple linear regression models based on terrain parameters as explanatory variables were capable to explain 30 to 91 % of the variability of snow depth for the respective single data sets. Elevation, slope, Northing, and the mean wind-sheltering index Sx (Winstral et al., 2002) were the most frequent parameters in the models. Even though similar parameters were the best predictors for most models, the transferability between sites appeared very limited. In that context a "global" model could only explain 23 % of the variability. In contrast, it could be shown that regression models which were developed for a specific winter can well be applied for other years (Chapter 3). This high temporal consistency of the snow cover of the two sites has been confirmed by studies of Schirmer et al. (2011) and Helfricht et al. (accepted for publication).

The good performance of the regression models could only be obtained if the input data were aggregated to spatial scales of hundreds of metres (400 m grid size). Two different approaches of aggregation were tested. The first was a manual definition of sub-areas with homogenous topography (Lehning et al., 2011; Kite and Kouwen, 1992; Rinaldo et al., 2006; Pomeroy et al., 2007). The second approach was an automatic division into a quadratic grid of a similar length scale. As the results were very similar for both approaches, the simpler automatic gridding method appears favourable. Principally, such an aggregation is a prerequisite to smooth the extremely large spatial heterogeneity of snow that is typically present at scales of a few metres (Shook and Gray, 1996; Watson et al., 2006; Schirmer and Lehning, 2011). Such large heterogeneity at small scales is also a main reason for the large deviations between point observations and areal means as identified in Chapter 2.

The high relevance of elevation for the snow-cover distributions has been pointed out in Chapter 3. Elevation was shown to be an important, if not the most important predictor for snow depth in most of the study sites. Positive elevation trends were also denoted for the index stations (Chapter 2). Chapter 4 and 5 presented an isolated, systematic analysis of the relationship between elevation and snow depth. Specifically, the research questions were:

How are altitudinal gradients reflected in snow-depth measurements?
How universal are they and how do they compare to published results?
Where is the maximum of the precipitation-elevation relationship and how is the flattening of the gradients reflected in the snow distribution on the ground?
Which variables have a significant impact on the characteristics of these gradients?

To analyse the elevation gradients, 100 m elevation bands were defined and the mean snow depth of each elevation zone was derived from the snow-depth maps. Different scales, ranging from slope transects to the entire data sets were investigated. In general, it could be shown that positive relationships between elevation and snow depth were evident, especially at the larger scales. Only very few slope transects were characterised by no or even negative trends. In principal, snow depth increased with elevation up to a certain elevation level, where the gradients flattened and finally even decreased. This shape appears to be typical for the elevation – snow-depth relationship. We attribute it to a general increase of precipitation with altitude that is modified by the interaction of gravity and wind with the snow cover. This modification is most pronounced in steep and exposed terrain that is particularly present in higher elevations. A high correlation of the elevation level of the maximum snow depth with the level of rocks in the

specific transect confirmed this hypothesis. The results suggest that the typical shape of the elevation – snow-depth relationship should be considered when applying elevation gradients for tasks like interpolation of snow-cover properties. Recently, such gradients were usually assumed to be consistently positive. Such an assumption will, however, lead to a strong overestimation of snow depth in higher elevations. Moreover, the presented studies (Chapter 4 and 5) confirm that magnitude and character of the elevation gradients appears variable, even at small distances. However, Chapter 5 indicated that the snow-depth gradients showed a reasonable collapse when scaled by relative elevation. This implies a certain degree of transferability between sites.

It has been speculated that elevation gradients of precipitation are characterised by a similar form as the typical shape of snow-depth gradients identified in Chapter 5 (Havlik, 1969; Blanchet et al., 2009). Such a shape could be caused by a precipitation maximum in a certain altitude, attributed to reduced condensation due to lower air pressure (Havlik, 1969) or by a wind-induced leeward shift of the local precipitation maximum (Carruthers and Choularton, 1983; Robichaud and Austin, 1988; Zängl, 2008; Zängl et al., 2008; Mott et al., 2014). We are not aware of any study that systematically addressed this question, probably due to the lack of adequate measurement data. It has therefore not been investigated if a similar shape is characteristic for liquid precipitation. On the one hand, one of the dominant processes, the preferential deposition of precipitation (Lehning et al., 2008) interacts with both, snow fall and rain. But the effect of the wind might be larger for snow due to lower fall speeds (Colle, 2004; Zängl, 2008). On the other hand, the precipitation signal is modified by redistribution of snow, once accumulated on the ground. In that context, Scipion et al. (2013) identified significant differences between the local precipitation field and the snow cover accumulated on the ground. Scipion et al. (2013) conclude that "the small-scale variability of snow depth on the ground cannot be explained by the snowfall variability because additional wind-induced processes control snow distribution on the ground".

In general, the presented findings are in agreement with most earlier studies. Most of these studies were limited by amount and quality of input data and usually restricted to single study sites. A unique feature of this work is the high quality of the input data which allowed to model development based on "real" snow distribution. For the first time, the systematic decrease of snow depth at higher elevations has been documented for a variety of data sets.

As a final synthesis it can be stated that statistical models and elevation gradients proved to be adequate methods when assessing the spatial heterogeneity of the snow cover. Spatial extrapolation or interpolation of limited data amount are common approaches in all types of applications that require spatial information on the state of the snow cover. However, our results emphasise that much care is required. Input data might not be representative for larger areas (Chapter 2 and Chapter 4), the transferability of statistical relationships appears rather limited (Chapter 3) and even the application of simple elevation lapse rates is accompanied by significant potential biases if the exact shape of the local gradient is not accounted for (Chapter 4 and Chapter 5).

All presented studies and results are limited by the nature of the data sets. Data from seven different locations have been available for this study but most of them originate from the European Alps and are far from representing the entire range of climatological and morphological conditions found in the mountains of the world. Moreover, the data only picture single points of time of one or few winter seasons. For most study sites presented, this point of time coincided with the maximum of the seasonal snow accumulation and reflects the cumulated snow fall of an entire winter. However, multiple assessments during a season would be of interest to study if and how the relationships between snow and terrain change in time. Time periods could be reduced to single precipitation events, to periods of redistribution of snow by wind or to short events during the ablation season. Such data sets have been obtained from terrestrial laser scanning surveys but are currently restricted to rather small areas (Grünewald et al., 2010; Egli et al., 2011; Schirmer et al., 2011; Mott et al., 2011a,b; Revuelto et al., 2014). For precipitation, operational weather radars could be applied to investigate the spatial characteristics of snow fall and rain while still in the air (Scipion et al., 2013; Mott et al., 2014). Such studies are currently not existing. The difference between the those measured precipitation fields and the snow accumulation on the ground was, however, found to be large (Scipion et al., 2013). Furthermore, for most study sites the snow cover has been surveyed just for single or very few years. Data sets from winter seasons characterised by different climatological conditions would be valuable to prove if results can be transformed to other years.

Nevertheless, it can be expected that an increasing number of large data sets are getting available in the near future. This is attributed to the combination of a rising interest of the hydrological community with rapid advances that are currently made in remote sensing of snow. This will finally result in significant cost reductions for data gathering. In that context, the NASA has currently launched a demonstration mission: Airborne LiDAR surveys are obtained weekly to monitor the snow cover of large catchments in California and Colorado (*http://www.jpl.nasa.gov/news/news.php?release=2013-154*).

A further limitation of this dissertation is that the analyses were restricted to alpine, non-vegetated regions. An expansion to vegetated areas would be possible although it must be considered that the accuracy of the data is clearly reduced in forested areas (Hopkinson et al., 2012). Moreover, additional processes such as interception of snow by trees would have to be considered in the statistical interpretations.

Finally, advances in model development might allow to apply physically based models to assess the spatial and temporal variability of the snow cover. Due to large computational demands, the application of such models is currently restricted to small areas or short periods of time. However, the fast enhancement of computational power might overcome computational limitations in the near future. Nonetheless, such physical models still depend on input data such as precipitation, snow depth, wind, temperature and radiation. These parameters are usually obtained from few meteorological stations and then extrapolated to the area of interest. However, as shown in this thesis, such an extrapolation is potentially problematic. It might be valid for parameters such as air temperature or radiation: Air temperature is characterised by a relatively constant elevation lapse rate that can be derived from a pair of stations in different altitudes. Longwave radiation strongly depends on the cloud coverage but is rather constant in space for clear sky or continuous cloud cover and shortwave radiation can be well modelled when interactions with the terrain are accounted for. Wind speed and wind directions can sufficiently be calculated with mesoscale atmospheric models, that are, however, computational very expensive. Contrary, we showed that the extrapolation of precipitation and snow depth might be problematic. The non-representativeness of the measurements requires much care when working with snow depth data from "index stations" and the non-linearity of the elevation gradients needs to be considered. The typical shape of the elevation – snow-

depth relationship, with an decrease in higher elevations, must therefore be accounted for in extrapolation schemes.

Alvarez-Mozos, J., M. A. Campo, R. Gimenez, J. Casali, and U. Leibar, 2011: Implications of scale, slope, tillage operation and direction in the estimation of surface depression storage. *Soil and Tillage Research*, **111 (2)**, 142–153, doi:10.1016/j.still.2010.09.004.

Anderton, S. P., S. M. White, and B. Alvera, 2004: Evaluation of spatial variability in snow water equivalent for a high mountain catchment. *Hydrological Processes*, **18 (3)**, 435–453, doi:10.1002/Hyp. 1319,2004.

Arakawa, O. and A. Kitoh, 2011: Intercomparison of the relationship between precipitation and elevation among gridded precipitation datasets over the Asian summer monsoon region. *Global Environ. Res*, **15**, 109–118.

Asaoka, Y. and Y. Kominami, 2012: Spatial snowfall distribution in mountainous areas estimated with a snow model and satellite remote sensing. *Hydrological Research Letters*, **6**, 1–6.

Balk, B. and K. Elder, 2000: Combining binary decision tree and geostatistical methods to estimate snow distribution in a mountain watershed. *Water Resources Research*, **36 (1)**, 13–26, doi:10.1029/ 1999wr900251.

Baltsavias, E., 1999: Airborne laser scanning: basic relations and formulas. *Journal of Photogrammetry and Remote Sensing*, **54**, 199–214.

Barnett, T. P., J. C. Adam, and D. P. Lettenmaier, 2005: Potential impacts of a warming climate on water availability in snow-dominated regions. *Nature*, **438 (7066)**, 303–309, doi:10.1038/nature04141.

Basist, A., G. D. Bell, and V. Meentemeyer, 1994: Statistical relationships between topography and precipitation patterns. *Journal of Climate*, **7 (9)**, 1305–1315, doi:10.1175/1520-0442(1994)007⟨1305: srbtap⟩2.0.co;2.

Baumgartner, A., E. Reichel, and G. Weber, 1983: *Der Wasserhaushalt der Alpen. Niederschlag, Verdunstung, Abfluss und Gletscherspende im Gesamtgebiet der Alpen im Jahresdurchschnitt fr̈ die Normalperiode 1931-1960.* Oldernburg, Munich, 343 pp.

Bavay, M., T. Grünewald, and M. Lehning, 2013: Response of snow cover and runoff to climate change in high Alpine catchments of Eastern Switzerland. *Advances in Water Resources*, doi:10.1016/j.advwatres. 2012.12.009.

Bavay, M., M. Lehning, T. Jonas, and H. Löwe, 2009: Simulations of future snow cover and discharge in Alpine headwater catchments. *Hydrological Processes*, **23 (1)**, 95–108, doi:10.1002/hyp.7195.

Bavera, D. and C. De Michele, 2009: Snow water equivalent estimation in the mallero basin using snow gauge data and MODIS images and fieldwork validation. *Hydrol Process*, **23 (14)**, 1961–1972, doi: 10.1002/hyp.7328.

Beniston, M., 1997: Snow pack in the Swiss Alps under changing climatic conditions: an empirical approach for climate impacts studies. *Climatic Change*, **36 (3/4)**, 281–300.

Beniston, M., F. Keller, and S. Goyette, 2003: Snow pack in the Swiss Alps under changing climatic conditions: an empirical approach for climate impacts studies. *Theoretical and Applied Climatology*, **74 (1-2)**, 19–31, doi:10.1007/s00704-002-0709-1.

Bernhardt, M. and K. Schulz, 2010: SnowSlide: A simple routine for calculating gravitational snow transport. *Geophysical Research Letters*, **37**, doi:10.1029/2010gl043086.

Bernhardt, M., G. Zängl, G. E. Liston, U. Strasser, and W. Mauser, 2009: Using wind fields from a high-resolution atmospheric model for simulating snow dynamics in mountainous terrain. *Hydrological Processes*, **23 (7)**, 1064–1075, doi:10.1002/hyp.7208.

Birkeland, K. W., K. J. Hansen, and R. L. Brown, 1995: The spatial variability of snow resistance on potential avalanche slopes. *Journal of Glaciology*, **41**, 183–190.

Blanchet, J., C. Marty, and M. Lehning, 2009: Extreme value statistics of snowfall in the Swiss Alpine region. *Water Resources Research*, **45**, 12, doi:10.1029/2009wr007916.

Blöschl, G., 1999: Scaling issues in snow hydrology. *Hydrological Processes*, **13 (14-15)**, 2149–2175.

Blöschl, G., R. B. Grayson, and M. Sivapalan, 1995: On the representative elementary area (rea) concept and its utility for distributed rainfall-runoff modelling. *Hydrological Processes*, **9 (3-4)**, 313–330, doi:10.1002/hyp.3360090307.

Blöschl, G. and R. Kirnbauer, 1992: An analysis of snow cover patterns in a small alpine catchment. *Hydrological Processes*, **6 (1)**, 99–109.

Blumer, F., 1994: Höhenabhängigkeit des Niederschlags im Alpenraum. Ph.D. thesis.

Bollmann, E., R. Sailer, C. Briese, J. Stotter, and P. Fritzmann, 2011: Potential of airborne laser scanning for geomorphologic feature and process detection and quantifications in high alpine mountains. *Zeitschrift für Geomorphologie*, **55**, 83–104, doi:10.1127/0372-8854/2011/0055s2-0047.

Bühler, Y., A. Hüni, M. Christen, R. Meister, and T. Kellenberger, 2009: Automated detection and mapping of avalanche deposits using airborne optical remote sensing data. *Cold Regions Science and Technology*, **57 (2-3)**, 99–106, doi:10.1016/j.coldregions.2009.02.007.

Bühler, Y., M. Marty, L. Egli, J. Veitinger, T. Jonas, P. Thee, and C. Ginzler, 2014: Spatially continuous mapping of snow depth in high alpine catchments using digital photogrammetry. *The Cryosphere Discuss.*

Bühler, Y., M. Marty, and C. Ginzler, 2012: High resolution DEM generation in high-alpine terrain using airborne remote sensing techniques. *Transactions in GIS*, **16 (5)**, 635–647, doi:10.1111/j.1467-9671.2012.01331.x.

Burrough, P. A., 1981: Fractal dimensions of landscapes and other environmental data. *Nature*, **294 (5838)**, 240–242.

Burrough, P. A., 1993: Fractals and geostatistical methods in landscape studies. *Fractals in Geography*, N. Lam and L. De Cola, Eds., Englewood Cliffs, New York, 87–121.

Carroll, S. S. and N. Cressie, 1996: A comparison of geostatistical methodologies used to estimate snow water equivalent. *Water Resources Bulletin*, **32 (2)**, 267–278.

Carruthers, D. J. and T. W. Choularton, 1983: A model of the feeder-seeder mechanism of orographic rain including stratification and wind-drift effects. *Quarterly Journal of the Royal Meteorological Society*, **109 (461)**, 575–588, doi:10.1002/qj.49710946109.

Cavalieri, D. J., et al., 2012: A comparison of snow depth on sea ice retrievals using airborne altimeters and an AMSR-E simulator. *Ieee Transactions on Geoscience and Remote Sensing*, **50 (8)**, 3027–3040, doi:10.1109/tgrs.2011.2180535.

Chang, A. T. C., R. E. J. Kelly, E. G. Josberger, R. L. Armstrong, J. L. Foster, and N. M. Mognard, 2005: Analysis of ground-measured and passive-microwave-derived snow depth variations in midwinter across the northern Great Plains. *Journal of Hydrometeorology*, **6 (1)**, 20–33, doi:10.1175/jhm-405.1.

Chang, K. T. and Z. X. Li, 2000: Modelling snow accumulation with a geographic information system. *International Journal of Geographical Information Science*, **14 (7)**, 693–707.

Choularton, T. W. and S. J. Perry, 1986: A model of the orographic enhancement of snowfall by the seeder-feeder mechanism. *Quarterly Journal of the Royal Meteorological Society*, **112 (472)**, 335–345.

Clark, M. P., et al., 2011: Representing spatial variability of snow water equivalent in hydrologic and land-surface models: A review. *Water Resources Research*, **47**, doi:10.1029/2011wr010745.

Cline, D., K. Elder, and R. Bales, 1998: Scale effects in a distributed snow water equivalence and snowmelt model for mountain basins. *Hydrological Processes*, **12 (10-11)**, 1527–1536, doi:10.1002/(sici)1099-1085(199808/09)12:10/11⟨1527::aid-hyp678⟩3.0.co;2-e.

Colle, B. A., 2004: Sensitivity of orographic precipitation to changing ambient conditions and terrain geometries: An idealized modeling perspective. *Journal of the Atmospheric Sciences*, **61 (5)**, 588–606, doi:10.1175/1520-0469(2004)061⟨0588:sooptc⟩2.0.co.

Dadic, R., J. G. Corripio, and P. Burlando, 2008: Mass-balance estimates for Haut Glacier d'Arolla, Switzerland, from 2000 to 2006 using DEMs and distributed mass-balance modeling. *Annals of Glaciology*, **49**, 22–26.

Dadic, R., R. Mott, M. Lehning, and P. Burlando, 2010a: Parameterization for wind-induced preferential deposition of snow. *Hydrological Processes*, **24 (14)**, 1994–2006, doi:10.1002/hyp.7776.

Dadic, R., R. Mott, M. Lehning, and P. Burlando, 2010b: Wind influence on snow depth distribution and accumulation over glaciers. *Journal of Geophysical Research-Earth Surface*, **115**, 8, doi:10.1029/2009JF001261.

Daly, C., M. Halbleib, J. I. Smith, W. P. Gibson, M. K. Doggett, G. H. Taylor, J. Curtis, and P. P. Pasteris, 2008: Physiographically sensitive mapping of climatological temperature and precipitation across the conterminous United States. *International Journal of Climatology*, **28 (15)**, 2031–2064, doi:10.1002/Joc.1688.

Daly, C., R. P. Neilson, and D. L. Phillips, 1994: A statistical-topographic model for mapping climatological precipitation over mountainous terrain. *Journal of Applied Meteorology*, **33 (2)**, 140–158, doi:0.1175/1520-0450(1994)033⟨0140:astmfm⟩2.0.co;2.

Daly, S. F., R. Davis, E. Ochs, and T. Pangburn, 2000: An approach to spatially distributed snow modelling of the Sacramento and San Joaquin basins, California. *Hydrological Processes*, **14 (18)**, 3257–3271, doi:10.1002/1099-1085(20001230)14:18⟨3257::aid-hyp199⟩3.0.co;2-z.

DeBeer, C. M. and J. W. Pomeroy, 2010: Simulation of the snowmelt runoff contributing area in a small alpine basin. *Hydrology and Earth System Sciences*, **14 (7)**, 1205–1219, doi:10.5194/hess-14-1205-2010.

Deems, J. S., S. R. Fassnacht, and K. J. Elder, 2006: Fractal distribution of snow depth from Lidar data. *Journal of Hydrometeorology*, **7 (2)**, 285–297.

Deems, J. S., S. R. Fassnacht, and K. J. Elder, 2008: Interannual consistency in fractal snow depth patterns at two Colorado mountain sites. *Journal of Hydrometeorology*, **9 (5)**, 977–988, doi:10.1175/2008jhm901.1.

Deems, J. S. and T. H. Painter, 2006: Lidar measurement of snow depth: Accuracy and error sources. *Proceedings International Snow Science Workshop ISSW 2006, Telluride, CO*, **Proceedings International Snow Science Workshop ISSW**, 384–391.

Deems, J. S., T. H. Painter, and D. C. Finnegan, 2013: Lidar measurement of snow depth: a review. *Journal of Glaciology*, **59 (215)**, 467–479, doi:10.3189/2013JoG12J154.

Dietz, A. J., C. Künzer, U. Gessner, and S. Dech, 2011: Remote sensing of snow - a review of available methods. *International Journal of Remote Sensing*, **33 (13)**, 4094–4134, doi:10.1080/01431161.2011.640964.

Durand, Y., G. Giraud, M. Laternser, P. Etchevers, L. Mèrindol, and B. Lesaffre, 2009: Reanalysis of 47 years of climate in the french alps (1958-2005): Climatology and trends for snow cover. *Journal of Applied Meteorology and Climatology*, **48 (12)**, 2487–2512, doi:10.1175/2009jamc1810.1.

Egli, L., 2008: Spatial variability of new snow amounts derived from a dense network of Alpine automatic stations. *Annals of Glaciology*, **49**, 51–55, doi:10.3189/172756408787814843.

Egli, L., N. Griessinger, and T. Jonas, 2011: Seasonal development of spatial snow-depth variability across different scales in the Swiss Alps. *Annals of Glaciology*, **52 (58)**, 216–222, doi:10.3189/172756411797252211.

Egli, L., T. Jonas, T. Grünewald, M. Schirmer, and P. Burlando, 2012: Dynamics of snow ablation in a small alpine catchment observed by repeated terrestrial laser scans. *Hydrological Processes*, **26 (10)**, 1574–1585, doi:10.1002/hyp.8244.

Elder, K., J. Dozier, and J. Michaelsen, 1991: Snow accumulation and distribution in an alpine watershed. *Water Resources Research*, **27 (7)**, 1541–1552, doi:10.1029/91wr00506.

Elder, K., W. Rosenthal, and R. E. Davis, 1998: Estimating the spatial distribution of snow water equivalence in a montane watershed. *Hydrological Processes*, **12 (10-11)**, 1793–1808.

Emerson, C. W., N. S. N. Lam, and D. A. Quattrochi, 1999: Multi-scale fractal analysis of image texture and pattern. *Photogrammetric Engineering and Remote Sensing*, **65 (1)**, 51–61.

Erickson, T. A., M. W. Williams, and A. Winstral, 2005: Persistence of topographic controls on the spatial distribution of snow in rugged mountain terrain, Colorado, United States. *Water Resources Research*, **41 (4)**, doi:10.1029/2003wr002973.

Erxleben, J., K. Elder, and R. Davis, 2002: Comparison of spatial interpolation methods for estimating snow distribution in the Colorado Rocky Mountains. *Hydrological Processes*, **16 (18)**, 3627–3649, doi:10.1002/Hyp.1239.

Essery, R., E. Martin, H. Douville, A. Fernandez, and E. Brun, 1999: A comparison of four snow models using observations from an alpine site. *Climate Dynamics*, **15 (8)**, 583–593, doi:10.1007/s003820050302.

Evans, I. S., 1972: General geomorphometry, derivatives of altitude, and descriptive statistics. *Spatial Analysis in Geomorphology*, R. Chorley, Ed., Harper & Row, London, 17–90.

Fang, X. and J. W. Pomeroy, 2009: Modelling blowing snow redistribution to prairie wetlands. *Hydrological Processes*, **23 (18)**, 2557–2569, doi:10.1002/hyp.7348.

Foppa, N., A. Stoffel, and R. Meister, 2005: Snow depth mapping in the alps: Merging of in situ and remotely-sensed data. *EARSeL eProceedings*, **4 (1)**, 119–129.

Fox, C. G. and D. E. Hayes, 1985: Quantitative methods for analyzing the roughness of the seafloor. *Reviews of Geophysics*, **23 (1)**, 1–48, doi:10.1029/RG023i001p00001, URL http://dx.doi.org/10.1029/RG023i001p00001.

Frei, A., M. Tedesco, S. Lee, J. Foster, D. K. Hall, R. Kelly, and D. A. Robinson, 2012: A review of global satellite-derived snow products. *Advances in Space Research*, **50 (8)**, 1007–1029, doi:10.1016/j.asr.2011.12.021.

Frei, C. and C. Schär, 1998: A precipitation climatology of the Alps from high-resolution rain-gauge observations. *International Journal of Climatology*, **18 (8)**, 873–900.

Gauer, P., 2001: Numerical modeling of blowing and drifting snow in Alpine terrain. *Journal of Glaciology*, **47 (156)**, 97–110.

Geist, T., B. Höfle, M. Rutzinger, and J. Stötter, 2009: Laser scanning - a paradigm change in topographic data acquisition for natural hazard management. *Sustainable Natural Hazard Management in Alpine Environments*, E. Veulliet, J. Stötter, and H. Weck-Hannemann, Eds., Springer, Dordrecht, Heidelberg, London, New York, Berlin, 309–344.

Geist, T. and J. Stötter, 2008: Documentation of glacier surface elevation change with multi-temporal airborne laser scanner data - case study: Hintereisferner and Kesselwandferner, Tyrol, Austria. *Zeitschrift für Gletscherkunde und Glazialgeologie*, **41**, 77–106.

Gerrard, J., 1990: *Mountain Environments: An Examination of the Physical Geography of Mountains*. MIT Press, London, 317 pp.

Golding, D. L., 1974: The correlation of snowpack with topography and snowmelt runoff on Marmot Creek Basin, Alberta. *Atmosphere*, **12 (1)**, 31–38, doi:10.1080/00046973.1974.9648368.

Goodchild, M. F. and D. M. Mark, 1987: The fractal nature of geographic phenomena. *Annals of the Association of American Geographers*, **77 (2)**, 265–278, doi:10.1111/j.1467-8306.1987.tb00158.x.

Gruber, S., 2007: A mass-conserving fast algorithm to parameterize gravitational transport and deposition using digital elevation models. *Water Resources Research*, **43 (6)**, W06 412, doi:10.1029/2006wr004868.

Grünewald, T. and M. Lehning, 2011: Altitudinal dependency of snow amounts in two small alpine catchments: can catchment-wide snow amounts be estimated via single snow or precipitation stations? *Annals of Glaciology*, **52 (58)**, 153–158.

Grünewald, T., M. Schirmer, R. Mott, and M. Lehning, 2010: Spatial and temporal variability of snow depth and ablation rates in a small mountain catchment. *The Cryosphere*, **4 (2)**, 215–225, doi:10.5194/tc-4-215-2010.

Grünewald, T., et al., 2013: Statistical modelling of the snow depth distribution in open alpine terrain. *Hydrology and Earth System Sciences*, **17 (8)**, 3005–3021, doi:10.5194/hess-17-3005-2013.

Havlik, D., 1969: Die Höhenstufe maximaler Niederschlagssummen in den Westalpen. *Freiburger Geographische Hefte*, **7**, 76.

Helbig, N., H. Lowe, and M. Lehning, 2009: Radiosity approach for the shortwave surface radiation balance in complex terrain. *Journal of the Atmospheric Sciences*, **66 (9)**, 2900–2912, doi:10.1175/2009jas2940.1.

Helfricht, K., J. Schöber, K. Schneider, R. Sailer, and M. Kuhn, accepted for publication: Inter-annual persistence of the seasonal snow cover in a glacierized catchment. *Journal of Glaciology*, **(13J197)**.

Hopkinson, C., T. Collins, A. Anderson, J. Pomeroy, and I. Spooner, 2012: Spatial snow depth assessment using LiDAR transect samples and public gis data layers in the Elbow River Watershed, Alberta. *Canadian Water Resources Journal*, **37 (2)**, 69–87, doi:10.4296/cwrj3702893.

Hopkinson, C., J. Pomeroy, C. De Beer, C. Ellis, and A. Anderson, 2011: Relationships between snowpack depth and primary LiDAR point cloud derivatives in a mountainous environment. *Remote Sensing and Hydrology (Proceedings of a symposium held at Jackson Hole, Wyoming, USA, September 2010) (IAHS Publ. 352).*, IAHS Publ., Vol. 352.

Hopkinson, C., M. Sitar, L. Chasmer, and P. Treitz, 2004: Mapping snowpack depth beneath forest canopies using airborne lidar. *Photogrammetric Engineering and Remote Sensing*, **70 (3)**, 323–330.

Hopkinson, C., et al., 2001: Mapping the spatial distribution of snowpack depth beneath a variable forest canopy using airborne laser altimetry. *58th Eastern Snow Conference, Ottawa*.

Hosang, J. and K. Dettwiler, 1991: Evaluation of a water equivalent of snow cover map in a small catchment-area using a geostatistical approach. *Hydrological Processes*, **5 (3)**, 283–290.

Houze, R. A., 2012: Orographic effects on precipitating clouds. *Reviews of Geophysics*, **50 (1)**, RG1001, doi:10.1029/2011rg000365.

Johnson, G. L. and C. L. Hanson, 1995: Topographic and atmospheric influences on precipitation variability over a mountainous watershed. *Journal of Applied Meteorology*, **34 (1)**, 68–87, doi: 10.1175/1520-0450-34.1.68.

Jonas, T., C. Marty, and J. Magnusson, 2009: Estimating the snow water equivalent from snow depth measurements in the Swiss Alps. *J Hydrol*, **378**, 161–167, doi:10.1016/j.jhydrol.2009.09.021.

Jost, G., M. Weiler, D. R. Gluns, and Y. Alila, 2007: The influence of forest and topography on snow accumulation and melt at the watershed-scale. *Journal of Hydrology*, **347 (1-2)**, 101–115, doi:10.1016/ j.jhydrot.2007.09.006.

Keller, H., T. Strobel, and F. Forster, 1984: Die räumliche und zeitliche Variabilität der Schneedecke in einem schweizerischen Voralpental. *DVWK-Mitteilungen*, **7 (Schneehydrologische Forschung in Mitteleuropa)**, 257–284.

Kirchhofer, W. and B. Sveruk, 1992: Mittlere jährliche korrigierte Niederschlagshöhen 1951-1980. *Hydrologischer Atlas der Schweiz*, Landeshydrologie und Geologie, Bern.

Kite, G. W. and N. Kouwen, 1992: Watershed modeling using land classifications. *Water Resources Research*, **28 (12)**, 3193–3200, doi:10.1029/92wr01819.

Klinkenberg, B., 1992: Fractals and morphometric measures: is there a relationship? *Geomorphology*, **5 (1-2)**, 5–20, doi:10.1016/0169-555x(92)90055-s.

Klinkenberg, B. and M. F. Goodchild, 1992: The fractal properties of topography: A comparison of methods. *Earth Surface Processes and Landforms*, **17 (3)**, 217–234, doi:10.1002/esp.3290170303.

Kuchment, L. S. and A. N. Gelfan, 2001: Statistical self-similarity of spatial variations of snow cover: verification of the hypothesis and application in the snowmelt runoff generation models. *Hydrological Processes*, **15 (18)**, 3343–3355.

Ku'zmin, P. P., 1960: Formirovanie snezhnogo pokrova i metody opredeleniya snegozapasov. *Gidrometeoizdat: Leningrad. (Published 1963 as Snow Cover and Snow Reserves. [English Translation by Israel Program for Scientific Translation, Jerusalem]. National Science Foundation: Washington, DC)*.

Lang, H., 1985: Hӧhenabhängigkeit der Niederschläge. *Der Niederschlag in der Schweiz*, B. Sevruk, Ed., Kümmerly + Frey, Bern, Beiträge zur Geologie der Schweiz - Hydrologie, Vol. 31, 149–157.

Lauscher, F., 1976: Weltweite Typen der Höhenabhängigkeit des Niederschlags. *Wetter und Leben*, **28**, 80–90.

Lehning, M., P. Bartelt, B. Brown, T. Russi, U. Stöckli, and M. Zimmerli, 1998: A network of automatic weather and snow stations and supplementary model calculations providing snowpack information for avalanche warning. *Proceedings of the International Snow Science Workshop "a merging of theory and practice", September 27 to October 1, 1998, Sunriver, Oregon.*, 225–233.

Lehning, M., P. Bartelt, B. Brown, T. Russi, U. Stöckli, and M. Zimmerli, 1999: SNOWPACK model calculations for avalanche warning based upon a new network of weather and snow stations. *Cold Regions Science and Technology*, **30 (1-3)**, 145–157, doi:10.1016/S0165-232X(99)00022-1.

Lehning, M., T. Gruenewald, and M. Schirmer, 2011: Mountain snow distribution governed by an altitudinal gradient and terrain roughness. *Geophysical Research Letters*, **38**, doi:10.1029/2011GL048927.

Lehning, M., H. Löwe, M. Ryser, and N. Raderschall, 2008: Inhomogeneous precipitation distribution and snow transport in steep terrain. *Water Resources Research*, **44 (7)**, W07404, doi: 10.1029/2007wr006545.

Lehning, M., I. Völksch, D. Gustafsson, T. A. Nguyen, M. Stähli, and M. Zappa, 2006: ALPINE3D: a detailed model of mountain surface processes and its application to snow hydrology. *Hydrological Processes*, **20 (10)**, 2111–2128, doi:10.1002/Hyp.6204.

Liston, G. E. and K. Elder, 2006: A distributed snow-evolution modeling system (SnowModel). *Journal of Hydrometeorology*, **7 (6)**, 1259–1276, doi:10.1175/Jhm548.1.

Liston, G. E., R. B. Haehnel, M. Sturm, C. A. Hiemstra, S. Berezovskaya, and R. D. Tabler, 2007: Instruments and methods simulating complex snow distributions in windy environments using SnowTran-3D. *Journal of Glaciology*, **53 (181)**, 241–256.

Litaor, M. I., M. Williams, and T. R. Seastedt, 2008: Topographic controls on snow distribution, soil moisture, and species diversity of herbaceous alpine vegetation, Niwot Ridge, Colorado. *Journal of Geophysical Research-Biogeosciences*, **113 (G2)**, doi:10.1029/2007jg000419.

Liu, C., K. Ikeda, G. Thompson, R. Rasmussen, and J. Dudhia, 2011: High-resolution simulations of wintertime precipitation in the Colorado headwaters region: Sensitivity to physics parameterizations. *Monthly Weather Review*, **139 (11)**, 3533–3553, doi:10.1175/mwr-d-11-00009.1.

Lopez-Moreno, J. I., S. R. Fassnacht, S. Begueria, and J. B. P. Latron, 2011: Variability of snow depth at the plot scale: implications for mean depth estimation and sampling strategies. *The Cryosphere*, **5 (3)**, 617–629, doi:10.5194/tc-5-617-2011.

Lopez-Moreno, J. I. and D. Nogues-Bravo, 2006: Interpolating local snow depth data: an evaluation of methods. *Hydrological Processes*, **20 (10)**, 2217–2232, doi:10.1002/Hyp.6199.

Lopez-Moreno, J. I. and M. Stähli, 2008: Statistical analysis of the snow cover variability in a subalpine watershed: Assessing the role of topography and forest, interactions. *Journal of Hydrology*, **348 (3-4)**, 379–394, doi:10.1016/j.jhydrol.2007.10.018.

Lundquist, J. D. and M. D. Dettinger, 2005: How snowpack heterogeneity affects diurnal streamflow timing. *Water Resources Research*, **41 (5)**, doi:10.1029/2004wr003649.

MacDonald, M. K., J. W. Pomeroy, and A. Pietroniro, 2009: Parameterizing redistribution and sublimation of blowing snow for hydrological models: tests in a mountainous subarctic catchment. *Hydrological Processes*, **23 (18)**, 2570–2583, doi:10.1002/hyp.7356.

MacDonald, M. K., J. W. Pomeroy, and A. Pietroniro, 2010: On the importance of sublimation to an alpine snow mass balance in the Canadian Rocky Mountains. *Hydrology and Earth System Sciences*, **14 (7)**, 1401–1415, doi:10.5194/hess-14-1401-2010.

Magnusson, J., T. Jonas, I. Lopez-Moreno, and M. Lehning, 2010: Snow cover response to climate change in a high alpine and half-glacierized basin in Switzerland. *Hydrology Research*, **41 (3-4)**, 230–240, doi:10.2166/nh.2010.115.

Mandelbrot, B., 1977: *Fractals: Form, Chance and Dimension.* W.H. Freeman and Company, San Francisco, CA.

Mandelbrot, B., 1982: *The Fractal Geometry of Nature.* W.H. Freeman and Company, New York.

Marchand, W. D. and A. Killingtveit, 2005: Statistical properties of spatial snowcover in mountainous catchments in Norway. *Nordic Hydrology*, **35 (2)**, 101–117.

Mark, D., 1975: Geomorphometric parameters: A review and evaluation. *Geografiska Annaler. Series A, Physical Geography*, **57 (3/4)**, 165–177.

Marsh, C. B., J. W. Pomeroy, and R. J. Spiteri, 2012: Implications of mountain shading on calculating energy for snowmelt using unstructured triangular meshes. *Hydrological Processes*, **26 (12)**, 1767–1778, doi:10.1002/hyp.9329.

Maune, D., 2001: *Digital Elevation Model Technologies and Applications: The DEM Users Manual.* American Society for Photogrammetry and Remote Sensing.

McKay, G. A. and D. M. Gray, 1981: The distribution of the snow cover. *Handbook of Snow*, D. Gray and D. Hale, Eds., Pergamon Press Canada Ltd., 153–190.

Melvold, K. and T. Skaugen, 2013: Multiscale spatial variability of lidar-derived and modeled snow depth on Hardangervidda, Norway. *Annals of Glaciology*, **54 (62)**, 273–281, doi:10.3189/2013AoG62A161.

Meromy, L., N. P. Molotch, T. E. Link, S. R. Fassnacht, and R. Rice, 2013: Subgrid variability of snow water equivalent at operational snow stations in the western USA. *Hydrological Processes*, **27 (17)**, 2383–2400, doi:10.1002/hyp.9355.

Molotch, N. P., M. T. Colee, R. C. Bales, and J. Dozier, 2005: Estimating the spatial distribution of snow water equivalent in an alpine basin using binary regression tree models: the impact of digital elevation data and independent variable selection. *Hydrological Processes*, **19 (7)**, 1459–1479, doi: 10.1002/Hyp.5586.

Moreno Baños, I., et al., 2009: Snowpack depth modelling and water availability from LIDAR measurements in eastern Pyrenees. 202-206 pp.

Mott, R., L. Egli, T. Grünewald, N. Dawes, C. Manes, M. Bavay, and M. Lehning, 2011a: Micrometeorological processes driving snow ablation in an Alpine catchment. *The Cryosphere*, **5 (4)**, 1083–1098, doi:10.5194/tc-5-1083-2011.

Mott, R. and M. Lehning, 2010: Meteorological modelling of very high resolution wind fields and snow deposition for mountains. *Journal of Hydrometeorology*, doi:10.1175/2010jhm1216.1.

Mott, R., M. Schirmer, M. Bavay, T. Grünewald, and M. Lehning, 2010: Understanding snow-transport processes shaping the mountain snow-cover. *The Cryosphere*, **4 (4)**, 545–559, doi:10.5194/tc-4-545-2010.

Mott, R., M. Schirmer, and M. Lehning, 2011b: Scaling properties of wind and snow-depth distribution in an Alpine catchment. *J. Geophys. Res.*, **116**, 1–8, doi:doi:10.1029/2010JD014886.

Mott, R., D. Scipión, M. Schneebeli, N. Dawes, A. Berne, and M. Lehning, 2014: Orographic effects on snow deposition patterns in mountainous terrain. *Journal of Geophysical Research: Atmospheres*, **119 (3)**, 1419–1439, doi:10.1002/2013jd019880.

Neumann, N. N., C. Derksen, C. Smith, and B. Goodison, 2006: Characterizing local scale snow cover using point measurements during the winter season. *Atmosphere-Ocean*, **44 (3)**, 257–269, doi:10.3137/ao.440304.

Nolin, A. W., 2010: Recent advances in remote sensing of seasonal snow. *Journal of Glaciology*, **56 (200)**, 1141–1150, doi:10.3189/002214311796406077.

Odermatt, D., D. Schläpfer, M. Lehning, M. Schwikowski, M. Kneubühler, and K. Itten, 2005: Seasonal study of directional reflectance properties of snow. *EARSeL eProceedings*, **4 (2)**, 203–214.

Peck, E. L. and M. J. Brown, 1962: An approach to the development of isohyetal maps for mountainous areas. *Journal of Geophysical Research*, **67 (2)**, 681–694, doi:10.1029/JZ067i002p00681.

Pentland, A. P., 1984: Fractal-based description of natural scenes. *Ieee Transactions on Pattern Analysis and Machine Intelligence*, **6 (6)**, 661–674.

Pipp, W. W., M. amd Locke, 1998: Local scale variability in storm snowfall and seasonal snowpack distributions in the Bridger Range, Montana. *Proceedings of the 66th Western Snow Conference. April 20 to 23 1998, Snowbird, Utah*, 26–37.

Plattner, C., L. Braun, and A. Brenning, 2006: Spatial variability of snow accumulation on vernagtferner, Austrian Alps, in winter 2003/04. *Zeitschrift für Gletscherkunde und Glazialgeologie*, **39**, 43–57.

Pohl, S., P. Marsh, and G. E. Liston, 2006: Spatial-temporal variability in turbulent fluxes during spring snowmelt. *Arctic Antarctic and Alpine Research*, **38 (1)**, 136–146, doi:10.1657/1523-0430(2006) 038[0136:svitfd]2.0.co;2.

Pomeroy, J., R. Essery, and B. Toth, 2004: Implications of spatial distributions of snow mass and melt rate for snow-cover depletion: observations in a subarctic mountain catchment. *Annals of Glaciology*, **38**, 195–201, doi:10.3189/172756404781814744.

Pomeroy, J., X. Fang, M. Solohub, and X. Guan, 2011: Marmot Creek hydrometeorological database (Nakiska Alpine Ridgetop AWS). IP3 Archive (www.usask.ca/ip3/data).

Pomeroy, J. W. and E. Brun, 2001: Physical properties of snow. *Snow Ecology: an Interdisciplinary Examination of Snow-covered Ecosystems*, D. A. W. H. G. Jones, J. W. Pomeroy and R. W. H. (eds.), Eds., Cambridge University Press, Cambridge, UK., 45–118.

Pomeroy, J. W., X. Fang, and C. Ellis, 2012: Sensitivity of snowmelt hydrology in Marmot Creek, Alberta, to forest cover disturbance. *Hydrological Processes*, **26 (12)**, 1892–1905, doi:10.1002/hyp.9248.

Pomeroy, J. W. and D. M. Gray, 1995: *Snowcover Accumulation, Relocation and Management.* National Hydrology Research Institute Science Report No. 7, Environment Canada: Saskatoon, 144 pp pp.

Pomeroy, J. W., D. M. Gray, T. Brown, N. R. Hedstrom, W. L. Quinton, R. J. Granger, and S. K. Carey, 2007: The cold regions hydrological model: a platform for basing process representation and model structure on physical evidence. *Hydrological Processes*, **21 (19)**, 2650–2667, doi:10.1002/hyp.6787.

Pomeroy, J. W., D. M. Gray, N. R. Hedstrom, and J. R. Janowicz, 2002: Prediction of seasonal snow accumulation in cold climate forests. *Hydrological Processes*, **16 (18)**, 3543–3558, doi:10.1002/hyp.1228.

Pomeroy, J. W., D. M. Gray, K. R. Shook, B. Toth, R. L. H. Essery, A. Pietroniro, and N. Hedstrom, 1998: An evaluation of snow accumulation and ablation processes for land surface modelling. *Hydrological Processes*, **12 (15)**, 2339–2367, doi:10.1002/(sici)1099-1085(199812)12:15⟨2339::aid-hyp800⟩3.0.co;2-l.

Pomeroy, J. W. and L. Li, 2000: Prairie and arctic areal snow cover mass balance using a blowing snow model. *Journal of Geophysical Research-Atmospheres*, **105 (D21)**, 26 619–26 634, doi:10.1029/ 2000jd900149.

Power, W. L. and T. E. Tullis, 1991: Euclidean and fractal models for the description of rock surface roughness. *Journal of Geophysical Research-Solid Earth and Planets*, **96 (B1)**, 415–424, doi:10.1029/ 90jb02107.

Prokop, A., M. Schirmer, M. Rub, M. Lehning, and M. Stocker, 2008: A comparison of measurement methods: terrestrial laser scanning, tachymetry and snow probing, for the determination of spatial snow depth distribution on slopes. *Annals of Glaciology*, **49 (1)**, 210–216.

Purves, R. S., J. S. Barton, W. A. Mackaness, and D. E. Sugden, 1998: The development of a rule-based spatial model of wind transport and deposition of snow. *Annals of Glaciology*, **26**, 197–202.

Raderschall, N., M. Lehning, and M. Schär, 2008: Fine-scale modeling of the boundary layer with wind field over steep topography. *Water Resources Research*, **44 (W07404)**, 1–18, doi:10.1029/ 2007WR006545.

Rasmussen, R., et al., 2001: Weather support to deicing decision making (WSDDM): A winter weather nowcasting system. *Bulletin of the American Meteorological Society*, **82 (4)**, 579–595.

Rasmussen, R. M., J. Hallett, R. Purcell, S. D. Landolt, and J. Cole, 2011: The hotplate precipitation gauge. *Journal of Atmospheric and Oceanic Technology*, **28 (2)**, 148–164, doi:10.1175/2010jtecha1375. 1.

Revuelto, J., J. I. López-Moreno, C. Azorin-Molina, and S. M. Vicente-Serrano, 2014: Topographic control of snowpack distribution in a small catchment in the central Spanish Pyrenees: intra- and inter-annual persistence. *The Cryosphere Discuss.*, **8 (2)**, 1937–1972, doi:10.5194/tcd-8-1937-2014.

Rice, R. and R. C. Bales, 2010: Embedded-sensor network design for snow cover measurements around snow pillow and snow course sites in the Sierra Nevada of California. *Water Resources Research*, **46**, doi:10.1029/2008wr007318.

Rinaldo, A., G. Botter, E. Bertuzzo, A. Uccelli, T. Settin, and M. Marani, 2006: Transport at basin scales: 1. Theoretical framework. *Hydrology and Earth System Sciences*, **10 (1)**, 19–29.

Robichaud, A. J. and G. L. Austin, 1988: On the modelling of warm orographic rain by the seeder-feeder mechanism. *Quarterly Journal of the Royal Meteorological Society*, **114 (482)**, 967–988, doi: 10.1002/qj.49711448207.

Rohrer, M., L. Braun, and H. Lang, 1994: Long-term records of snow cover water equivalent in the Swiss Alps 1. analysis. *Nordic Hydrology*, **25**, 53–64.

Sandau, R., 2010: *Digital Airborne Camera. Introduction and Technology.* Springer, Heidelberg, Germany.

Schaffhauser, A., R. Fromm, P. Jörg, G. Luzi, L. Noferini, and R. Sailer, 2008: Remote sensing based retrieval of snow cover properties. *Cold Reg Sci Technol*, **54**, 164–175.

Schirmer, M. and M. Lehning, 2011: Persistence in intra-annual snow depth distribution: 2. Fractal analysis of snow depth development. *Water Resources Research*, **47 (9)**, W09 517, doi:10.1029/ 2010wr009429.

Schirmer, M., V. Wirz, A. Clifton, and M. Lehning, 2011: Persistence in intra-annual snow depth distribution: 1 Measurements and topographic control. *Water Resources Research*, **47 (9)**, W09 516, doi:10.1029/2010wr009426.

Schmidt, S., B. Weber, and M. Winiger, 2009: Analyses of seasonal snow disappearance in an alpine valley from micro- to meso-scale (Loetschental, Switzerland). *Hydrological Processes*, **23 (7)**, 1041–1051, doi:10.1002/Hyp.7205.

Schneiderbauer, S. and A. Prokop, 2011: The atmospheric snow-transport model: SnowDrift3D. *Journal of Glaciology*, **57 (203)**, 526–542.

Schöber, J., S. Achleitner, K. Schneider, R. Sailer, F. Schöberl, J. Stötter, and R. Kirnbauer, 2011: The potential of airborne laser scanning driven snow depth observations for modelling snow cover, snow water equivalent and runoff in alpine catchments. *European Geosciences Union (EGU) General Assembly 2011*, Geophysical Research Abstracts, Vol. 13.

Schwarb, M., C. Daly, C. Frei, and C. Schär, 2001: Mittlerere jährliche Niederschlagsḧohen im europäischen Alpenraum 1971 -1990. *Hydrologischer Atlas der Schweiz*, Landeshydrologie und Geologie, Bern.

Schweizer, J., J. B. Jamieson, and M. Schneebeli, 2003: Snow avalanche formation. *Reviews of Geophysics*, **41 (4)**, doi:10.1029/2002rg000123.

Scipion, D. E., R. Mott, M. Lehning, M. Schneebeli, and A. Berne, 2013: Seasonal small-scale spatial variability in alpine snowfall and snow accumulation. *Water Resources Research*, **49 (3)**, 1446–1457, doi:10.1002/wrcr.20135.

Seligman, G., 1936: *Snow Structure and Ski Fields.* International Glaciological Society, Cambridge, UK, 555 pp.

Sevruk, B., 1997: Regional dependency of precipitation-altitude relationship in the Swiss Alps. *Climatic Change*, **36 (3-4)**, 355–369.

Seyfried, M. S. and B. P. Wilcox, 1995: Scale and the nature of spatial variability - field examples having implications for hydrologic modeling. *Water Resources Research*, **31 (1)**, 173–184.

Shepard, M. K., B. A. Campbell, M. H. Bulmer, T. G. Farr, L. R. Gaddis, and J. J. Plaut, 2001: The roughness of natural terrain: A planetary and remote sensing perspective. *Journal of Geophysical Research-Planets*, **106 (E12)**, 32 777–32 795.

Shook, K. and D. M. Gray, 1996: Small-scale spatial structure of shallow snowcovers. *Hydrological Processes*, **10 (10)**, 1283–1292.

Skaloud, J., J. Vallet, K. Keller, G. Veyssiàre, and O. Kölbl, 2006: An eye for landscapes - rapid aerial mapping with handheld sensors. *GPS World*, **17 (5)**, 26–32.

Sovilla, B., J. N. McElwaine, M. Schaer, and J. Vallet, 2010: Variation of deposition depth with slope angle in snow avalanches: Measurements from Vallee de la Sionne. *Journal of Geophysical Research-Earth Surface*, **115**, doi:10.1029/2009jf001390.

Speight, J., 1974: A parametric approach to landform regions. *Progress in Geomorphology, Special Publication*, Institute of British Geographers, Alden & Mowbray Ltd at the Alden Press, Oxford, Vol. 7, 213–230.

Spreen, W., 1947: A determination of the effect of topography upon precipitation. *Transactions, American Geophysical Union*, **28 (2)**, 285–290, doi:10.1029/TR028i002p00285.

Steppuhn, H. and G. Dyck, 1974: Estimating true basin snowcover. *Proceedings of Interdisciplinary Symposium on Advanced Concepts and Techniques in the Study of Snow and Ice Resources*, N. A. of Science, Ed., 314–328.

Sturm, M. and C. Benson, 2004: Scales of spatial heterogeneity for perennial and seasonal snow layers. *Annals of Glaciology*, **38 (1)**, 253–260, doi:10.3189/172756404781815112.

Sun, W., G. Xu, P. Gong, and S. Liang, 2006: Fractal analysis of remotely sensed images: A review of methods and applications. *International Journal of Remote Sensing*, **27 (22)**, 4963–4990, doi:10.1080/01431160600676695.

Taud, H. and J. Parrot, 2006: Measurement of dem roughness using the local fractal dimension. *Geomorphologie : relief, processus, environnement*, **4/2005**, 327–338.

Tinkham, W. T., A. M. S. Smith, H. P. Marshall, T. E. Link, M. J. Falkowski, and A. H. Winstral, 2014: Quantifying spatial distribution of snow depth errors from LiDAR using random forest. *Remote Sensing of Environment*, **141**, 105–115, doi:10.1016/j.rse.2013.10.021.

Trujillo, E., J. A. Ramirez, and K. J. Elder, 2007: Topographic, meteorologic, and canopy controls on the scaling characteristics of the spatial distribution of snow depth fields. *Water Resources Research*, **43 (W07409)**, 1–17, doi:10.1029/2006WR005317.

Trujillo, E., J. A. Ramirez, and K. J. Elder, 2009: Scaling properties and spatial organization of snow depth fields in sub-alpine forest and alpine tundra. *Hydrological Processes*, **23 (11)**, 1575–1590, doi:10.1002/Hyp.7270.

Vallet, J., 2011: Quick deployment heliborne handheld lidar system for natural hazard mapping. *Gi4DM - Geoinformation for Disaster management Conference , 3-7 May 2011*.

Vallet, J. and J. Skaloud, 2005: Helimap: Digital Imagery/LiDAR handheld airborne mapping system for natural hazard monitoring. *6 setmana Geomatica, Barcelona. Fev. 2005*, 1–10.

Varhola, A., N. C. Coops, M. Weiler, and R. D. Moore, 2010: Forest canopy effects on snow accumulation and ablation: An integrative review of empirical results. *Journal of Hydrology*, **392 (3-4)**, 219–233, doi:10.1016/j.jhydrol.2010.08.009.

Veitinger, J., B. Sovilla, and R. S. Purves, 2014: Influence of snow depth distribution on surface roughness in alpine terrain: a multi-scale approach. *The Cryosphere*, **8**, 547–569, doi:10.5194/tc-8-547-2014.

Warren, S. G., 1982: Optical properties of snow. *Reviews of Geophysics*, **20 (1)**, 67–89.

Wastl, C. and G. Zängl, 2008: Analysis of mountain-valley precipitation differences in the Alps. *Meteorologische Zeitschrift*, **17 (3)**, 311–321, doi:10.1127/0941-2948/2008/0291.

Watson, F. G. R., T. N. Anderson, W. B. Newman, S. E. Alexander, and R. A. Garrott, 2006: Optimal sampling schemes for estimating mean snow water equivalents in stratified heterogeneous landscapes. *Journal of Hydrology*, **328 (3-4)**, 432–452, doi:10.1016/j.jhydrol.2005.12.032.

Wehr, A. and U. Lohr, 1999: Airborne laser scanning - an introduction and overview. *Journal of Photogrammetry & Remote Sensing*, **54**, 68–82.

Winstral, A., K. Elder, and R. E. Davis, 2002: Spatial snow modeling of wind-redistributed snow using terrain-based parameters. *Journal of Hydrometeorology*, **3 (5)**, 524–538.

Winstral, A. and D. Marks, 2002: Simulating wind fields and snow redistribution using terrain-based parameters to model snow accumulation and melt over a semi-arid mountain catchment. *Hydrological Processes*, **16 (18)**, 3585–3603, doi:10.1002/hyp.1238.

Winstral, A. and D. Marks, 2014: Long-term snow distribution observations in a mountain catchment: Assessing variability, time stability, and the representativeness of an index site. *Water Resources Research*, **50 (1)**, 293–305, doi:10.1002/2012wr013038.

Wipf, S., V. Stoeckli, and P. Bebi, 2009: Winter climate change in alpine tundra: plant responses to changes in snow depth and snowmelt timing. *Climatic Change*, **94 (1-2)**, 105–121, doi:10.1007/s10584-009-9546-x.

Wirz, V., M. Schirmer, S. Gruber, and M. Lehning, 2011: Spatio-temporal measurements and analysis of snow depth in a rock face. *The Cryosphere*, **5 (4)**, 893–905, doi:10.5194/tc-5-893-2011.

Witmer, U., 1986: *Erfassung, Bearbeitung und Kartierung von Schneedaten in der Schweiz*, Geographica Bernensia, Vol. G25. Bern.

Wood, E. F., M. Sivapalan, K. Beven, and L. Band, 1988: Effects of spatial variability and scale with implications to hydrologic modeling. *Journal of Hydrology*, **102 (1-4)**, 29–47, doi:10.1016/0022-1694(88)90090-X.

Wood, J., 1996: The geomorphological characterisation of digital elevation models. Ph.D. thesis.

Xu, T. B., I. D. Moore, and J. C. Gallant, 1993: Fractals, fractal dimensions and landscapes - a review. *Geomorphology*, **8 (4)**, 245–262, doi:10.1016/0169-555x(93)90022-t.

Yang, D. and M.-K. Woo, 1999: Representativeness of local snow data for large scale hydrologic investigations. *Hydrological Processes*, **13 (12-13)**, 1977–1988, doi:10.1002/(sici)1099-1085(199909)13:12/13⟨1977::aid-hyp894⟩3.0.co;2-b.

Yang, D. Q., B. E. Goodison, J. R. Metcalfe, V. S. Golubev, R. Bates, T. Pangburn, and C. L. Hanson, 1998: Accuracy of NWS 8 standard nonrecording precipitation gauge: Results and application of WMO intercomparison. *Journal of Atmospheric and Oceanic Technology*, **15 (1)**, 54–68.

Zängl, G., 2008: The temperature dependence of small-scale orographic precipitation enhancement. *Quarterly Journal of the Royal Meteorological Society*, **134 (634)**, 1167–1181, doi:10.1002/qj.267.

Zängl, G., D. Aulehner, C. Wastl, and A. Pfeiffer, 2008: Small-scale precipitation variability in the alps: Climatology in comparison with semi-idealized numerical simulations. *Quarterly Journal of the Royal Meteorological Society*, **134 (636)**, 1865–1880, doi:10.1002/qj.311.

Zingg, T., 1963: Übersicht über die Schneeverhältnisse in der Schweiz. II. Teil: Neuschneeverhältnisse. *Schnee und Lawinen im Winter 1961/62.*, Davos-Weissfluhjoch., Vol. 26.

Curriculum vitae

Grünewald Thomas

Date of birth: 23.10.1982
Place of birth: Eggenfelden, Germany
Nationality: German

Scientific education

06/2011 - 07/2014	**PHD** at EPF Lausanne (Civil- and Environmental Engineering) and WSL Institute for Snow and Avalanche Research SLF Topic: "*Small scale investigation and statistical modeling of mountain snow depth variability*"
02/2009 - 05/2011	Scientific assistant at WSL Institute for Snow and Avalanche Research SLF, Davos (CH)
12/2008	Master of Science (MSc)
02/2008 - 11/2008	Master theses at WSL Institute for Snow and Avalanche Research SLF Topic: *"Bestimmung der räumlichen und zeitlichen Variabilität von Schneewasseräquivalenten im Wannengrat Einzugsgebiet (Davos, Ch) während der Ablationsphase mit Terrestischem Laserscanner (Riegl LPM321)"*
11/2007 - 12/2008	Academic studies MSc "Global change and sustainable development", main focus natural hazards at University of Innsbruck (AT):
11/2007	Bachelor of Science (BSc) Geo- and atmospheric sciences, focus Geography
09/2006 – 07/2007	Academic studies Geography at University of Durham (UK): Grant: ERASMUS
03/2005 - 09/2007	Academic studies Geography (Diploma) and BSc "Geosciences and Atmospheric Sciences" at University of Innsbruck (AT)
10/2004	Vordiplom Geography
10/2002 – 09/2005	Academic studies Geography (Diploma) University of Regensburg (GER)
06/2002	Abitur
1993 – 2002	Secondary school: Maximilian-von-Montgelas-Gymnasium Vilsbiburg; Natural scientific education

Scientific publications

Peer-reviewed

Grünewald, T., Bühler, Y., and Lehning, M.: Elevation dependency of mountain snow depth. The Cryosphere Discuss, 8, 3665-3698, DOI:10.5194/tcd-8-3665-2014, 2014.

Grünewald, T. and Lehning, M.: Are flat-field snow depth measurements representative? A comparison of selected index sites with areal snow depth measurements at the small catchment scale., Hydrol Process, 7, DOI: 10.1002/hyp.10295, 2014.

Bavay, M., Grünewald, T., and Lehning, M.: Response of snow cover and runoff to climate change in high alpine catchments of Eastern Switzerland, Advances in Water Resources, 55, 4-16, Doi:10.1016/j.advwatres.2012.12.009, 2013.

Grünewald, T., Stötter, J., Pomeroy, J. W., Dadic, R., Moreno Baños, I., Marturià, J., Spross, M., Hopkinson, C., Burlando, P., and Lehning, M.: Statistical modelling of the snow depth distribution in open alpine terrain, Hydrol. Earth Syst. Sci. , 17, 3005-3021, Doi:10.5194/hess-17-3005-2013, 2013.

Mott, R., Gromke, C., Grünewald, T., and Lehning, M.: Relative importance of advective heat transport and boundary layer decoupling in the melt dynamics of a patchy snow cover, Advances in Water Resources, 55, 88-97 Doi:10.1016/j.advwatres.2012.03.001, 2013.

Egli, L., Jonas, T., Grünewald, T., Schirmer, M., and Burlando, P.: Dynamics of snow ablation in a small alpine catchment observed by repeated terrestrial laser scans, Hydrological Processes, 26, 1574-1585, Doi:10.1002/hyp.8244, 2012.

Grünewald, T., Dierer, S., Cattin, R., Steiner, P., Steinkogler, W., Fundel, F., and Lehning, M.: Mapping frequencies of icing on structures in Switzerland, Journal of Wind Engineering and Industrial Aerodynamics, 107–108, 76-82, Doi:10.1016/j.jweia.2012.03.022, 2012.

Veas, E., Grasset, R., Ferencik, I., Grünewald, T., and Schmalstieg, D.: Mobile augmented reality for environmental monitoring, Pers Ubiquit Comput, 1-17, Doi:10.1007/s00779-012-0597-z, 2012.

Grünewald, T., and Lehning, M.: Altitudinal dependency of snow amounts in two small alpine catchments: Can catchment-wide snow amounts be estimated via single snow or precipitation stations?, Ann. Glaciol., 52, 153-158, 2011.

Lehning, M., Grünewald, T., and Schirmer, M.: Mountain snow distribution governed by an altitudinal gradient and terrain roughness, Geophys. Res. Lett., 38, L19504 Doi:10.1029/2011gl048927, 2011.

Mott, R., Egli, L., Grünewald, T., Dawes, N., Manes, C., Bavay, M., and Lehning, M.: Micrometeorological processes driving snow ablation in an alpine catchment, Cryosphere, 5, 1083-1098, Doi:10.5194/tc-5-1083-2011, 2011.

Grünewald, T., Schirmer, M., Mott, R., and Lehning, M.: Spatial and temporal variability of snow depth and ablation rates in a small mountain catchment, The Cryosphere, 4, 215-225, Doi:10.5194/tc-4-215-2010, 2010.

Kruijff, E., Mendez, E., Veas, E., Grünewald, T., Simoni, S., Luyet, V., Salminen, O., Nurminen, A., and Lehtinen, V.: Hydrosys: On-site monitoring and management of environmental processes using handheld devices, in: Geohydroinformatics: Integrating gis and water engineering, edited by: Anand, S. A., R.J., Jackson, M., Vairavamoorthy, K., Ware, M., CRC Press., 2010.

Mott, R., Schirmer, M., Bavay, M., Grünewald, T., and Lehning, M.: Understanding snow-transport processes shaping the mountain snow-cover, The Cryosphere, 4, 545-559, Doi:10.5194/tc-4-545-2010, 2010.

Non-peer-reviewed

Lehning, M., Grünewald, T., Marty, C., Mott, R., and Stähli, M.: Kleinräumige Schneeverteilung und Einfluss der Topographie, Alpine Schnee- und Wasserresourcen gestern, heute, morgen. Forum für Wissen, 13-18, 2012.

Dierer, S., Cattin, R., Grünewald, T., Lehning, M., and Steiner, P.: Modelling the risk of icing - mapping and forecasting icing on structures, Windtech International., June 2010, 2010.

Conference Proceedings

Grünewald, T., and Lehning, M.: Can a point measurement represent the snow depth in its vicinity? A comparison of areal snow depth measurements with selected index sites., in: Proceedings of the International Snow Science Workshop 27 October 7 to 11, Grenoble, France. 69-72., Proceedings of the International Snow Science Workshop 27 October 7 to 11, Grenoble, France. 69-72., 2013.

Kruijff, E., Mendez, E., Veas, E., and Grünewald, T.: Hydrosys: On-site monitoring of environmental processes using mobile augmented reality. Proceedings of environmental information systems and services, ENVIP'2010, 2010.

Grünewald, T., Schirmer, M., and Lehning, M.: Measurements of small scale spatial and temporal variability of snow depth and SWE in a small mountain catchment., in: Proceedings of the International Snow Science Workshop 27 September to 2 October 2009, Davos, Switzerland. 151-154., 2009.

Mott, R., Schirmer, M., Grünewald, T., and Lehning, M.: Understanding snow transport processes shaping the mountain snow-cover, in: Proceedings of the International Snow Science Workshop 27 September to 2 October 2009, Davos, Switzerland. , Proceedings of the International Snow Science Workshop 27 September to 2 October 2009, Davos, Switzerland. 141-145., 2009.

Lehning, M., Grünewald, T., and Fierz, C.: Assessment of mountain snow transport based on measured wind and simulated snow cover, in: Proceedings of the International Snow Science Workshop, 1-6 October, Telluride, CO USA, 2006, 815-819, 2006.

Conference Presentations

Grünewald, T., and Lehning, M.: Do snow depth measurement at typical flat-field locations represent their surrounding?, Davos Atmosphere and Cryosphere Assembly 2013: Air, Ice & Process Interactions, Davos, Switzerland, July 8-12, 2013, 2013.

Helbig, N., Löwe, H., Grünewald, T., Magnusson, J., Lehning, M., and Jonas, T.: Characterizing the spatial snow depth distribution in mountainous terrain Davos Atmosphere and Cryosphere Assembly, Davos, 2013, 2013.

Grünewald, T., and Lehning, M.: Can a point measurement represent the snow depth in its vicinity? A comparison of areal snow depth measurements with selected index sites., ICAM 2013 - International Conference on Alpine Meteorology, Kranjska Gora, Slovenia, 3 - 7 June 2013, 2013.

Grünewald, T., and Lehning, M.: Statistical modelling of the snow depth distribution for two glaciated catchments, One decade of airborne laserscanning at Hintereisferner, 3.-6. October 2012, Obergurgl, Austria, 2012.

Grünewald, T., Schirmer, M., and Lehning, M.: Statistical modeling of the small-scale spatial variability of snow depth, European Geoscience Union General Assembly, April, 7rd to 12th 2012, Vienna, Austria, 2012.

Lehning, M., Mott, R., Grünewald, T., and Schirmer, M.: Physical and statistical descriptions of mountain snow distributions, International symposium on Seasonal snow and Ice, 28 May–1 June 2012, Lahti, Finland, 2012.

Trujillo, E., Grünewald, T., and Lehning, M.: Uncertainty and reliability of snow depth measurements, AGU fall meeting, 3-7 December 2012, San Francisco, USA, 2012.

Grünewald, T., Mendez, E., Roos, U., Danioth, C., and Phillips, M.: Monitoring infrastructure stability in alpine permafrost, European Geoscience Union General Assembly, April, 3rd to 8th 2011, Vienna, Austria, 2011.

Bavay, M., Grünewald, T., Magnusson, J., and Lehning, M.: Modelling the climate change impact on snow and runoff in the alpine space, AGU fall meeting, 5-9 December 2011, San Francisco, USA, 2011.

Dierer, S., Grünewald, T., Cattin, R., Lehning, M., and Steiner, P.: Atmospheric icing - a challenge in site assessment, European Wind Energy Conference. 20.-23.4.2010 Warschau, 2010, 2010.

Grünewald, T., and Lehning, M.: Altitudinal dependency of snow amounts in two alpine catchments. Can catchment wide snow amounts be estimated via single snow stations and precipitation gradients?, International symposium on snow, ice and humanity in a changing climate, 21-25 June 2010, Sapporo, Japan, 2010.

Grünewald, T., Steinkogler, W., Dierer, S., Cattin, R., Steiner, P., and Lehning, M.: A new map of the icing potential for Switzerland, INTERNATIONAL SYMPOSIUM ON SNOW, ICE AND HUMANITY IN A CHANGING CLIMATE, 21-25 June 2010, Sapporo, Japan, 2010.

Lehning, M., Grünewald, T., and Schirmer, M.: The role of a roughness scaling parameter in describing alpine snow distribution, AGU Fall Meeting, 3-17 December 2010 San Francisco, USA, 2010.

Mott, R., Grünewald, T., Schirmer, M., Wirz, V., and Lehning, M.: Understanding snow deposition on mountain slopes, European Geoscience Union General Assembly, Mai, 2nd to 7th 2010, Vienna, Austria. 2010.

Grünewald, T., Schirmer, M., and Lehning, M.: Can the total snow amount in an alpine catchment be estimated from flat field snow measurements? European Geoscience Union General Assembly Wien 2009.

Lehning, M., Grünewald, T., Dadic, R., Mott, R., Schirmer, M., and Wirz, V.: How much snow is there on the mountain, where and when?, AGU fall meeting, 14-18 December 2009, San Francisco, USA, 2009.